# MODELING WATER QUALITY IN SOUTHERN SASKATCHEWAN WATERSHEDS

A Thesis Submitted to the

College of Graduate and Postdoctoral Studies

In Partial Fulfillment of the Requirements

for the Degree of Master of Science in the

Department of Civil, Geological and Environmental Engineering

University of Saskatchewan

Saskatoon.

By

**Asif Ahmed Abir**

## PERMISSION TO USE

In presenting this thesis in partial fulfilment of the requirements for a Postgraduate degree from the University of Saskatchewan, I agree that the Libraries of this University may make it freely available for inspection. I further agree that permission for copying of this thesis in any manner, in whole or in part, for scholarly purposes may be granted by the professors who supervised my thesis work or, in their absence, by the Head of the Department or the Dean of the College in which my thesis work was done. It is understood that any copying or publication or use of this thesis or parts thereof for financial gain shall not be allowed without my written permission. It is also understood that due recognition shall be given to me and to the University of Saskatchewan in any scholarly use which may be made of any material in my thesis.

Requests for permission to copy or to make other use of material in this thesis in whole or part should be addressed to:

Head of the Department of Civil, Geological, and Environmental Engineering
University of Saskatchewan
57 Campus Drive
Saskatoon, Saskatchewan
Canada, S7N 5A9

OR

Dean
College of Graduate and Postdoctoral Studies
University of Saskatchewan
116 Thorvaldson Building, 110 Science Place
Saskatoon, Saskatchewan S7N 5C9 Canada

## ABSTRACT

The presence of accumulated nutrients in surface waters is a great concern for water quality. In Saskatchewan, for many streams, data on water quality is limited both spatially and temporally. An eco-hydrological model is a relatively low-cost method to help assess water quality where there are limited measurements. The study area is located in the Canadian prairie region where potholes are the dominant landscape feature and farming is an extensive activity. Potholes are closed-surface depressions that have a significant role in the prairie hydrologic cycle, flood mitigation, and water quality.

The current modelling study was conducted in three southern Saskatchewan watersheds: Pipestone Creek above Moosomin Lake, Swift Current Creek below Rock Creek, and Lightning Creek near Carnduff. The hydrological model SWAT (the Soil and Water Assessment Tool) with the Probability Distributed Landscape Depressions module (SWAT-PDLD) (with seasonally variable soil erodibility) used in simulating flow and water quality results were compared to SWAT with its in-built pond routine (SWAT-lumped). Model results were then used to determine pond spilling and non-spilling period to examine whether any relationships between observed nutrient loading and streamflow differed during spilling and non-spilling periods.

Both the SWAT-PDLD and SWAT-lumped models showed “good” performance for calibration period and “satisfactory” performance for validation period respectively for streamflow simulation based on statistical metrics for Pipestone Creek and Lightning Creek watershed. However, the SWAT-PDLD performed “good” for sediment export, total phosphorus export and total nitrogen export simulation whereas the SWAT-lumped model performed “satisfactory” for the same cases. Simulation results were improved using SWAT-PDLD over SWAT-lumped model. Spilling and non-spilling

events were identified and categorized based on pond outflow contribution to streamflow. Both models could not satisfactorily simulate the streamflow for the Swift Current Creek watershed.

It has been noticed that the observed total nitrogen load was significantly higher during model-predicted spilling periods than non-spilling periods in the Lightning Creek watershed. However, observed sediment export and total phosphorus export did not appear any different between spilling and non-spilling events. In the Pipestone Creek watershed, the relationship between loadings and streamflow did not appear to be different during spilling and non-spillling periods for sediment export, nitrogen, and phosphorus.

## ACKNOWLEDGMENTS

All praises goes to my almighty Allah and I am thankful to him for giving me the ability, knowledge and strength to pursue my MSc. successfully.

I am expressing my deeply gratitude to my supervisors Dr. Kerry A. Mazurek and Dr. Gordon Putz for giving me the opportunity and continuous support and guideline to pursue my MSc. at the University of Saskatchewan. I am also grateful to my Advisory committee members Dr. Warren Helgason, Dr. Saman Razavi and Dr. John-Mark Davies for their valuable comments and suggestions to improve my research work. Special gratitude to Dr. Balew A. Mekonnen for the technical support and continuous guidance throughout the research period.

I acknowledge the support of Dr. John-Mark Davies for providing the required water quality data which was a crucial part of my thesis work. I also like to thank Mr. Robert Alary, Data, GIS and Government Information, University of Saskatchewan for providing high resolution DEM data. Special gratitude goes to Dan McKenney and Pia Papadopol from Natural Resources Canada (NRC) for providing gridded climate data.

I also greatly acknowledge the financial support provided by Natural Sciences and Engineering Research Council of Canada (NSERC) to Dr. Putz in the form of Discovery Grants.

I like to thank Tracy McArthur, departmental assistant of the Hydrotechnical lab and my fellow lab mates for making a nice work environment in the lab.

In the end, I am thankful to my family members and friends for providing me the continuous mental support and inspiration to pursue my degree.

## DEDICATION

This thesis work is dedicated to my parents Momotaz Begum and Md. Abdus Satter who sacrificed their whole life for my better future.

## TABLE OF CONTENTS

## LIST OF TABLES

## LIST OF FIGURES

## LIST OF SYMBOLS

$area_{hru}$ area of the HRU;

$b_{melt}$ daily melt factor ;

$c$ storage capacity of landscape depressions;

$conc_{NO3,mobile}$ concentration of nitrate in the mobile water;

$conc_{orgN}$ concentration of organic nitrogen;

$conc_{sedP}$ concentration of phosphorus attached to sediment;

$covsoil$ soil cover index;

$CFRG$ coarse fragment factor;

$CN$ daily curve number ;

$C_{USLE}$ USLE cover and management factor;

$depth_{surf}$ depth of the surface layer;

$E_{can}$ evaporation from water stored on the vegetation canopy;

$E_d$ adjusted potential evapotranspiration from the vegetation canopy;

$E_k$ soil evaporation (mm) for different soil layer;

$E_o$ potential evapotranspiration

$E_s$ sublimation from the snowpack;

$E_{soil,z}$ soil evaporative demand at depth $z$;

$E_{sub}$ daily sublimation;

$E_s'$ maximum sublimation adjusted for plant water use;

$E_s''$ maximum potential for soil water evaporation;

$E_t$ maximum transpiration;

| | |
|---|---|
| $Ho$ | extraterrestrial radiation; |
| $I$ | infiltration into the soil layer; |
| $I_a$ | initial abstractions prior to runoff ; |
| $k_{d,perc}$ | phosphorus percolation coefficient; |
| $K_{USLE}$ | USLE soil erodibility factor; |
| $LAI$ | vegetation leaf area index; |
| $LS_{USLE}$ | USLE topographic factor; |
| $minP_{act,ly}$ | phosphorus in the active mineral pool; |
| $minP_{sta,ly}$ | phosphorus in the stable mineral pool; |
| n | number of observed data; |
| N | Nitrogen; |
| $N_2$ | Nitrogen gas; |
| $NO_2^-$ | Nitrite ion; |
| $NO_3^-$ | Nitrate ion; |
| $NO3_{conc,z}$ | concentration of the nitrate in the soil at depth $z$; |
| $NO3_{lat,ly}$ | nitrate removed in lateral flow; |
| $NO3_{perc,ly}$ | nitrate moved to the underlying layer by percolation; |
| $NO3_{rain}$ | nitrate added by rainfall; |
| $NO3_{surf}$ | nitrate removed in surface runoff; |
| $orgC_{ly}$ | organic carbon in the layer; |
| $orgN_{fsh,surf}$ | nitrogen in the fresh organic pool in the top 10 mm; |
| $orgN_{hum,ly}$ | concentration of humic organic nitrogen in the layer; |

$orgN_{surf}$ organic nitrogen transported to the main channel in surface runoff;

$orgP_{act,ly}$ phosphorus in the active organic pool;

$orgP_{frsh,ly}$ phosphorus in the fresh organic pool in the soil layer;

$pai$ phosphorus availability index;

$P$ total daily precipitation depth;

$P_{dec,ly}$ phosphorus decomposed from the fresh organic P pool;

$P_{int}$ precipitation intercepted and stored in the vegetation canopy,

$P_{min,ly}$ phosphorus mineralized from the fresh organic P pool;

$P_{mina,ly}$ phosphorus mineralized from the humus active organic P pool;

$P_{perc}$ phosphorus moving from the top 10 mm into the first soil layer;

$P_{solution,ly}$ phosphorus in solution;

$P_{solution,surf}$ phosphorus in solution in the top 10 mm;

$P_{surf}$ soluble phosphorus lost in surface runoff;

$P_{thr}$ precipitation in the form of rain that is not intercepted on vegetation surfaces;

$P_{USLE}$ USLE support practice factor;

$Q$ daily total flow leaving the HRU;

$Q_i$ observed flow;

$q_{peak}$ peak runoff rate;

$Q_{gwd}$ groundwater recharge to the deep aquifer that is lost from the watershed;

$Q_{gws}$ baseflow from the shallow aquifer;

$Q_{lk}$ lateral flow from top soil layer to bottom soil layers;

$Q_{lat,ly}$ water discharged from the soil layer by lateral flow;

$Q_{sim}$ simulated flow;

$Q_{surf}$ daily surface runoff;

$\bar{Q}$ average observed flow;

$R_{day}$ daily precipitation;

$R_{int\ (i)}$ daily initial amount of free water held in the canopy;

$R_{int\ (f)}$ daily final amount of free water held in the canopy;

$R_{NO3}$ concentration of nitrogen in the rain;

$R_{vap}$ upward movement of water from the shallow aquifer;

$rsd_{surf}$ material in the residue pool;

$S$ retention parameter;

$sed$ daily sediment yield;

$S_k$ water stored in different soil layers;

$S_{melt}$ snowmelt water from the snowpack;

$S_{pack}$ snow stored on the soil surface;

$S_{sa}$ water stored in the shallow aquifer;

$S_{thr}$ precipitation in the form of snow that is not intercepted on vegetation surfaces;

$sedP_{surf}$ phosphorus transported with sediment to the main channel in surface runoff;

$sno_{cov}$ fraction of the HRU area covered by snow;

$SNO_{(i)}$ water in the snowpack on a given day before considering for sublimation;

$SW_{ly,excess}$ daily drainable volume of water in the soil layer;

$SNO_{melt}$ daily amount of snowmelt;

$SW_t$ final soil water content;

| | |
|---|---|
| $SW_0$ | initial soil water content; |
| $\Delta S$ | daily change in water storage of the HRU; |
| $t$ | time (days); |
| TOT N | total Nitrogen; |
| TOT P | total phosphorus; |
| $T_{av}$ | daily mean air temperature; |
| $T_k$ | plant transpiration (mm) from different soil layer; |
| $T_{melt}$ | base temperature above which snowmelt will occur; |
| $T_{mn}$ | daily minimum air temperature; |
| $T_{mx}$ | daily maximum air temperature; |
| $T_{snow}$ | daily snowpack temperature; |
| $TT_{perc}$ | travel time for percolation; |
| $\Delta t$ | length of time steps; |
| WDPM | Wetland DEM Ponding Model |
| $w_{perc,ly}$ | water percolating to the underlying soil layer; |
| $w_{perc,surf}$ | water percolating to the first soil layer; |
| $W_{pk}$ | water percolating from upper soil layer to the next soil layers; |
| $z$ | depth below the surface; |
| $\beta_{min}$ | rate coefficient for mineralization of the humus active organic nutrients; |
| $\beta_{NO3}$ | nitrate percolation coefficient; |
| $\gamma_{sw,ly}$ | nutrient cycling water factor for the soil layer; |
| $\gamma_{tmp,ly}$ | nutrient cycling temperature factor for the soil layer; |

$\delta_{ntr.ly}$ residue decay rate constant;

$\varepsilon_{N;sed}$ nitrogen enrichment ratio;

$\varepsilon_{P;sed}$ phosphorus enrichment ratio;

$\lambda$ latent heat of vaporization;

$\rho_b$ bulk density of the top soil layer.

## LIST OF ABBREVIATIONS

| | |
|---|---|
| AAFC | Agriculture and Agri-Food Canada |
| AET | Actual Evapotranspiration |
| CANSIS | Canadian Soil Information Service |
| CHRM | Cold Regions Hydrological Model |
| DEM | Digital Elevation Model |
| DHI | Danish Hydrological Institute |
| GIS | Geographic Information System |
| HEW | Hydrologic Equivalent Wetland |
| HRU | Hydrologic Response Unit |
| HYDAT | Hydrometric Database |
| MESH | Modélisation Environmentale Communautaire – Surface and Hydrology |
| MUSLE | Modified Universal Soil Loss Equation |
| NCDA | Non-contributing Drainage Area |
| NRC | Natural Resources Canada |
| NSE | Nash and Sutcliffe Efficiency |
| NSERC | Natural Sciences and Engineering Research Council of Canada |
| PBIAS | Percent Bias |
| PD | Puddle Delineation |
| PDLD | Probability Distributed Landscape Depressions |
| PET | Potential Evapotranspiration |
| PFRA | Prairie Farm Rehabilitation Administration |

| | |
|---|---|
| QUAL2E | Enhanced Stream Water Quality Model |
| RSR | Standardized version of Root mean Square error |
| SCS | Soil Conservation Service |
| SGIC | Saskatchewan Geospatial Imagery Collaborative |
| SPARROW | SPAtially Referenced Regression On Watershed Attributes |
| SUFI | Sequential Uncertainty FItting |
| SWA | Saskatchewan Watershed Authority |
| SWAT | Soil and Water Assessment Tool |
| SWAT-CUP | SWAT Calibration and Uncertainty Procedures |
| TN/TOT N | Total Nitrogen |
| TP/TOT P | Total Phosphorus |
| TSS | Total Suspended Solids |
| USEPA | United States Environmental Protection Agency |
| USLE | Universal Soil Loss Equation |
| WINTRA | Winter Nutrient Field Transport Model |
| WSA | Water Security Agency |

# CHAPTER 1: INTRODUCTION

## 1.1 Background

Water quality in streams in the Canadian prairie region has been a matter of concern for several decades (Wheater and Gober 2013). More intensive agricultural practice over the past decades (1971-2006) (Statistics Canada 2011) has resulted in adverse impacts on water, quality which has threatened aquatic ecosystems (Wheater and Gober 2013). However, water quality data in Saskatchewan tend to be sparse in both time and location. An absence of water quality data makes it challenging for policy makers to make decisions with respect to watershed management. To help "fill in the blanks", it is therefore important to be able to simulate streamflow water quality. Computational modelling of water quality requires both simulation of streamflow and the processes related to water quality constituents.

The hydrology of the Canadian prairie region is complex due to the cold climate and the numerous landscape depressions or "potholes." The prairie pothole region (Figure 1) covers three Canadian provinces (Saskatchewan, Manitoba, and Alberta) and five states in the United States (Minnesota, Iowa, North and South Dakota, and Montana), where potholes are the dominant landscape feature and farming is an extensive activity (Upadhyay *et al*. 2018). Potholes are closed-surface depressions that have a significant role in the prairie hydrologic cycle, flood mitigation, and water quality (Upadhyay *et al.* 2018). The dynamic connectivity among depressions and their variable storage capacity strongly influence the hydrology of this region (Shaw *et al*. 2011). The depressions fill and then spill and overland flow makes connections among them, which induces higher surface runoff that moves down to the main streams along with accumulated sediment and nutrients (Muhammad *et al.* 2019). A large amount of surface runoff does not flow until the storages are filled and the depressions "spill" to contribute to streamflow. There are also non-

contributing areas where the surface runoff does not contribute to the major river system of the basin due to the wetland storage as well as poor and internal drainage (Fang *et al.* 2007).

With respect to the cold climate of this region, the freeze-thaw cycle is an important characteristic that affects surface runoff during snowmelt, infiltration, and nutrient transport (Bechmann and Sharpley 2005). The fill-and-spill mechanism of the depressions is a unique characteristic of the prairie region during freeze-thaw cycles (Fang *et al*. 2007). During freeze-thaw cycles increased soil erodibility occurs. As a result, mobilization and transport of sediment is expected to be higher during the snowmelt period (McConkey *et al*. 1996).

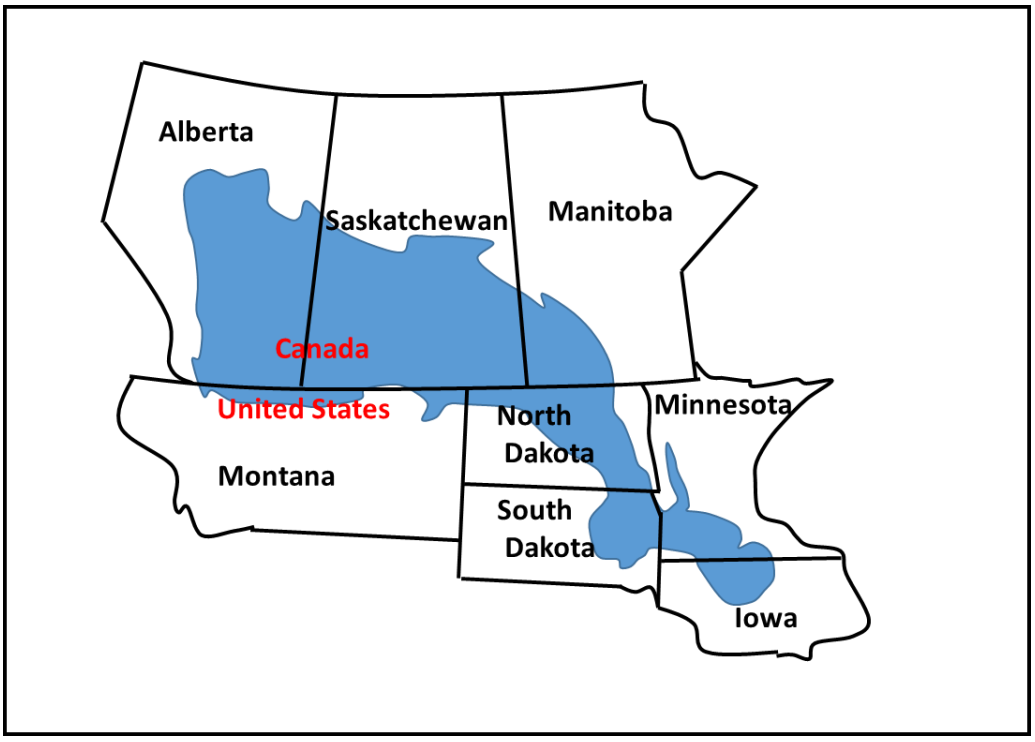


Figure 1.1: Prairie Pothole Region of North America (adapted from Howerter 2014).

Water quality issues in Saskatchewan are primarily related to algal growth in lakes, reservoirs and potholes and in some cases immediate downstream effects from sewage outflows into watercourses (Pomeroy *et al*. 2005). Landscape depressions are a trap for sediment and nutrients (Du *et al.* 2005; Almendinger *et al.* 2014). The landscape depressions are capable of storing water

for long periods, in which water quality deteriorates due to eutrophication (Neely and Baker 1989). Eutrophication is the process of enrichment of minerals and nutrients in the water body which triggers aquatic plant and algal growth and results in depletion of oxygen (Chislock *et al.* 2013). It may occur naturally *i.e*. with solar radiation, abundance of carbon dioxide and soil nutrients, or through anthropogenic activities *i.e*. with increased usage of fertilizer in agricultural fields (de Jonge and Elliott 2001; Smith and Schindler 2009; Chislock *et al.* 2013).

Sedimentation in water bodies in prairie watersheds was noticed in the early 1900s after introducing agricultural activities on a large scale (Acton and Gregorich 1995, Boer et al. 2005, Koroluk and de Boer 2007). Sediment is a concern because of the potential impacts on fish (Kjelland e*t al*. 2015), as sediments can cover egg deposition sites, smother juveniles, interfere with gills, and alter benthic communities that serve as food (USEPA 1983). Sediment also carries other pollutants to the waterbody (Koroluk and de Boer 2007). For example, phosphorus can be transported into streams in a form bound to sediments (Novotny 2003).

This study will use the hydrological model SWAT (Soil and Water Assessment Tool), modified with a probability distributed algorithm to account for dynamic storage in landscape depressions and for seasonality in soil erodibility (called SWAT-PDLD), to assess water quality in three small watersheds in southern Saskatchewan that are dominated by numerous landscape depressions. Specifically, the research is focused on determining the sediment and nutrient loading in streamflow. SWAT-PDLD was developed by Mekonnen *et al.* (2016a-c) but was only tested in two large Saskatchewan watersheds.

### 1.2 Objectives

The objectives of the work are as follows:

1. To assess how the SWAT-PDLD model with seasonally variable soil erodibility performs in simulating flow and water quality for three additional southern Saskatchewan watersheds different than those tested by Mekonnen *et al.* (2016a-c); and
2. To use SWAT-PDLD to identify when depressions were contributing to streamflow and when they were not, and then to examine whether the observed relationship between nutrient concentrations and load in the river and discharge are different between the two cases.

### 1.3 Scope of the Study

The scope of this study includes computational modelling and analysis of existing water quality data. The study will estimate the streamflow, sediment loads, nitrogen, and phosphorus export using Mekonnen *et al.'s* (2016a-c) modified version of SWAT (SWAT-PDLD) for three watersheds in southern Saskatchewan, as well as SWAT with its Pond module. The scope does not include measurements of water quality in the field or the collection of water samples for analysis.

### 1.4 Organization of the Thesis document

This thesis document contains six chapters including this introductory chapter. Chapter 2 provides a literature review of the hydrology of the cold climate prairie region, previous SWAT modeling work for the prairie region, and how depressions are handled in hydrological modelling of the prairie region. Chapter 3 reviews the mechanics of the SWAT model. Next, Chapter 4 explains the detailed methodology of the research work and describes the data collection, model setup, calibration and validation, and sensitivity analysis. Chapter 5 mainly presents the simulation results, model performance, and discussion of the results, as well as an analysis of the water quality data in the watershed during spill and non-spill periods. Finally, Chapter 6 presents the conclusions of the research work and recommendations for future work.

# CHAPTER 2: LITERATURE REVIEW

## 2.1 Overview of Prairie Hydrology and Water Quality

The numerous surface-water depressions of the prairie pothole region have been discussed as being geographically isolated (Tiner 2003); however, this idea is controversial (Mushet *et al.* 2015, Hay *et al.* 2017). Over space and time, the connectivity among these water bodies can vary (Leibowitz and Vining 2003, Winter and LaBaugh 2003). It is believed that the surface water depressions of the prairie pothole region play an important role in the hydrologic cycle (Eisenlohr and Sloan 1968, Cohen *et al.* 2016). In the case of flood control, surface water depressions can collect and store precipitation and surface runoff resulting in reduced or delayed flow input to the stream channel with reduced peak streamflow (DeLaney 1995, Ludden *et al.* 1983, Hay *et al.* 2017).According to Pomeroy *et al.* (2007), the key features that represent the cold climate of the prairie region are moderate precipitation, seasonal frozen soil and snow coverage that stores a considerable amount of water, a poor drainage system due to glacial geomorphic structures, and irregular and large runoff events. Furthermore, available soil moisture is a key factor influencing surface runoff to the stream. Fang and Pomeroy (2007) found that low antecedent soil moisture decreased snowmelt runoff, whereas the volume of runoff resulting from snowmelt increased when the preceding fall soil moisture content was high.

The water budget of the prairie pothole region is a matter of concern during summer because summer precipitation is exceeded by evapotranspiration; therefore, the most crucial input to the prairie landscape depression water budget is considered to be upland snowmelt (Hayashi *et al.* 1998, LaBaugh *et al.* 1998, Fang and Pomeroy 2008, Mekonnen 2016). The next most important inputs are direct precipitation on the depression and surface runoff during intense rainfall events.

On the other hand, evapotranspiration and lateral flow of shallow groundwater are the main means of water leaving the depressions (Woo and Rowsell 1992, van der Kamp and Hayashi 2009). However, due to the low hydraulic conductivity of the deeper soil layers, the influence of deep groundwater interaction on the water balance of the depressions is limited (van der Kamp and Hayashi 2009).

It is reported that agricultural management practices are responsible for high concentrations of N and P in prairie runoff because they maintain a high degree of soil nutrients in agricultural land (Buda *et al.* 2009; Hansen *et al.* 2002; Liu *et al.* 2013; Moog and Whiting 2002). Management practices, such as tillage and crop choice, and antecedent soil moisture conditions impact the transport of P and N in a watershed (Jamieson and Enright 2003; Christopher *et al.* 2007). It has also been identified that nutrient loss is affected by hydrologic and weather factors (runoff over frozen soils, temperature, total rainfall, rainfall intensity, *etc*.), which are also linked to the water chemistry in runoff (Townsend-Small *et al.* 2011, Tisseuil *et al.* 2008, Shrestha *et al.* 2011, Liu *et al.* 2013, Lintern *et al.* 2018). Nutrient loadings (manure and fertilizers) reach streams through surface runoff, but Hargrave and Shaykewich (1997) indicate that nutrient loading is also correlated with sediment loss. Liu *et al.* (2013) noted that the important factors controlling the nutrient concentration or loads are the volume of runoff, the snow water equivalent, flow rate, and runoff duration.

Major water quality concerns in reservoirs in the prairie region include eutrophication. A high intensity of algal blooms, eutrophication, and growth of non-native species are consequences of excess nutrient enrichment in water bodies (Burford *et al.* 2007, Xu *et al.* 2010, Connelly *et al.* 2007, Morales-Marín *et al.* 2017**).** Reservoirs reduce incoming upland flow velocities and this

results in the deposition of a large amount of nutrients within a reservoir (Morales-Marín *et al.* 2017).

Several past studies demonstrated that pothole wetlands in prairie catchments trap nutrients from surface runoff (Neely and Baker 1989, Crumpton and Goldsborough 1998). Moreover, potholes are connected to the downstream water body by draining surface runoff; thus, they are potential sources of excess nutrient and sediment pollution of water quality to the receiving streams (Leibowitz and Vining 2003; Winter and LaBaugh 2003). Researchers also found that prairie wetlands in Canada are contaminated due to increased use of pesticides (Donald *et al.* 2000, Waite *et al.* 2002). The possible origins of pesticide and herbicides loadings to prairie wetlands are atmospheric sources such as wet and dry deposition (Jantunen *et al.* 2008), surface runoff events, or contaminated groundwater inflow (Waite *et al.* 1992, Donald *et al.* 2000). It is estimated that the maximum acceptable concentration level of pesticides was exceeded in nearly 24% of the wetlands in the province of Saskatchewan according to Canadian guidelines for the protection of aquatic life (Messing *et al.* 2011).

## 2.2 Review of Modelling Work

### 2.2.1 Streamflow

The North American prairie pothole region, which consists of many depression-dominated areas, is complex to model hydrologically. Modelling in the region is reliant on a clear understanding of the dynamic "filling-spilling-merging-splitting processes" of the depressions (Nasab *et al.* 2017). The sizes, storages, and interactions of potholes vary over time, and they are spatially distributed over a watershed. However, most hydrologic models and their default approaches fail to account for these dynamic processes.

According to various literature, there is no doubt that wetland hydrologic function is a key for modelling wetland-dominated watersheds (Bengtson and Padmanabhan 1999; Hayashi *et al.* 2004). However, the selection of the modelling approach to incorporate wetlands into a hydrologic model is a controversial topic. A fully-distributed approach based on GIS was developed to represent wetlands in prairie regions to characterize wetlands and their effects on flow and water quality at a finer scale (Liu *et al.* 2018). Simulation of hydrologic processes with detailed spatial distribution and providing output in user-defined spatial and temporal scales is possible. However, fully-distributed approaches are normally useful for a site-specific wetland assessment with a high degree of computational requirements. Pomeroy *et al.* (2007) and Fang and Pomeroy (2008) introduced the Cold Regions Hydrological Model (CRHM) to simulate the water balance for individual closed wetlands with no provision of calibration. CRHM was also designed considering snow management and to represent the potential impact of enhanced runoff on wetlands during dry periods (Fang and Pomeroy 2008). However, CRHM is still developing its water quality module for prairie watersheds.

The MESH (Modélisation Environmentale Communautaire - Surface and Hydrology) model has been used to predict streamflow in the prairie region of Saskatchewan (Pietroniro *et al.* 2006). However, it is also not fully capable of water quality assessment, as it does not simulate all the commonly required water quality parameters (Mekonnen 2016). Further, water management practices for irrigation and agricultural management are not included in MESH (Nazemi and Wheater 2015).

Besides these North American models, there are some advanced hydrological models developed in Europe, *e.g.* MIKE SHE by DHI (Danish Hydrological Institute). However, MIKE SHE is a fully distributed commercial model and therefore it is not suitable for simulating a large-

area watershed. Moreover, a well-developed agricultural management practices module is unavailable.

SWAT is a semi-distributed model developed by Arnold *et al.* (1993), which is one of the most widely used models to predict the impact of different land management practices on water and nutrient export over long periods of time. However, very few studies have considered the influence of wetlands in simulating streamflow using SWAT.

Shrestha *et al.* (2012a) used the pond feature in SWAT to attempt to consider all depressions that contribute surface runoff to a watershed, however that approach does not simulate the dynamic characteristics of landscape depressions of the prairie pothole region (Nasab *et al.* 2017). The SWAT pond feature considers wetlands in a lumped approach. This means the numerous wetlands in a sub-watershed are summed and considered as a single virtual pond for each sub watershed. Depending on the sub watershed size and wetland geometry, the lumped approach can simulate watershed streamflow with moderate success. However, the lumped approach is not close to the actual scenario for the prairie region where the heterogeneity of surface storage capacity is very challenging to represent in a hydrologic model (Hossain 2017). Therefore, to more representatively incorporate landscape depressions some modification of the SWAT model is necessary.

A variety of approaches have been used to represent landscape depressions within SWAT for modelling in the prairie pothole region. The Hydrologic Equivalent Wetland (HEW) concept, coupled with the SWAT model, has been used in several studies (Wang *et al*. 2008, Perez-Valdivia *et al.* 2017 and Yang *et al.* 2010). HEW was originally developed by Wang *et al.* (2008) by introducing a variable drainage area that contributes to the wetlands for a watershed in northwestern Minnesota. Moreover, a non-linear functional relationship between runoff and

wetland characteristics such as surface area and volume that was first introduced by Quinton *et al.* (2003) was also observed by Wang *et al.* (2008).

The HEW approach was incorporated into the wetland module available in the SWAT model. According to Wang *et al.* (2008), the HEW has hydrologic characteristics that are identical to the actual distributed wetlands. The geometric properties required by the HEW are the surface area (SA) at normal and maximum water level, volume of the HEW at normal water level ($V_{nor}$), volume of the HEW during maximum water level ($V_{mx}$) and the fraction of the sub-basin area that drains into HEW. The unique aspect of this study was the values of all the parameters that describe the HEW were selected by model calibration. In total, the HEW was defined by six calibrated parameters: the fraction of sub-basin area that drains into wetlands, the volume of water stored in the wetland during normal water level (WET_NVOL), the volume of water stored in the wetland during maximum water level, the longest tributary channel length in a sub-basin, the Manning's n value for the tributary channel and the Manning's n value for the main channel.

A linear relationship was used between the volume and depth of the wetland in the HEW approach, as the surface area does not change significantly with water elevation (Wang *et al.* 2008). The normal and maximum storage of the distributed wetlands are calculated based on the geometry and mean normal and maximum water level of the HEW. The spilling of water from the HEW is controlled by $V_{nor}$ to a threshold value of $V_{mx.}$ So, it is necessary to adjust these two parameters to correctly represent the water budget of the distributed wetlands and to simulate the water fill and spill effect on streamflow. Moreover, to validate the assumed linear relationship between WET_NVOL and SA, the calibrated values of WET_NVOL were plotted against corresponding SA.

A significant outcome of the work using the HEW approach is that SWAT utilizing a wetlands module provides better streamflow simulations than SWAT without using a wetlands assumption (Wang *et al.* 2008). A satisfactory performance was found using the SWAT model with the HEW approach in the Otter Tail River watershed (Minnesota) for streamflow (daily, monthly and annual). In that study (Wang *et al.* 2008), better prediction of streamflow was noticed for upstream gauging stations than for downstream stations.

A recent study based on the HEW approach was conducted by Perez-Valdivia *et al.* (2017) for the Pipestone Creek watershed, Saskatchewan. The study found that the contribution of wetlands to runoff and streamflow on the Canadian prairies during a selected period is not obvious. Similarly, Stichling and Blackwell (1957) stated that the contributing drainage area to runoff varies with time.

Perez-Valdivia *et al.* (2017) considered a non-contributing drainage area (NCDA), which is characterized by numerous landscape depressions with no or low connectivity to the stream network. The NCDA was determined from the gross drainage area and effective drainage area of the watershed. In a normal runoff year, the wetlands in the NCDA are not expected to fill and spill, which results in no streamflow contribution from the depressions to the main channel. Further, they indicated there is a threshold water level in the wetlands and, after reaching that threshold water level, the wetlands start connecting with other wetlands and spilling downstream to the main channel. This effect of prairie wetlands is more significantly noticeable during large magnitude low-frequency runoff events (Vining 2002, Perez-Valdivia *et al.* 2017). The model was calibrated for relatively wet periods during which most of the years had larger peaks and volumes of streamflow compared to those during normal periods. The selected calibration period may be a

reason that the model had difficulty predicting streamflow for daily time steps during dry years. No water quality analysis was performed in the study.

Yang *et al.* (2010) used the HEW approach coupled with SWAT to assess the effect of wetland restoration in the Broughton's Creek watershed in western Manitoba to develop a better understanding of watershed function. The focus of the research was to check the influence of wetlands on water quantity through flood attenuation and on water quality through retention of sediment and nutrients. Sediment and nutrient (phosphorus and nitrogen) loading to the wetlands and streams was estimated based on wetland and stream drainage area as well as nutrient export coefficients. An observation from the study is that almost half of the nutrients routed to the stream were absorbed by the in-stream processes and the remaining half portion of nutrients were exported to the outlet of the watershed. Moreover, a significant amount of stream flow and nutrient reduction was noticed due to wetland restoration.

In the cases discussed above a consideration of prairie landscape depressions was attempted using the existing pond or wetland module in the SWAT model. A different approach was introduced by Evenson *et al.* (2016) that uses a "Pothole" representation that works at the HRU level instead of at the sub-watershed. Moreover, a new contributing area for simulating the watershed was introduced, which includes active fill and spill pathways of all the HRUs to the stream network. Significant improvement of seasonal streamflow was noticed; however, a huge computational capacity is required to handle thousands of HRUs created in this approach.

Nasab *et al.* (2017) introduced a Puddle Delineation (PD) algorithm coupled with SWAT (PD-SWAT). The PD algorithm also works at the HRU level and is used to quantify topographic characteristics and the hierarchical relationships of depressions. The approach is initiated by determining puddle centres, threshold elevations and the grid cells comprising each depression.

The initial steps identify the lower elevation puddles on the land surface and forms the first level of puddles. After combining several elevations of puddles, the higher elevation puddles are formed, and a hierarchical relationship is established. The relationships developed result in a drainage network that represents the hydrologic connectivity among puddles. The typical SWAT lumped approach generally overestimates the outflow discharge even when considering the depressions. However, the PD-SWAT approach significantly reduces the surface runoff considering the threshold control of depressions at the HRU level (Nasab *et al.* 2017). Nasab *et al*. (2017) stated that the depressions act as a "gatekeeper" for controlling the timing of surface runoff movement.

Probability distributed models have also been used to represent fill and spill of prairie wetland depressions (Mekonnen *et al.* 2016a). Recently, Mekonnen *et al.* (2016a-c) applied a probability distributed approach coupled with the SWAT model called SWAT-PDLD. SWAT-PDLD was used to model two large Canadian prairie watersheds and produced satisfactory results for both streamflow and water quality assessment. The focus of that study was to represent dynamic storage capacity of depressions and their impact on fill and spill phenomena. The landscape depressions receive precipitation and upland runoff from HRUs as input and evapotranspiration and seepage remove water stored in the depressions. The net amount of water from this input and output either fills or empties the depressions. The storage capacity ($c$) of a depression is a ratio of storage volume and surface area. A frequency distribution (exponential distribution) is applied in the PDLD model for representing storage capacity (volume per surface area) of depressions within the watershed.

Hossain (2017) describes a probability distribution (PDM) approach coupled with the MESH (Modelisation Environmentale Communautaire -Surface and Hydrology) model for hydrologic modelling in the Canadian prairie region. A hybrid modelling approach using MESH, PDM and

system dynamics (for lake operation), were used to simulate the natural hydrological processes on the prairies. An improved parameterization method was also developed.

A brief summary of modelling studies using SWAT and its modifications are listed in Table 2.1

### 2.2.2 Sediment and Water Quality

The prairie pothole region of North America is an area of approximately 715,000 $km^2$ (Euliss *et al.* 2002), a large portion of which is used for agricultural cropland (Messing *et al.* 2011). Due to the advancement of modern technology, the use of manure and fertilizer for crops and pasture has increased on agricultural fields (Morales-Marín *et al.* 2017). The forms and sources of nitrogen (N) and phosphorus (P) that contribute to nutrient loading vary with agricultural practices, living and dead biomass, *etc*. Nitrite ($NO_2^-$), nitrate ($NO_3^-$), ammonia ($NH_3$), and ammonium ($NH_4^+$) are the inorganic sources of N that can accumulate in prairie potholes (Neely and Baker 1989). Orthophosphate ($PO_4^{3-}$), used on agricultural land as fertilizer (inorganic form), and organic P, formed normally by biological processes acting on manure and plant matter, are the primary sources of P that accumulate in prairie potholes (Mitsch and Gosselink 1993).

Limited modelling approaches have been reported to simulate sediment and water quality in the prairie region. Most of the existing hydrological models are unable to representatively quantify sediment mobilization and nutrient export due to the complex hydrology and dynamic characteristics of landscape depressions of prairie watersheds (Mekonnen *et al.* 2016b).

To estimate upland soil erosion, the soil erodibility factor (K) is an important parameter for sediment export modelling and typically, an average annual value of soil erodibility factor is used (Wischmeier and Smith 1978). However, soil erodibility has been found to be much greater during the snowmelt period in the spring than during the summer (Wall *et al.* 1988a); therefore seasonal

Table 2.1: Summary of modelling studies using SWAT and its modifications

| No. | Study | Author(s) | Study Area | Goal | Modification |
|---|---|---|---|---|---|
| 01 | Development and Application of SWAT to Landscapes with Tiles and Potholes | Du *et al.* 2005 | Story and Boone Counties in central Iowa, USA | An enhanced SWAT model (SWAT_M) was compared to an older version of SWAT (2000) on a watershed in central Iowa. | SWAT_M |
| 02 | Using Hydrologic Equivalent Wetland Concept Within SWAT to Estimate Streamflow in Watersheds with Numerous Wetlands | Wang *et al*. 2008 | Northwestern Minnesota, USA | Introduced HEW coupled with the SWAT model and simulated the streamflow in the upper portion of the Otter Tail River watershed in northwestern Minnesota | HEW |
| 03 | Water quantity and quality benefits from wetland conservation and restoration in the Broughton's Creek Watershed | Yang *et al.* 2008 | Southwestern Manitoba, Canada | Effect of different wetland restoration scenarios on stream flow and sediment loading through HEW concept | HEW |
| 04 | Simulated environmental effects of wetland restoration scenarios in a typical Canadian prairie watershed | Yang *et al.* 2010 | Western Manitoba, Canada | Effect of different wetland restoration scenarios on stream flow and sediment using HEW concept | HEW |
| 05 | Scenarios to Investigate the Effect of Wetland Position in a Watershed on Nutrient Loadings | Melles *et al.* 2010 | South central Manitoba, Canada | Examine the relative effects of restoring drained wetland with different scenarios | N/A |
| 06 | Hydrological modeling of Alberta using SWAT Model: a preliminary report | Karim C. Abbaspour 2012 | Alberta, Canada | Quantification of Alberta's water resources including all components of the water balance at the sub-basin spatial and monthly temporal scale | N/A |
| 07 | Modelling of climate-induced hydrologic changes in the Lake Winnipeg watershed | Shrestha *et al.* 2012a | Upper Assiniboine River catchment, Manitoba, Canada | Investigation of the climate-induced hydrologic changes in two snowmelt-driven catchments using the SWAT model | N/A |
| 08 | Modeling Climate Change Impacts on Hydrology and Nutrient Loading in the Upper Assiniboine River Catchment | Shrestha *et al.* 2012b | Upper Assiniboine River catchment, Manitoba, Canada | Study on climate-induced changes in hydrologic and nutrient fluxes in the Upper Assiniboine River catchment, located in the Lake Winnipeg watershed | N/A |
| 09 | Use of the Soil and Water Assessment Tool to Scale Sediment Delivery from Field to Watershed in an Agricultural Landscape with Topographic Depressions | Almendinger *et al.* 2014 | Eastern Minnesota, USA | Investigating landscape depression influence on watershed hydrology and sediment yield | SWAT (Modification to account for surface water-groundwater interactions of ponds, wetland and reservoirs). |

Table 2.1 continued

| No. | Study | Author(s) | Study Area | Goal | Modification |
|---|---|---|---|---|---|
| 10 | An improved representation of geographically isolated wetlands in a watershed-scale hydrologic model | Evenson *et al.* 2016 | North Dakota, USA | An improved representation of GIW hydrologic processes particularly with respect to inter-GIW fill and spill hydrology | Modification of representing GIW and better simulation of fill and spill |
| 11 | Incorporated landscape depression heterogeneity into the Soil and Water Assessment Tool (SWAT) using a probability distribution | Mekonnen *et al.* 2016a | Moose Jaw River basin & Assiniboine River basin, Canada | Probability distributed model of depression storage is introduced into the SWAT model to better handle landscape storage heterogeneity | SWAT-PDLD |
| 12 | Sediment Export Modeling in Cold Climate Prairie Watersheds | Mekonnen *et al.* 2016b | Kamsack & Moose Jaw River Watershed, Canada | Application of SWAT PDLD with seasonal varying soil erodibility factor was tested to simulate daily sediment export in a cold climate prairie watershed | SWAT-PDLD |
| 13 | Modeling of nutrient export and Effects of management practices in a cold- Climate prairie watershed: Assiniboine river Watershed, Canada | Mekonnen *et al.* 2016c | Assiniboine river Watershed, Canada | Application of SWAT-PDLD model with seasonally varying soil erodibility to simulate the daily nutrient export in a cold climate prairie watershed. | SWAT-PDLD |
| 14 | Hydrological modeling of the Pipestone Creek watershed using the Soil Water Assessment Tool (SWAT): Assessing impacts of wetland drainage on hydrology | Perez-Valdivia *et al.* 2017 | Pipestone Creek Watershed, SK, Canada | Impact of wetland drainage on hydrology of prairie watershed using HEW approach | HEW |
| 15 | SWAT Modeling for Depression-Dominated Areas: How Do Depressions Manipulate Hydrologic Modeling? | Tahmasebi Nasab *et al.* 2017 | North Dakota, USA | SWAT coupled with Puddle Delineation (PD) algorithm. | PD-SWAT |
| 16 | Depressional wetlands affect watershed hydrological, biogeochemical, and ecological functions | Evenson *et al.* 2018 | North Dakota, USA | Effect of potentially vulnerable depressional wetlands influence on watershed functions | Modification of representing GIW and better simulation of fill and spill |
| 17 | SWAT Modeling of Non-Point Source Pollution in Depression-Dominated Basins under Varying Hydroclimatic Conditions | Nasab *et al.* 2018 | Red River of the North Basin (RRB), USA | To improve hydrologic and non-point source water quality modelling and calibration for depression-dominated basins under wet and dry hydroclimatic conditions | N/A |
| 18 | Assessing the Importance of Potholes in the Canadian Prairie Region under Future Climate Change Scenarios | Muhammad *et al.* 2018a | Upper Assiniboine River Basin at Kamsack, Canada. | Application of SWAT to project streamflow under the potential impacts of climate change | Geographically isolated wetlands (GIWs) module was added to the model to simulate GIWs (i.e., potholes) |

Table 2.1 continued

| No. | Study | Author(s) | Study Area | Goal | Modification |
|---|---|---|---|---|---|
| 19 | Multi-Model Approaches for Improving Seasonal Ensemble Streamflow Prediction Scheme with Various Statistical Post-Processing Techniques in the Canadian Prairie Region | Muhammad *et al.* 2018b | Upper Assiniboine River basin (UARB) at Kamsack, Saskatchewan, Canada | To improve decision-making capacity by developing a framework to evaluate the forecast skill of an ensemble of hydrologic models. | The WATFLOOD model + SWAT |
| 20 | Impact of model structure on the accuracy of hydrological modeling of a Canadian Prairie watershed | Muhammad *et al.* 2019 | Upper Assiniboine River Basin at Kamsack, Canada. | Application of SWAT with three structural variants is utilized to assess the degree of accuracy associated with increasing model complexity | SWAT (Lumped, semi and fully discretized) |

variation of the soil erodibility factor is required for water quality modelling (Dickinson *et al.* 1986). The freeze-thaw cycle plays a significant role in soil erosion (Wall *et al.* 1988a). It causes increased sediment mobilization (Dickinson *et al.* 1975, McConkey *et al.* 1996) during surface runoff in the spring due to snowmelt and limited infiltration into frozen or partially frozen soil (Granger *et al.* 1984).

Researchers suggest for cold climate regions a varying soil erodibility factor should be used for different seasons to better represent the seasonal sediment loading pattern (McConkey *et al.* 1996). Mekonnen *et al.* (2016b) introduced SWAT-PDLD with the seasonal variation of soil erodibility due to the freeze-thaw cycle for prairie watersheds. The SWAT-PDLD model was successfully calibrated and validated for sediment export for two depression dominated watersheds in the Moose Jaw and Assiniboine River basins in Saskatchewan, Canada.

The Modified Universal Soil Loss Equation (MUSLE) which is used to estimate soil erosion in the SWAT-PDLD model. The modification to represent seasonal variation was to use different soil erodibility factors (K) for the spring and summer season than for other periods of the year. Moreover, this approach also performed well for nutrient export modelling of the prairie

watersheds because nutrient (e.g. phosphorus) transport is highly connected to sediment movement (Mekonnen *et al.* 2016c).

SWAT and the HEW approach was used to examine if wetland restoration and conservation in prairie watershed can significantly reduce the sediment loading and nutrient export (Yang *et al.* 2010). However, a combined approach considering both wetland and variable stream drainage area effects with empirical nutrient export coefficients was necessary for predicting the nutrient export at the outlet of the watershed.

Application of an improved understanding of SWAT Impoundment tools (IT) and parameterization for sediment simulation has been presented by Jalowska and Yuan (2019). SWAT Impoundment tools are the default SWAT Pond or Wetland modules that can be used to provide a lumped representation of landscape depressions in a watershed. An important factor in wetland sediment export is the balance between settling of sediment and flow through removal of sediment which depends on the sediment concentration in the waterbody. SWAT utilizes an equilibrium sediment concentration concept to estimate how much sediment is trapped in the wetland. The equilibrium sediment concentration has to be specified through a calibration process of model parameters representing landscape, wetland, channel, and reservoir characteristics. Also, the fraction of the sub-basin area that drains into the wetland is a crucial factor for simulation of wetland sediment export. The study concluded that simulation of sediment export from wetlands is more sensitive to the type of impoundment rather than streamflow.

Almendinger *et al.* (2014) also emphasized the importance of parameterization for simulating sediment yield and phosphorus trapping in depression dominated watersheds. The existing SWAT pond and wetland tools were tested for different watersheds. They noted the pond module has more outflow control than the wetland module. Excessive sediment export was simulated by SWAT

when no ponds were considered. After activating the Pond or Wetland module, SWAT predicted less sediment export than without a wetland representation and better results were achieved when a calibrated parameter (USLE P) was used. They concluded it is a challenge to achieve a parameterization in standard SWAT that effectively represents ponds and wetlands in prairie watersheds, hence the depressional storage for the watershed must be represented (Almendinger *et al.* 2014).

Another study using the SWAT lumped modelling approach to assess water quality was published by Melles *et al.* (2010) for the Lake Winnipeg watershed in the prairie region. The effect of non-point source pollution from farms on nutrient loading to Lake Winnipeg was examined, and the influence of wetland restoration and positioning within the watershed was also investigated. The study results indicated that wetland restoration reduced the annual total nitrogen and total phosphorus loading significantly. Moreover, wetland position within sub-watersheds can more effectively predict nutrient loading than a single wetland position modeled at the outlet, and parameterization was a crucial factor in predicting better seasonal nutrient export. The study also found that seasonal variation of nutrient export was correlated with streamflow.

Shrestha *et al.* (2012b) conducted a study using the SWAT model in the upper Assiniboine River catchment that focused on the effect of climate change on the hydrology and nutrient loading in the prairie watershed. The study considered non-point sources as an input for nutrient modelling and tracked the transformations of several forms of nitrogen and phosphorus in HRUs of the watershed. The calibration and validation result for daily total nitrogen and total phosphorus loading were unsatisfactory according to NSE criteria; however, calibration and validation for monthly loading results was satisfactory. The authors indicated calibration of parameters for nutrient loading instead of concentration, missing observed data during low flow periods and

uncertainty in application rates of fertilizer contributed to poor calibration and validation results for daily loading.

Nutrient transport modelling studies in prairie watersheds have been reported using models other than SWAT. Two examples are presented here. Costa *et al.* (2017) introduced a hybrid modelling approach called Winter Nutrient field Transport (WINTRA), which is based on the CRHM model and several process-based algorithms that represent the snowpack and soil $NO_3^-$ interactions. The goal of this study was to simulate only field scale $NO_3^-$ during the snowmelt period in the prairie region (Stepper catchment, a sub-basin of Lake Winnipeg watershed). The study considered several phases for nitrate movement and export during the snowmelt period and implemented them through the WINTRA model. Initially, when snowmelt starts, accumulation of ions ($NO_3^-$) occurred and their concentration gradually increases in the runoff, which moves to the edge of the field. Later, a transition of the $NO_3^-$ occurred to snowpack input to the soil. Finally, when complete snowmelt occurred, $NO_3^-$ then moved to the stream from the thawing soil. The model requires hourly input climate data so that it can better capture the flow and nutrient movement; however, it is very challenging to obtain hourly data for this region. The nutrient model showed variable results (a Nash-Sutcliffe efficiency (described later in equation 4.1) of -7.03 to 0.97) depending on location and simulation period. Total nitrogen and total phosphorus loading were not assessed in the study.

Morales-Marín *et al.* (2017) published an assessment of annual nutrient loading (Total Phosphorus and Nitrogen) in a prairie basin (Lake Diefenbaker) using the SPAtially Referenced Regression On Watershed (SPARROW) model. The SPARROW model is based on nonlinear physically-based functions and applies both statistical and empirical approaches. The model requires a combination of water quality observations and high-resolution landscape information,

which makes the model time-intensive for setup. The assessment estimated that 27% of the Lake Diefenbaker catchment area consisted of non-contributing drainage areas (prairie potholes) which were disconnected from the main channel network (contributing drainage areas). Morales-Marín *et al.* (2017) considered both anthropogenic and natural sources as nutrient input to the model and reported satisfactory performance.

### 2.3 Summary

Various modelling options are available to simulate streamflow in watersheds in the prairie region. However, their performance can greatly differ depending upon the hydrology and topography of the location. The semi-distributed modelling approach is a widespread method that divides the watershed in many sub-watersheds. SWAT is a semi-distributed physically-based hydrological model that has been widely used in various types of watersheds (Gassman *et al.* 2007). Currently, SWAT is used extensively to simulate streamflow and water quality in small to major size agricultural watersheds. SWAT is also used to assess changes in streamflow and water quality due to the environmental impacts of various land uses, soil types and topography for extended time periods with varying time scales. The advantages of using the SWAT model are its wide variety of applications (Gassman *et al.* 2007) specially for incorporating ponds, usefulness for agricultural dominated areas, and open access to its source code (Neitsch *et al.* 2011).

The existence of numerous landscape depressions in the prairie region significantly affects the surface runoff and the infiltration processes (Hayashi *et al.* 2003; Hayashi *et al.* 2004). Typically, the SWAT pond module considers the depressions by aggregating all of them and applying a lumped approach per sub-basin to simulate fill and spill processes (Almendinger et al. 2014). Although this approach improves streamflow simulation the heterogeneity of the storage capacity of the depressions is not considered (Wang et al. 2008; Yang et al. 2010). Consequently, the

applicability of the standard SWAT model is challenged like other models to simulate streamflow and water quality in prairie watersheds in the depression dominated region. Attempts to consider multiple individual depressions in a hydrologic model is complex, data intensive and has a high level of computational demand. Alternatively, a probability distributed approach to consider the heterogeneity and number of depressions in a prairie watershed appears to be quite feasible (Mekonnen *et al.* 2016a).

In the study described in this thesis a modified version of the SWAT model (SWAT-PDLD) has been used where a probability distribution is incorporated into the SWAT Pond Module as in Mekonnen (2016a). This modification allows the model to consider the variable storage capacities of wetlands within sub-basins (Mekonnen *et al.* 2016a). The study further investigates the applicability of SWAT-PDLD modelling of streamflow, sediment export and nutrient export in three small prairie watersheds *i.e.* Pipestone Creek above Moosomin Lake, Swift Current Creek below Rock Creek and Lightning Creek near Carnduff.

# CHAPTER 3: STREAMFLOW AND WATER QUALITY MODELLING IN SWAT

## 3.1 Introduction

This chapter discusses the process representations used in the SWAT model to simulate streamflow and water quality. This discussion is based primarily on the Soil and Water Assessment Tool Theoretical Documentation (Neitsch *et al.* 2011), with other references provided as needed.

## 3.2 Watershed Representation

The Soil and Water Assessment Tool (SWAT) simulates hydrological processes in a watershed. SWAT partitions an overall physical watershed into several spatially explicit sub-watersheds (or sub-basins) that are spatially and hydraulically connected to the watershed main channel. The watershed and sub-watershed delineation (boundary and streamflow network) are created based on topographic analysis of a Digital Elevation Model (DEM).

Sub-basins are further divided into hydrologic response units (HRUs). An HRU is a unique combination of land use, soil texture, and land slope. Unlike a sub-watershed, an HRU is not identified spatially; rather it represents a percentage of a sub-watershed area (Gassman *et al.* 2007). A schematic depiction of how a watershed is represented in SWAT is given in Figure 3.1.

The advantages of utilizing HRUs in representing portions of watershed sub-basins include increased accuracy in export predictions from a sub-basin and better representation of the diversity of land use, slope and vegetation cover in a sub-basin (Grath 2016, Arnold *et al.* 2012).

## 3.3 Water Balance Components

Precipitation is the primary input of water into the SWAT hydrologic simulation within a watershed. Precipitation can be intercepted by vegetative and land surfaces and returned to the atmosphere via evaporation and sublimation. The remaining portions are distributed as

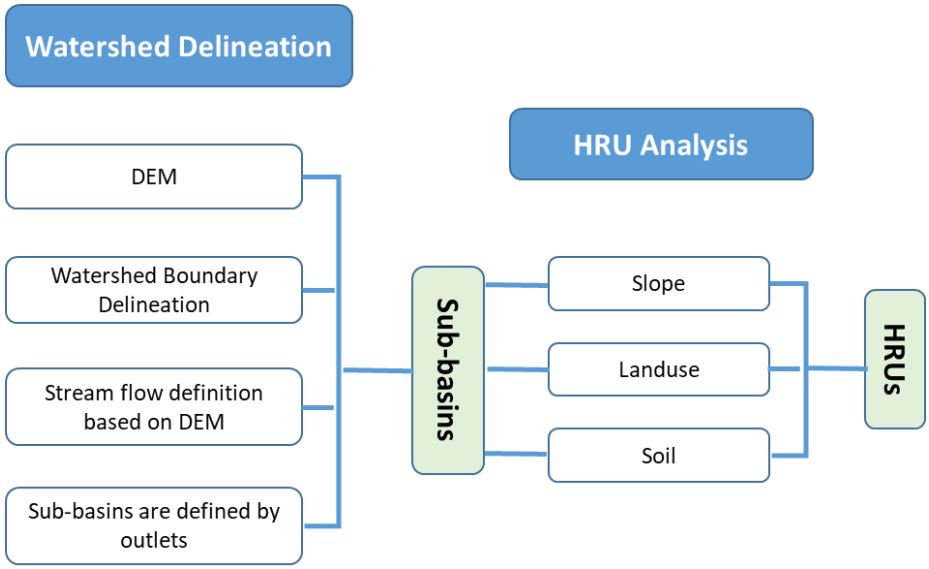


Figure 3.1: Schematic concepts of watershed delineation in the SWAT model (adapted from Grath 2016).

infiltration down through the soil profile and by lateral flow and surface runoff to the watershed stream network. Figure 3.2 shows a schematic representation of the hydrologic cycle modelled by SWAT.

The soil profile can be subdivided into multiple layers within SWAT and infiltration occurs through the soil surface to soil layers. The first soil layer receives infiltration from the soil surface and releases water as evapotranspiration, percolation to the next soil layer, and lateral flow. This process continues for each defined soil layer down to the shallow aquifer. Upward movement of water (revap) can occur from the shallow aquifer to the soil layers. The shallow aquifer can also lose water through baseflow (return flow) to the stream network and by groundwater infiltration to a deep aquifer. The potential water storage components in each HRU are the snowpack, soil profile (0-2 meters), shallow aquifer (typically 2-20 meters), and deep aquifer (more than 20 meters) (Molina-Navarro *et al.* 2016).

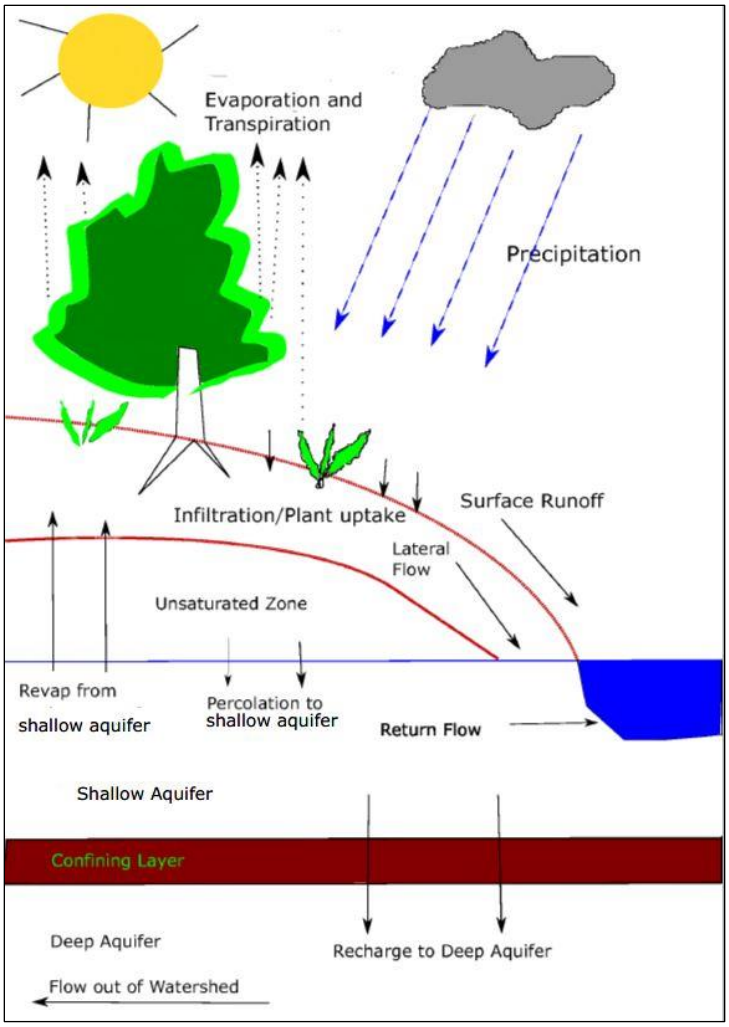


Figure 3.2: Schematic representation of the hydrologic cycle (adapted from Neitsch *et al.*, 2011).

The water storage components of each HRU and the associated water movement pathways are represented in Figure 3.3. Water balance calculations in SWAT are typically conducted on a daily time step. In Figure 3.3 on day i, P is the precipitation (mm); $P_{int}$ is precipitation intercepted and stored in the vegetation canopy, $E_{can}$ is the amount of evaporation from water stored on the vegetation canopy (mm); $P_{thr}$ is the amount of precipitation in the form of rain that is not intercepted on vegetation surfaces (mm); $S_{thr}$ is the amount of precipitation in the form of snow that is not intercepted on vegetation surfaces (mm water equivalent); $S_{pack}$ is the *snow* stored on

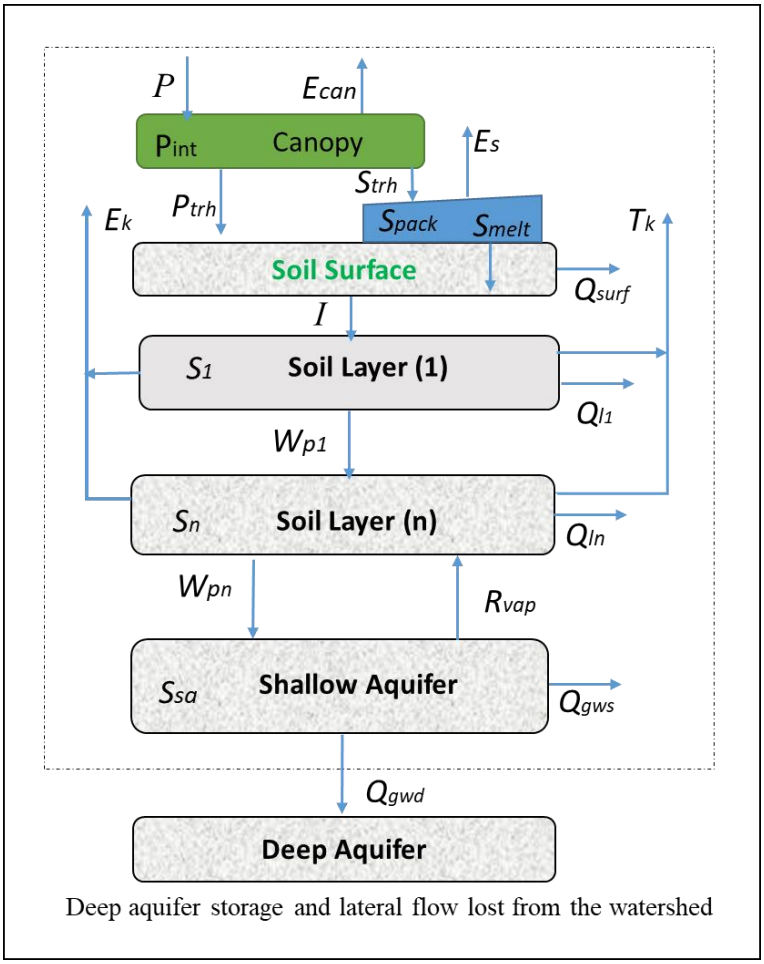


Figure 3.3: Components of the water balance representation for an HRU.

the soil surface (mm water equivalent); $S_{melt}$ is snowmelt water from the snowpack (mm); $E_s$ is the sublimation from the snowpack (if present) (mm); $T_k$ is the plant transpiration (mm) from soil layer 1 to n; $E_k$ is the amount of soil evaporation (mm) from soil layer 1 to n; $Q_{surf}$ is the amount of surface runoff (mm); $I$ is the amount of infiltration (mm) into the soil layer 1; $W_{pk}$ is the amount of water (mm) percolating from the an upper soil layer to the next soil layer or to the shallow aquifer for layers 1 to n; $S_k$ is the water stored in soil layer 1 to n (mm); $Q_{lk}$ is the lateral flow from soil layers 1 to n (mm); $R_{vap}$ is the upward movement of water from the shallow aquifer to soil layer $k$ (mm); $S_{sa}$ is the water stored in the shallow aquifer (mm); $Q_{gws}$ is the baseflow from the shallow

aquifer (mm); and $Q_{gwd}$ is groundwater recharge to the deep aquifer (mm) that is lost from the watershed.

All SWAT model computations are performed at the HRU level (Arnold *et al.* 2012). Runoff, lateral flow and return flow (the water returning from the shallow aquifer to streamflow) are estimated for each HRU within a sub-basin and added together to calculate the daily contribution of a sub-basin to the stream network (Bioteau *et al.* 2002, Mendes *et al.* 2006). In standard versions of SWAT there are no interactions between HRUs in a sub-basin.

The water balance calculations are done for the "Land Phase" of the model and then the runoff, lateral flow and return flow is routed through the stream network (the "Routing Phase" of the model). The routing phase deals with the movement of water, sediments, and other water quality constituents through the channel network to the watershed outlet.

### 3.4 Components of the HRU Water Balance

#### 3.4.1 Precipitation

Precipitation includes both rainfall and snowfall (expressed as water equivalent). The SWAT model decides whether to represent the precipitation as rainfall or snow based on the mean daily temperature. If the daily mean air temperature is less than 0 °C, it is often assumed that precipitation falls as snow. Further, snow is generally assumed to melt on days when the maximum temperature exceeds 0 °C. However, in reality, both snowfall and snow melt temperature is not exactly 0 °C and can be varied within the model. In a cold climate region, snow is a major contributor to the total annual precipitation and strongly influences the surface and subsurface hydrological cycles (Faria *et al.* 2000).

SWAT only considers data from a single precipitation gauge station that is nearest to the centroid of each sub-basin (Tuo *et al.* 2016). Later, SWAT reads a data file with daily precipitation readings as well as the maximum and minimum daily temperatures for each sub-basin which are distributed to corresponding HRUs within the sub-basin. The model partitions the precipitation (rainfall/snowfall) between that intercepted and held in the vegetation canopy (and eventually lost to evaporation) and the amount that falls to the soil surface.

## 3.5 Vegetation Canopy Storage and Evaporation

### 3.5.1 Canopy Interception and Storage

Precipitation first contacts the plant canopy, which traps a significant portion of rainfall as well as snowfall, and releases the remaining precipitation to the soil surface. The density of plant cover influences the interception process and also reduces the erosive energy of droplets. Therefore, canopy interception is a primary function that affects infiltration, surface runoff, and evapotranspiration.

### 3.5.2 Evaporation of Canopy Intercepted Rainfall

SWAT simulates evaporation of precipitation that has been intercepted and stored in the plant canopy. The amount of water it removes from canopy storage each day is based upon potential evapotranspiration ($E_o$). If $E_o$ is less than the amount of free water held in the plant canopy, then

$$E_{can} = E_o \tag{3.1}$$

$$R_{int(f)} = R_{int(i)} - E_{can} \tag{3.2}$$

where $E_{can}$ is the amount of evaporation from free water held in the canopy on a given day (mm), and $R_{int\,(i)}$ and $R_{int\,(f)}$ are the initial and final amount of free water held in the canopy on a given day (mm) respectively. If $E_o$ is greater than the amount of free water held in the canopy, then

$$E_{can} = R_{int(i)} \tag{3.3}$$

$$R_{int(f)} = 0 \tag{3.4}$$

### 3.6 Snowpack Storage and Snowmelt

Snowfall is accumulated on the land surface as a snowpack; the amount of water stored there is calculated via a snow-water equivalent. The depth and water content of the snowpack increases following additional snowfall and will decrease via melt or sublimation. The snowpack storage component of SWAT can be set to a simple, uniform snow cover model or a more complex model that allows non-uniform cover due to shading and drifting to be represented (Neitsch *et al.* 2011). Snowmelt is included with rainfall in the calculation of runoff and percolation.

Snowmelt in SWAT is calculated as a linear function of the average snowpack depth, maximum air temperature and a base temperature for snowmelt. The standard equation used in SWAT to estimate snowmelt is:

$$SNO_{melt} = b_{melt} \,.\, sno_{cov} \,.\, (\frac{T_{snow}+T_{mx}}{2} - T_{melt}) \tag{3.5}$$

where $SNO_{melt}$ is amount of snowmelt on a given day (mm $H_2O$), $b_{melt}$ is the melt factor for the day (mm $H_2O$/day-$^oC$), $sno_{cov}$ is the fraction of the HRU area covered by snow, $T_{snow}$ is the snowpack temperature on a given day ($^oC$), $T_{mx}$ is the maximum air temperature on a given day ($^oC$) and $T_{melt}$ is the base temperature ($^oC$) above which snowmelt will occur.

The melt factor varies seasonally with the maximum and minimum values in summer and winter respectively. In rural areas, the melt factor varies from 1.4-6.9 mm $H_2O$/day-$^oC$ (Huber and Dickinson 1988), whereas urban areas have a higher melt factor (3.0-8.0 mm $H_2O$/day-$^oC$) due to compression of snowpack by traffic and pedestrians.

The snowpack temperature ($T_{snow}$ ) is a function of mean daily air temperature during preceding days. A lagging factor is used to combine the previous and current day's snowpack temperature.

### 3.7 Evapotranspiration from Soil Layers

Evapotranspiration is a crucial factor in determining water loss from the watershed and a major component of the water balance. It is a term that combines evaporation from the soil layers and transpiration from plants. Evaporation is the process of transforming available surface water to vapor, whereas transpiration is a similar process that only occurs through the plant body in the presence of sunlight (Pidwirny 2006). A representation of evaporation and transpiration is presented in Figure 3.4.

A large amount of water is returned to the atmosphere through evapotranspiration. While $E_o$ is an estimation of the theoretical maximum potential to remove water, the Actual Evapotranspiration (AET) is the quantity of water actually removed from the soil layers and soil surface. AET consists of transpiration from vegetation growth in the soil, evaporation of water held within the soil, and sublimation of water from the snowpack (if present) on the soil surface. AET is calculated by SWAT after the determination of $E_o$ and the canopy evaporation $E_{can}$. The remaining potential water demand after accounting for water lost in the vegetation canopy is given by:

$$E_d = E_o - E_{can} \tag{3.6}$$

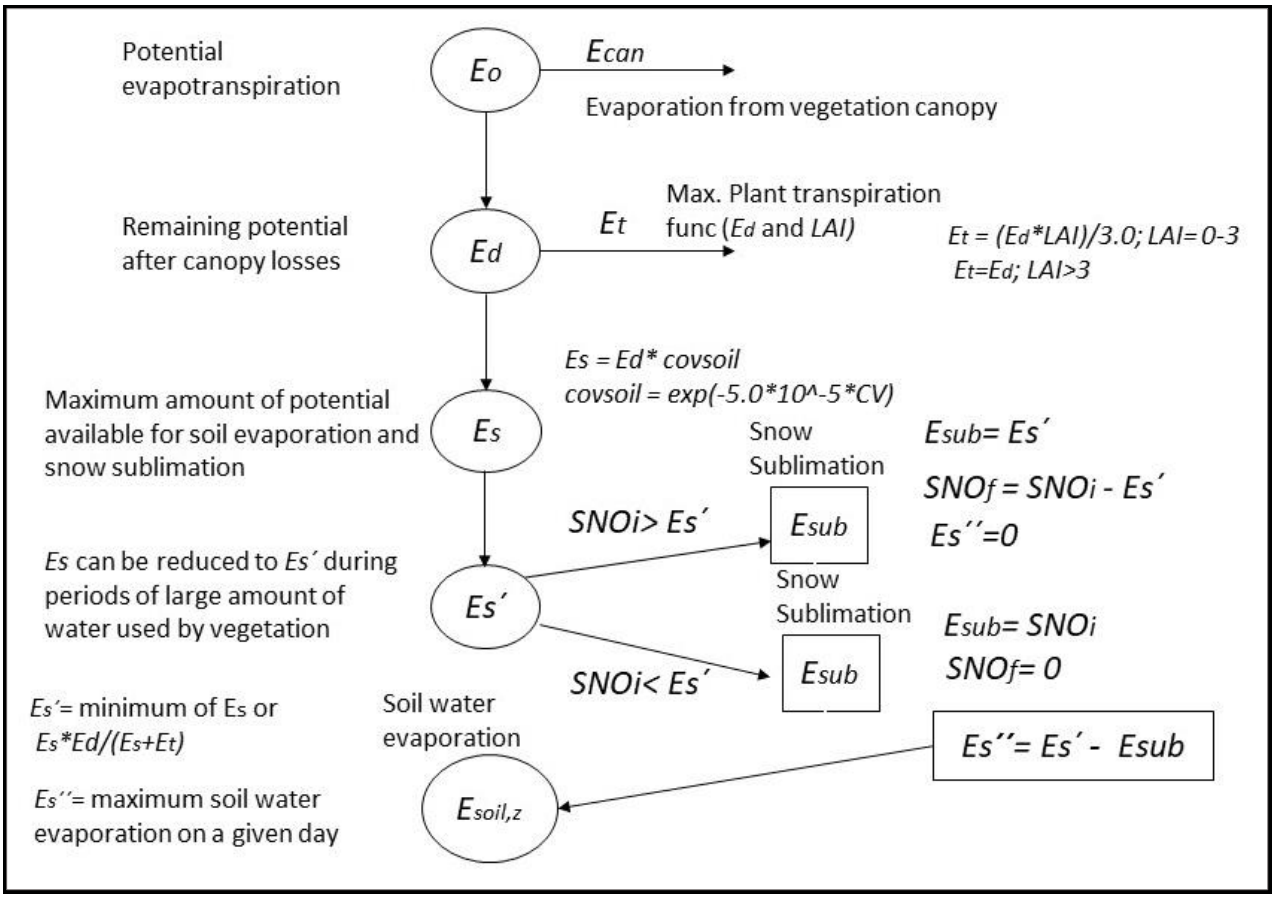


Figure 3.4: Evaporation (canopy and soil) and transpiration (plant) process in SWAT.

where $E_d$ is the potential evapotranspiration adjusted for evaporation of free water from the vegetation canopy (mm $H_2O$). SWAT estimates the plant transpiration, snowpack sublimation and soil evaporation in succession based upon vegetation, snowpack and soil profile characteristics to calculate AET following the method of Ritchie (1972).

### 3.7.1 Potential Evapotranspiration (PET)

Potential Evapotranspiration is an estimate of the theoretical maximum water demand by the environment in the presence of a sufficient water source. According to Soil Science of America (2008), Potential Evapotranspiration ($E_o$) is a loss of water by evaporation from the soil surface and by transpiration from plants for a given area during a specified period. SWAT provides three

alternative methods to estimate Potential Evapotranspiration ($E_o$) among which the Hargreaves method is the most convenient to use because it requires only temperature data. The other two more comprehensive methods are the Penmen-Monteith and the Priestley-Tylor, which each require input data such as solar radiation, wind speed, and relative humidity in addition to temperature.

The Hargreaves method is:

$$\lambda E_o = 0.0023 * H_o * (T_{mx} - T_{mn})^{0.5} * (T_{av} + 17.8) \quad (3.7)$$

where $\lambda$ is the latent heat of vaporization (MJ kg$^{-1}$), $E_o$ is the potential evapotranspiration (mm d$^{-1}$), *Ho* is the extraterrestrial radiation (MJ m$^{-2}$ d$^{-1}$), $T_{mx}$ is the maximum air temperature for a given day ($^o$C), $T_{mn}$ is the minimum air temperature for a given day ($^o$C), and $T_{av}$ is the mean air temperature for a given day ($^o$C). In this study, the Hargreaves method will be used to calculate PET.

### 3.7.2 Transpiration

As noted above, the Hargreaves equation will be used to estimate PET in this research. When the Hargreaves method and Priestley-Taylor method are used for calculating PET, SWAT calculates transpiration using the following equations:

$$E_t = \frac{E_d * LAI}{3.0} \quad 0 \leq LAI \leq 3.0 \quad (3.8)$$

$$E_t = E_d; \quad LAI > 3.0 \quad (3.9)$$

where $E_t$ is the maximum transpiration on a given day (mm $H_2O$), $E_d$ is the potential evapotranspiration adjusted for evaporation of free water in the canopy (mm $H_2O$), and *LAI* is the vegetation leaf area index. The *LAI* is the ratio of the one-sided developed area of green leaves per

unit land surface area which is an important parameter that characterizes the plant canopy structure (Zhao *et al.* 2012). The *LAI* expresses the amount of foliage and is an indicator of plant capacity for transpiration and capture of sunlight through the canopy (Zhao *et al.* 2012).

### 3.7.3 Sublimation and Evaporation

The amount of soil evaporation and snowpack sublimation is affected by vegetation shading of the land surface. The equation for the maximum potential for sublimation or soil evaporation ($E_s$) on a given day is:

$$E_s = E_d * covsoil \quad (3.10)$$

where *covsoil* is the soil cover index. The soil cover index is a function of above ground biomass and crop residue. The amount of sublimation or soil evaporation reduces due to higher amount of aboveground biomass and vice versa. The maximum potential for sublimation ($E_s$) can be reduced to a minimum amount ($E_s'$ ) during periods of large amount of water used by vegetation. The equation of $E_s'$ is:

$$E_s' = E_s * E_d / (E_s + E_t) \quad (3.11)$$

#### 3.7.3.1 Sublimation

After calculating the maximum potential for sublimation or soil evaporation ($E_s$) for a day, SWAT tries to meet the evaporative demand first by removing water from the snowpack. When the existing water content of the snowpack is higher than the potential sublimation or the soil evaporation demand, the amount of sublimation ($E_{sub}$) on a given day (mm $H_2O$) is:

$$E_{sub} = E_s' \quad (3.12)$$

where $E_s'$ is the maximum sublimation/soil evaporation adjusted for plant water use on a given day (mm $H_2O$). If the existing water content of the snowpack is less than the sublimation or soil evaporation demand then:

$$E_{sub} = SNO_{(i)} \quad (3.13)$$

where $SNO_{(i)}$ is the amount of water in the snowpack on a given day before considering for sublimation (mm $H_2O$).

### 3.7.3.2 Evaporation

If the sublimation/soil evaporative maximum potential exceeds the estimated amount of sublimation, then SWAT partitions the remaining potential to the soil layers for water loss by evaporation. The amount of soil evaporative loss is determined as a function of soil depth as follows:

$$E_{soil,z} = E_s'' * \frac{z}{z+\exp(2.374-0.00713*z)} \quad (3.14)$$

where $E_{soil,z}$ is the soil evaporative demand at depth z (mm $H_2O$), $E_s''$ is the maximum potential for soil water evaporation on a given day (mm $H_2O$), and z is the depth below the surface. It is worth noting that the vast majority of the evaporative demand occurs in the near surface portion of the soil profile. The amount of evaporative demand for an individual soil layer is the difference between evaporative demands of the upper and lower boundaries of soil layer.

## 3.8 Infiltration

Infiltration is the entry of water into the upper soil layer through the soil surface. Infiltrated water supplies plant demand for growth and recharges aquifers. The infiltration rate depends on the rainfall intensity or rate of snowmelt, vegetation cover, soil permeability, soil temperature and

initial moisture content. Within SWAT the volume of infiltration can be calculated directly based upon soil characteristics and rainfall intensity, or estimated as the difference between the amount of precipitation reaching the soil surface and surface runoff. The second approach using the SCS curve number method within SWAT is used in this research project (see Section 4.7.2 below). Direct calculation of infiltration within SWAT using the Green and Ampt method can be conducted if sub-hourly precipitation data is available.

## 3.9 Surface Runoff

### 3.9.1 Background

Surface runoff ($Q_{surf}$) occurs when the rate of precipitation received at the soil surface and/or rate of snowmelt exceeds the infiltration capacity of the soil . Low infiltration capacity may occur due to high antecedent soil moisture content, limited soil water storage capacity, frozen soil, or low physical permeability of the soil (Beven 2000). Vegetation cover and the magnitude of the land slope are other factors that influence surface runoff (Hofmann *et al.* 1983, Rehman *et al.* 2015) .

SWAT enables the user to calculate surface runoff using the Soil Conservation Service (SCS) curve number method or the Green and Ampt infiltration method. The first approach can determine surface runoff directly based on precipitation, canopy storage, surface storage, infiltration and soil moisture. On the other hand, the Green and Ampt infiltration method determines surface runoff indirectly by subtracting infiltration from precipitation and meltwater on the soil surface. However, in Green and Ampt method, the canopy storage model must be considered separately. SWAT calculates the maximum canopy storage available in a vegetation growth cycle based on the leaf area index. The SCS curve number method requires daily precipitation data to determine surface

runoff, whereas the Green and Ampt infiltration method needs sub-daily data, which is unavailable for this study.

### 3.9.2 SCS Curve Number Method

The SCS curve number is a function of soil permeability, land use and antecedent soil moisture. In the curve number method, the curve numbers vary non-linearly with the moisture content of the soil. The curve number decreases as the soil moisture approaches the wilting point and increases when the soil moisture approaches saturation. For estimation of runoff over frozen soil, SWAT makes a provision that, below 0˚C (in first soil layer), runoff increases but significant infiltration can also occur in dry frozen soil.

The daily surface runoff calculation based upon SCS curve number is

$$Q_{surf} = \frac{(P-I_a)^2}{P-I_a+S} \tag{3.15}$$

$$S = 25.4\left(\frac{1000}{CN} - 10\right) \tag{3.16}$$

where $Q_{surf}$ is daily surface runoff (mm $H_2O$), $P$ is the total precipitation depth for the day (mm $H_2O$), $I_a$ is the initial abstractions that consist of surface storage, interception and infiltration prior to runoff (mm $H_2O$), $S$ is the retention parameter (mm $H_2O$) and $CN$ is the curve number for the day.

In urban and rural areas, the curve number varies based on land use and soil permeability. Soils are classified based on infiltration rate (their drainage capacity) and sorted into hydrologic soil groups. A lower curve number is used for the soils that have very high infiltration rates (*e.g.*, hydrologic soil group A) and vice versa. However, the same hydrologic soil group may have different curve numbers for different land uses and hydrologic conditions. Normally, the bare soil

and urban developed areas (paved) have higher curve numbers than agricultural fields or grasslands.

SWAT determines the initial abstractions ($I_a$) based on the amount of evaporation from canopy ($E_{can}$), maximum amount of transpiration ($E_t$), maximum amount of sublimation ($E_s$) and soil water evaporation ($E_{soil}$). It is worth noting that surface runoff will only occur when $P > I_a$.

### 3.9.3 Lateral Subsurface Flow

Interflow or lateral subsurface flow originates below the soil surface and above the vadose zone. Lateral subsurface flow contributes to the streamflow within the watershed and is significant in areas having high hydraulic conductivity and a semipermeable or impermeable soil layer at a shallow depth in the soil profile (Neitsch *et al.* 2011). Water can accumulate above the impermeable layer forming a saturated zone of water that acts as a source of lateral subsurface flow (Neitsch *et al.* 2011).

Lateral subsurface flow is calculated simultaneously with redistribution. Redistribution is the continuous movement of water through a soil profile after input of water has suspended and continues until the water content throughout the soil profile is uniform. It occurs in a soil profile when the soil temperature is above 0$^{o}$C. The redistribution technique of SWAT uses a storage routing technique to predict flow through each soil layer in the root zone. A kinematic storage model developed by Sloan and Moore (1984) is used in SWAT to predict lateral flow in each layer of soil. The model is sensitive to variation in soil conductivity, slope, and soil water content. The model considers a two dimensional cross-section along a flow path down a steep hill slope to simulate the subsurface flow. The model is based on a mass water balance with the entire hillslope segment used as the control volume.

### 3.10 Percolation

Water in the soil can flow under saturated or unsaturated conditions. SWAT can directly model only saturated flow which is driven by gravity and usually occurs in the downward direction (known as percolation). SWAT assumes uniform flow distribution within a given layer. However, SWAT records the water content of different soil layers. Percolation is calculated for each soil layer in the profile. The equation for percolation is

$$w_{perc,ly} = SW_{ly,excess} \cdot (1 - e^{\frac{-\Delta t}{TT_{perc}}}) \quad (3.17)$$

where $w_{perc,ly}$ is the amount of water percolating to the underlying soil layer on a given day (mm $H_2O$), $SW_{ly,excess}$ is the drainable volume of water in the soil layer on a given day (mm $H_2O$), $\Delta t$ is the length of time steps (hrs), and $TT_{perc}$ is the travel time for percolation (hrs) depends on water content in the soil layer when completely saturated (mm $H_2O$) as well as at field capacity (mm $H_2O$) and saturated hydraulic conductivity for the layer (mm/h) .

No percolation is allowed from a soil layer if the temperature in the layer is 0°C or below. Lateral subsurface flow in the soil profile is calculated simultaneously with percolation (Manel and Mosbahi 2012). The portion of water that percolates out of the lowest layer of soil enters the vadose zone, which is an unsaturated zone between the bottom of the soil profile and the top of the aquifer.

### 3.11 Return Flow

A portion of precipitation ultimately recharges the groundwater aquifers after percolating through the soil layer(s). Base flow or return flow is the amount of groundwater that contributes to streamflow. SWAT partitions groundwater into a shallow aquifer and a deep aquifer and simulates both aquifers. The shallow aquifer is an unconfined aquifer that contributes to the

streamflow in the main channel within the watershed. However, the deep aquifer is a confined aquifer that contributes to streamflow outside of the watershed. The shallow aquifer contributes base flow to the reach when the amount of water stored in shallow aquifer exceeds a threshold value.

### 3.12 Water Storages

#### 3.12.1 Soil Water Content

For each HRU, SWAT provides a continuous daily simulation of the overall water budget that includes runoff, precipitation, interception, infiltration, snowmelt, redistribution of groundwater between zones (*e.g.*, shallow to deep aquifers), and evapotranspiration (Figure 3.3). The daily change in storage from an HRU (assuming a single soil layer) is given as:

$$\Delta S = P - ET_a - Q_{sur} - Q_l \ - w_p - Q_{gws} \quad (3.18)$$

$\Delta S$ is the change in water storage of the HRU on day i (mm); $ET_a$ is the amount of evapotranspiration on day i (mm); $Q_{sur}$ is the amount of surface runoff on day i (mm); $Q_l$ is the lateral flow on day i (mm); $w_p$ is the amount of water percolating to the underlying soil layer on day i (mm) and $Q_{gws}$ is the base flow from the shallow aquifer on day i (mm).

The active processes in the soil profile are infiltration, evapotranspiration, withdrawal by plants, lateral outflow and outflow toward the lower horizons. In the SWAT model, the overall water balance for the soil component of each HRU is represented as:

$$SW_t = SW_0 + \sum_{i=1}^{t} (\mathrm{P} - ET_a - Q_{sur} - Q_l - Q_{gws}) \quad (3.19)$$

where $SW_t$ is the final soil water content (mm $H_2O$), $SW_0$ is the initial soil water content on day 0 (mm $H_2O$), $t$ is time (days). SWAT has the capability to represent multiple soil layers in the HRU

water balance if increased complexity is required. The total flow predicted from an HRU which contributes to the streamflow on day i can be represented as:

$$Q = Q_{sur} + Q_l + Q_{gws} \quad (3.20)$$

where *Q* is the total flow leaving the HRU on day i (mm).

### 3.13 Water Quality

Water quality modeling in SWAT mainly includes simulation of sediment loading and adsorbed nutrient transport due to soil erosion, application of fertilizer on agricultural fields and subsequent dissolution in surface and subsurface runoff (as non-point sources), and wastewater discharges into streams and waterbodies (as point-sources).

### 3.14 Sediment Transport

Soil erosion is a result of the detachment of soil particles due to the erosive force of raindrops and surface runoff. The soil particles transport to small rills and finally reach a continuously-flowing stream or river. Sediment particles can also transport nutrients (N and P) (Novotny 2003, Mekonnen *et al*. 2016b). SWAT uses the Modified Universal Soil Loss Equation (MUSLE) (Williams 1975) to compute erosion that occurred in the watershed by rainfall and runoff. MUSLE uses a runoff factor instead of rainfall energy as in the original USLE. The MUSLE equation is:

$$sed = 11.8\left(Q_{surf} q_{peak} area_{hru}\right)^{0.56} K_{USLE} C_{USLE} P_{USLE} LS_{USLE} CFRG \quad (3.21)$$

where $sed$ is the sediment yield on a given day (metric tons), $Q_{surf}$ is the surface runoff volume (mm$H_2O$/ha), $q_{peak}$ is the peak runoff rate ($m^3$/s), $area_{hru}$ is the area of the HRU (ha), $K_{USLE}$ is the USLE soil erodibility factor (0.013 metric ton $m^2$ hr/($m^3$-metric ton cm)), $C_{USLE}$ is the USLE cover and management factor (dimensionless), $P_{USLE}$ is the USLE support practice factor

(dimensionless), $LS_{USLE}$ is the USLE topographic factor (dimensionless) and $CFRG$ is the coarse fragment factor (dimensionless).

The soil erodibility factor has an important influence on the amount of soil erosion even if all other factors remain constant. This factor depends on soil properties but also varies seasonally (McConkey *et al*. 1996) The standard version of SWAT uses an average value of $K_{USLE}$ for all seasons for a specific type of soil. SWAT-PDLD, used in this research, uses seasonal soil erodibility values and this will be discussed in Chapter 4.

The cover and management factor ($C_{USLE}$) represents the effect of plant canopy on erosion by reducing the effective rainfall energy of intercepted raindrops. The support practice factor ($P_{USLE}$) is used for measuring soil loss for specific support practice (*e.g.* contour tillage, strip-cropping *etc.)* with up and down slope culture. During low to moderate intensity storms, contour tillage and planting provides protection against erosion however they failed during occasional severe storms. According to Wischmeier and Smith (1978) contour tillage is effective on slopes of 3 to 8 percent.

### 3.15 Nutrient Transport

Nutrient transport is the movement of nutrient compounds in soil and water in a watershed and involves the transformation of those compounds as they move through the soil and water environment. The nutrient cycle for nitrogen and phosphorus in SWAT is simulated at the HRU level. The nutrient transport modelling is discussed below as a background for the total nitrogen and total phosphorus loading that has been conducted in this study.

### 3.15.1 Nitrogen

#### 3.15.1.1 Nitrogen Cycle

Nitrogen is the most abundant gaseous element in nature which is also required for plant growth. The gaseous form of nitrogen is unusable to plants so it must be converted to a usable form (*i.e.* $NH_4^+$ and $NO_3^-$ *etc*.) in the soil by microorganisms which is called fixation. The fixed nitrogen can be absorbed by plants. Nitrogen re-enters the soil as an organic form from plant residue and animal waste as a part of decomposition. The decomposition process releases ammonia and triggers the nitrification process which converts ammonium to nitrite and nitrate. Moreover, ammonia and nitrate can be added to the soil through fertilizer application. Plants uptake these nitrogen forms from the soil. Finally, nitrogen gas can be released to atmosphere by transforming nitrate through the denitrification process to complete the nitrogen cycle.

Nitrogen is mainly present in three pools in a soil profile: organic forms associated with humus, mineral forms held by soil colloids, and mineral forms in solution (Gorham 1991, Groenigen *et al*. 2015, Berg and Meehan 2017). The input of nitrogen into the soil can happen by rainfall, fertilizer, manure, or residue application, and fixation by bacteria (Groenigen *et al*. 2015). The removal of nitrogen occurs mainly by plant uptake, leaching, volatilization, denitrification, and erosion (Groenigen *et al.* 2015).

Nitrogen chemical species are extremely reactive and soluble in water (Berg and Meehan 2017), which makes them highly mobile and it is challenging to predict movement between different pools and conversion between forms in the soil (Berg and Meehan 2017). SWAT considers five different forms of nitrogen (Figure 3.5) including both organic and inorganic ($NH_4^+$ and $NO_3^-$) forms in the soil. Fresh plant residue is converted to humic substances (organic

compounds of soil) via microbial and other organisms decomposition processes in the soil. This conversion happens first to stable humic substances and then to the active humic substance which leads to mineralization that produces $NH_4^+$ and $NO_3^-$.

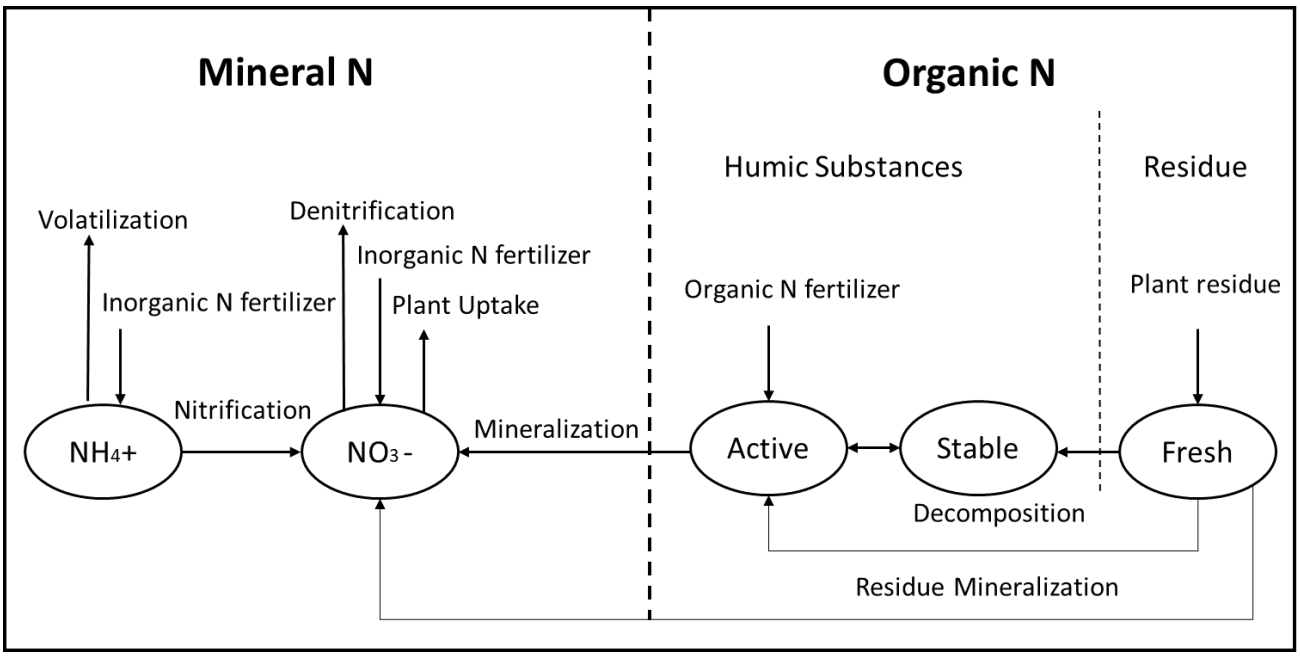


Figure 3.5: SWAT soil nitrogen forms and the process of N conversion (adapted from Neitsch *et al*. 2011)

### 3.15.1.2 Initialization of Soil Nitrogen Levels

SWAT can initialize the total concentration of nitrate ($NO_3$) in different pools in each of the soil layers with a default value at the beginning of the simulation if initial nitrate concentration is unavailable. There is a developed relationship of nitrate concentration with depth. The equation used to represent the distribution of initial nitrate concentration over the soil depth is

$$NO3_{conc,z} = 7 * exp((-z)/1000) \quad (3.22)$$

where $NO3_{conc,z}$ is the concentration of the nitrate in the soil at depth *z* (mg/kg or ppm) and z is the depth from the soil surface (mm).

The equation used to estimate of the amount of organic nitrogen in the form of soil humus is:

$$orgN_{hum,ly} = 10^4 \left(\frac{orgC_{ly}}{14}\right) \quad (3.23)$$

where $orgN_{hum,ly}$ is the concentration of humic organic nitrogen in the layer (mg/kg or ppm) and $orgC_{ly}$ is the amount of organic carbon in the layer (%). Organic carbon has been specified for each soil layer in the soil database.

Nitrogen in the fresh organic pool is calculated for the top 10 mm of the soil profile only using Equation 3.24 and varies with HRU:

$$orgN_{fsh,surf} = 0.0015 * rsd_{surf} \quad (3.24)$$

where $orgN_{fsh,surf}$ is the nitrogen in the fresh organic pool in the top 10 mm (kg N/ha), and $rsd_{surf}$ is material in the residue pool for the top 10 mm of soil (kg/ha) which varies with HRU.

The ammonium ($NH_4^-$) pool for soil nitrogen is considered 0 ppm initially.

#### 3.15.1.3 Atmospheric Deposition of Nitrogen

For wet deposition of nitrogen, the absorption of $NH_4^+$ and $NO_3^-$on soil particle surfaces and in water through precipitation input is defined as the wet deposition of nitrogen (Erisman and Draaijers 1995). Atmospheric nitrogen is converted to nitric acid in presence of lightning discharge (Franzblau and Popp 1989) and added to the soil during rainfall. The amount of wet nitrogen deposition range from 5-11 kg N $ha^{-1}$ $yr^{-1}$ across the Great Plains *i.e.* Alberta, Saskatchewan and Manitoba (Köchy and Wilson 1997).

The amount of nitrate added to the soil through precipitation and wet deposition is estimated with the following equations:

$$NO3_{rain} = 0.01 * R_{NO3} * R_{day} \quad (3.25)$$

where $NO3_{rain}$ is nitrate added by rainfall (kg N/ha), $R_{NO3}$ is the concentration of nitrogen in the rain (mg N/L) and $R_{day}$ is the amount of precipitation on a given day ($mmH_2O$). The default value of $R_{NO3}$ in SWAT is 1.0 mg N/L.

In dry deposition of nitrogen, deposition results from the direct input of particulate materials containing $NH_4^+$ and $NO_3^-$ to water or vegetation surfaces (Erisman and Draaijers 1995). However, information related to dry deposition rates are not well defined in most of the studies. The amount of total nitrogen deposition (combination of wet and dry deposition) rate in southern Ontario has found 15 kg N/ha/yr. In SWAT, an average daily dry deposition is applied to the soil surface for each sub-basin.

#### 3.15.1.4 Decomposition and Mineralization of Nitrogen

Decomposition is the breakdown of fresh organic plant residue into simpler organic components (Gorham 1991). Mineralization is the transformation of the simpler plant-unavailable organic nitrogen compounds to inorganic nitrogen compounds that are available for plant uptake (Berg and Meehan 2017). In SWAT, decomposition and mineralization of the fresh organic nitrogen pool is only simulated in the first soil layer.

#### 3.15.1.5 Nitrification and Ammonia Volatilization

Nitrogen can be added to the soil in both organic and inorganic forms. However, plants can only uptake nitrogen in inorganic forms (Berg and Meehan 2017). Inorganic nitrogen fertilizer can be added to soil as ammonia or as nitrate. The transformation of ammonia to nitrate via nitrite is a two-step process called nitrification (Berg and Meehan 2017). Ammonia volatilization is the gaseous loss of ammonia during surface application of ammonia fertilizer to a calcareous soil

(Berg and Meehan 2017). SWAT simulates both processes using combined methods developed by Reddy *et al.* (1979) and Godwin *et al.* (1984).

### 3.15.1.6 Nitrate Movement

Minerals in soil are mainly negatively charged at normal pH. Under normal soil conditions nitrate anions are repulsed from soil particle surfaces (Berg and Meehan 2017). Further nitrate anions are excluded from particle surfaces due to the attraction of cations (*e.g.* $Na^+$, $K^+$) which has a direct impact on the transport of $NO_3^-$ through the soil (Jury *et al.* 1991). SWAT considers nitrate mobilization from soil surfaces by surface runoff, lateral flow or percolation. The equation used to simulate nitrate partitioning and export in surface runoff is:

$$NO3_{surf} = \beta_{NO3} * conc_{NO3,mobile} * Q_{surf} \quad (3.26)$$

where $NO3_{surf}$ is the nitrate removed in surface runoff (kg N/ha), $\beta_{NO3}$ is the nitrate percolation coefficient, $conc_{NO3,mobile}$ is the concentration of nitrate in the mobile water for the top 10 mm of soil (kg N/mm$H_2O$) and $Q_{surf}$ is the surface runoff generated on a given day (mm $H_2O$).

The equations describing nitrate export in lateral flow are:

$$NO3_{lat,ly} = \beta_{NO3} * conc_{NO3,mobile} * Q_{lat,ly} \text{ (for top 10 mm)} \quad (3.27)$$

$$NO3_{lat,ly} = conc_{NO3,mobile} * Q_{lat,ly} \text{ (for lower layers)} \quad (3.28)$$

where $NO3_{lat,ly}$ is the nitrate removed in lateral flow (kg N/ha) and $Q_{lat,ly}$ is the water discharged from the soil layer by lateral flow (mm$H_2O$).

Nitrate movement to the underlying soil layer through percolation is calculated by Equation 3.29

$$NO3_{perc,ly} = conc_{NO3,mobile} * w_{perc,ly} \quad (3.29)$$

where $NO3_{perc,ly}$ is the nitrate moved to the underlying layer by percolation (kg N/ha) and $w_{perc,ly}$ is the amount of water percolating to the underlying soil layer on a given day (mm$H_2O$).

### 3.15.1.7 Organic Nitrogen Movement

Organic nitrogen is associated with the sediment loading from the HRU and transported by surface runoff to the main channel. Changes in sediment loading will affect the organic nitrogen loading hence organic N is not instantly soluble in water and major portions move with soil particles (Burwell *et al*. 1977). The amount of organic nitrogen transported with sediment to the stream is estimated by the following equation:

$$orgN_{surf} = 0.001 * conc_{orgN} * \frac{sed}{area_{hru}} * \varepsilon_{N;sed} \quad (3.30)$$

where $orgN_{surf}$ is the amount of organic nitrogen transported to the main channel in surface runoff (kg N/ha), $conc_{orgN}$ is the concentration of organic nitrogen in the top 10 mm soil layer (g N/metric ton soil), $sed$ is the sediment yield on a given day (metric tons), $area_{hru}$ is the HRU area (ha), and $\varepsilon_{N;sed}$ is the nitrogen enrichment ratio. The enrichment ratio is defined as the ratio of organic nitrogen concentration that is transported with the sediment to the concentration of organic nitrogen in the soil surface layer.

### 3.15.1.8 Leaching of Nitrogen

Leaching of nitrogen is the loss of nitrogen with water moving downward through the soil profile (Berg and Meehan 2017). The positively charged (cations) plant essential nutrients are attracted and sorbed to negatively charged soil particles. After plants extract cations from the soil solution, soil particles release cations to soil pore water to bring it back into nutrient equilibrium.

On the other hand negatively charged (anion) nitrate is not attracted or sorbed by soil particles. Therefore, nitrate has high tendency to leach (Berg and Meehan 2017). SWAT uses the same algorithm to calculate nitrate leaching that is used for loss of nitrate in surface runoff and lateral flow.

#### 3.15.1.9 Denitrification of Nitrogen

Denitrification is the process of nitrate ($NO_3^-$) reduction to $N_2$ or $N_2O$ gases by bacteria under anaerobic (reduced) condition (Berg and Meehan 2017). Denitrification can occur when the cropping system is ponded such as rice cultivation (Garcia and Tiedje 1982). There is a threshold value of moisture content in the soil in SWAT when denitrification can occur.

#### 3.15.1.10 Total Nitrogen Loading

Total nitrogen is the combined loading of organic and inorganic nitrogen (*i.e.*, $NO_3^-$) that is exported by SWAT. According to (Harmel et al. 2006) approximately 75% of the nitrogen lost from fields is in particulate form and most of it moves with sediment. Whereas, the dissolved nitrogen (*i.e.* $NO_3^-$) moves with surface runoff. SWAT models total nitrogen for particulate forms based on the sediment export model. The dissolved nitrogen (nitrate nitrogen) is calculated based on the runoff export model. This study will calibrate and validate the model for total nitrogen loading.

The equation of total nitrogen export (TOT N) is:

$$TOT\ N = NO3_{surf} + NO3_{lat,ly} + orgN_{surf} \quad (3.31)$$

### 3.15.2 Phosphorus

Plants require less phosphorus than nitrogen. However, the most important functions of phosphorus are to store and transfer energy that is needed for plant growth and reproductive processes (Malhotra *et al*. 2018).

#### 3.15.2.1 Phosphorus cycle

Phosphorus is not as freely available as nitrogen in the environment because most of it is held in rocks and sediment. Phosphorus is present in mineral soils in the following three major forms: organic phosphorus, insoluble mineral phosphorus and soluble phosphorus in soil solution (Berg and Meehan 2018, Malhotra *et al*. 2018). Other sources of phosphorus on agricultural fields in addition to the soil are fertilizers, manure or plant residue application (Beegle and Durst 2002). The loss of phosphorus from agricultural land occurs by plant uptake and soil erosion (Malhotra *et al*. 2018).

Phosphorus is less soluble and mobile than nitrogen in environments (Berg and Meehan 2018, Beegle and Durst 2002). It forms some insoluble compounds that are close to the soil surface and readily available for transport in the surface runoff (Beegle and Durst 2002). According to Sharpley and Syers (1979), phosphorus is mainly exported from most of the watersheds through surface runoff. SWAT represents three organic and three inorganic forms of phosphorus in the soil (Fig 3.6). Organic phosphorus consists of fresh crop residue and biomass. Fresh plant residue is converted to humic substances via microbial and other organisms mediated decomposition in the soil. This conversion happens first to stable humic substance and then to the active humic substance which leads to the mineralization process. Mineralization occurs in the soil through bacteria that make phosphorus available for plants for uptake. The transformation between the soluble pool and

the active pool is rapid however, the transformation between the active pool and the stable pool is a slower process.

### 3.15.2.2 Initialization of soil Phosphorus Levels

As for nitrogen SWAT can initialize the concentration of phosphorus in the different pools. At the beginning of a simulation, for unmanaged land under native vegetation SWAT assumes the concentration of phosphorus in the solution pool is 5 mg/kg soil in all soil layers. In this study, for crop land the concentration is set 25 mg/kg soil (the default SWAT value).

The concentration of phosphorus in the active and stable mineral pool is initialized using Equation 3.32 and 3.33:

$$minP_{act,ly} = P_{solution,ly} * \frac{1-pai}{pai} \quad (3.32)$$

$$minP_{sta,ly} = 4 * minP_{act,ly} \quad (3.33)$$

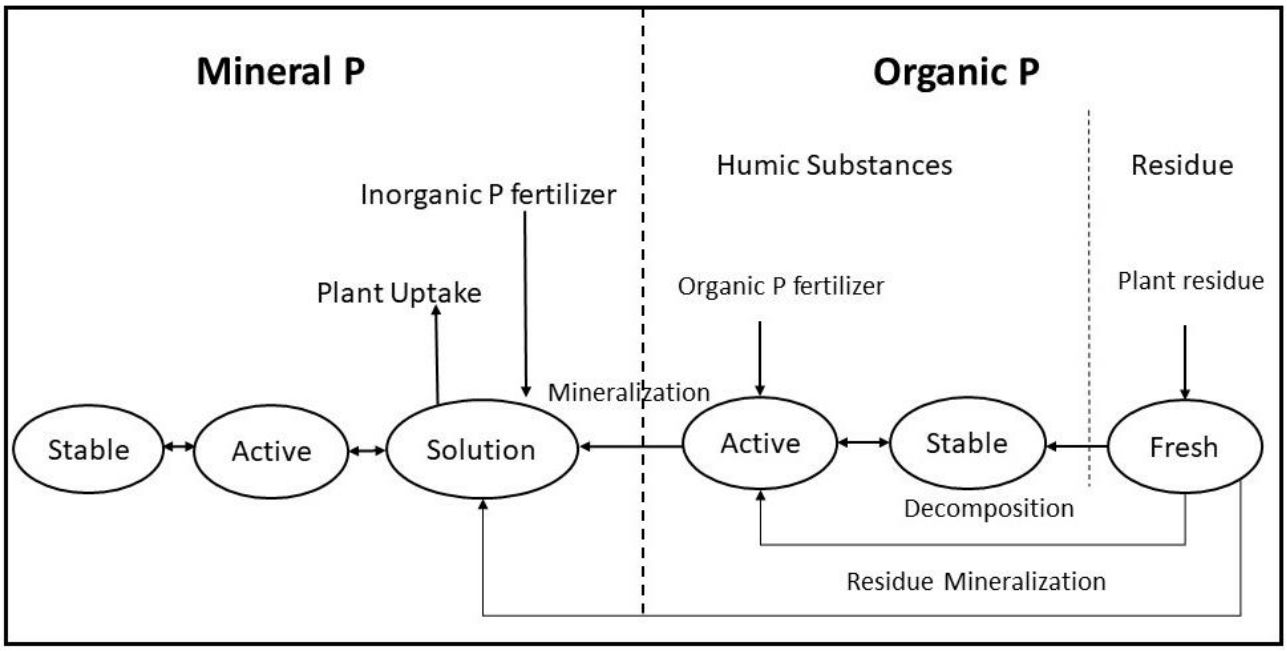


Figure 3.6: SWAT soil phosphorus pools and process of P movement (adapted from Neitsch *et al.* 2011).

where $minP_{act,ly}$ is the amount of phosphorus in the active mineral pool (mg/kg), $minP_{sta,ly}$ is the amount of phosphorus in the stable mineral pool (mg/kg), $P_{solution,ly}$ is the amount of phosphorus in solution (mg/kg), and $pai$ is the phosphorus availability index and it is a function of soluble phosphorus fertilizer added to the soil. SWAT assumes the concentration of organic phosphorus based on a ratio of 1:8 with the organic nitrogen level in humic materials.

### 3.15.2.3 Mineralization and Decomposition of Phosphorus

The definitions of mineralization and decomposition are described earlier in the nitrogen section. SWAT uses the same algorithm forms for both nitrogen and phosphorus mineralization. Temperature and water factors are used in the mineralization and decomposition equation. Mineralization is considered for two sources: the fresh organic P pool which deals with the crop residue and microbial biomass and active organic P pool which considered soil humus. Both mineralization and decomposition happens when the soil temperature is above 0°C.

SWAT calculates the phosphorus decomposition from crop residue in fresh organic pool using Equation (3.34):

$$P_{dec,ly} = 0.2 * \delta_{ntr.ly} * orgP_{frsh,ly} \quad (3.34)$$

where $P_{dec,ly}$ is the phosphorus decomposed from the fresh organic P pool (kg P/ha), $\delta_{ntr.ly}$ is the residue decay rate constant (dimensionless) calculated based on C:N and C:P ratio on the residue in the soil layer, and $orgP_{frsh,ly}$ is the phosphorus in the fresh organic pool in the soil layer (kg P/ha), which is measured from the material in the residue pool for the top 10 mm of soil. Later, $P_{dec,ly}$ is added to the humus organic phosphorus pool in the soil layer.

The mineralization process from crop residue in fresh organic pool is

$$P_{min,ly} = 0.8 * \delta_{ntr.ly} * orgP_{frsh,ly} \quad (3.35)$$

where, $P_{min,ly}$ is the phosphorus mineralized from the fresh organic P pool (kg P/ha). This amount of mineralized phosphorus is added to the solution phosphorus pool in the soil layer.

The mineralization process from active organic P pool which considers soil humus is

$$P_{mina,ly} = 1.4 * \beta_{min} * \left(\gamma_{tmp,ly} * \gamma_{sw,ly}\right)^{1/2} * orgP_{act,ly} \quad (3.36)$$

where, $P_{mina,ly}$ is the phosphorus mineralized from the humus active organic P pool (kg P/ha), $\beta_{min}$ is the rate coefficient for mineralization of the humus active organic nutrients (dimensionless), $\gamma_{tmp,ly}$ is the nutrient cycling temperature factor for the soil layer (dimensionless), $\gamma_{sw,ly}$ is the nutrient cycling water factor for the soil layer (dimensionless), and $orgP_{act,ly}$ is the amount of phosphorus in the active organic pool (kg P/ha). $P_{mina,ly}$ later surpluses to the solution phosphorus pool in the same soil layer.

### 3.15.2.4 Soluble Phosphorus Movement

Phosphorus movement in soil solution occurs mainly through diffusion over small distances (1-2 mm). This happens due to the concentration gradient of phosphorus. The equation for phosphorus transport through surface runoff is:

$$P_{surf} = \frac{P_{solution,surf} * Q_{surf}}{\rho_b * depth_{surf} * k_{d,perc}} \quad (3.37)$$

where $P_{surf}$ is the amount of soluble phosphorus lost in surface runoff (kg P/ha), $P_{solution,surf}$ is the amount of phosphorus in solution in the top 10 mm (kg P/ha), $Q_{surf}$ is the amount of surface runoff on a given day (mm $H_2O$), $\rho_b$ is the bulk density of the top soil layer ($Mg/m^3$), $depth_{surf}$

is the depth of the surface layer (10 mm), and $k_{d,perc}$ is the phosphorus percolation coefficient ($m^3$/kg).

SWAT also considers phosphorus transport (organic and mineral) with sediment transported in surface runoff. The equation is:

$$sedP_{surf} = 0.001 * conc_{sedP} * \frac{sed}{area_{hru}} * \varepsilon_{P;sed} \quad (3.38)$$

where $sedP_{surf}$ is the amount of phosphorus transported with sediment to the main channel in surface runoff (kg P/ha), $sed$ is the sediment yield on a given day (metric tons), $conc_{sedP}$ is the concentration of phosphorus attached to sediment in the top 10 mm (g P/metric ton soil), $area_{hru}$ is the area of the HRU (ha), and $\varepsilon_{P;sed}$ is the phosphorus enrichment ratio. $conc_{sedP}$ is calculated based on the amount of organic and mineral phosphorus in the fresh, stable and active pool. The phosphorus enrichment ratio is calculated based on the concentration of sediment in surface runoff.

### 3.15.5 Leaching of Phosphorus

SWAT considers leaching of soluble phosphorus from the top 10 mm of soil only into the first soil layer due to the low mobility of phosphorus. The equation of leaching is:

$$P_{perc} = \frac{P_{solution,surf} * w_{perc,surf}}{10 * \rho_b * depth_{surf} * k_{d,perc}} \quad (3.39)$$

where $P_{perc}$ is the amount of phosphorus moving from the top 10 mm into the first soil layer (kg P/ha), $w_{perc,surf}$ is the amount of water percolating to the first soil layer from the top 10 mm on a given day (mm $H_2O$), $depth_{surf}$ is the depth of the surface layer (10 mm), and $k_{d,perc}$ is the phosphorus percolation coefficient ($m^3$/kg).

### 3.15.6 Total Phosphorus Loading

Total phosphorus is a combination of organic and inorganic phosphorus (*i.e.*, $PO_4^{3-}$) compounds in water (Murphy 2007) and loading consists of both soluble and insoluble forms. SWAT calculates phosphorus removed from fields in particulate form based on the sediment export model. The soluble phosphorus is calculated based on the runoff export model. SWAT estimates the total phosphorus (TOT P) load using following equation:

$$TOT\ P = P_{surf} + sedP_{surf} \tag{3.40}$$

## 3.16 Loading Phases Simulated by the SWAT Model

The land phase and channel routing phase are the two main export categories that SWAT simulates. The amount of water, sediments, nutrients and pesticide exported to the main channel occurs in the land phase. The routing phase deals with the movement of water, sediments, nutrients, *etc.* through the channel network to the watershed outlet. Surface runoff, lateral flow and return flow is predicted separately in each HRU and routed to predict the total runoff in the watershed.

SWAT follows a command structure by Williams and Hann (1972) for water, sediment, nutrients and pesticides routing through the stream network to the main channel. Moreover, SWAT models the transformation of chemicals in the streams and streambed to keep track of mass flow in the channel. During channel routing, when water flows downstream losses occur by evaporation, transmission through the bed and anthropogenic usage. Direct rainfall and point source discharge are supplements to the flow in the channel. SWAT uses the variable storage coefficient method by Williams (1969) or the Muskingum routing method for flow routing in the channel.

Sediment transport in the channel is controlled by simultaneous simulation of erosion and deposition. SWAT considers peak channel velocity to calculate the maximum amount of sediment

erosion from a reach. Available stream power is used by SWAT for complete removal of loose and deposited bed materials. However, excess stream power causes bed degradation which is adjusted for stream bed erodibility and cover.

The instream water quality component of the model controls nutrient transformations in the channel. The instream nutrient transformation mechanisms that are used in SWAT were adopted from the QUAL2E model by (Brown and Barnwell 1987). The model is capable of tracking both dissolved nutrients in the stream and absorbed nutrients to the sediment. The dissolved nutrients are transported with water whereas the absorbed nutrients are deposited with sediment in the channel bed.

# CHAPTER 4: METHODOLOGY

## 4.1 SWAT Model

A recent version of the Soil and Water Assessment Tool (SWAT) model, SWAT 2012, was used in this study. Several modifications have been considered in this version and earlier versions to better simulate cold climate hydrology. According to Fontaine *et al*. (2002), SWAT incorporates a seasonally variable snowmelt rate. Further, to represent enhanced surface runoff and reduced infiltration for frozen soil conditions, SWAT modifies the curve number value (Tolson and Shoemaker 2007). Moreover, this study used an additionally modified version of SWAT 2012 that includes a probability distributed pond storage algorithm (Mekonnen *et al.* 2016a) and seasonally adjusted soil erodibility factors (Mekonnen *et al.* 2016b).

## 4.2 Pond Module

The SWAT model offers several modules that potentially could be used to simulate contributions to streamflow from landscape depressions *i.e*. the Pothole, Wetland, and Pond modules (Neitsch *et al.* 2011). Only the Pond and Wetland modules allow runoff contribution from any HRU within a sub-basin to be routed through them, which happens in reality (Almendinger *et al*. 2014). In this research, the Pond module was used to compare its simulated flow results to the probability distributed storage approach of Mekonnen *et al.* (2016a), which is an adaptation of the Pond routine. Moreover, water quality simulation is available in the Pond routine. The surface runoff processes considered in the Pond module are described in Figure 4.1.

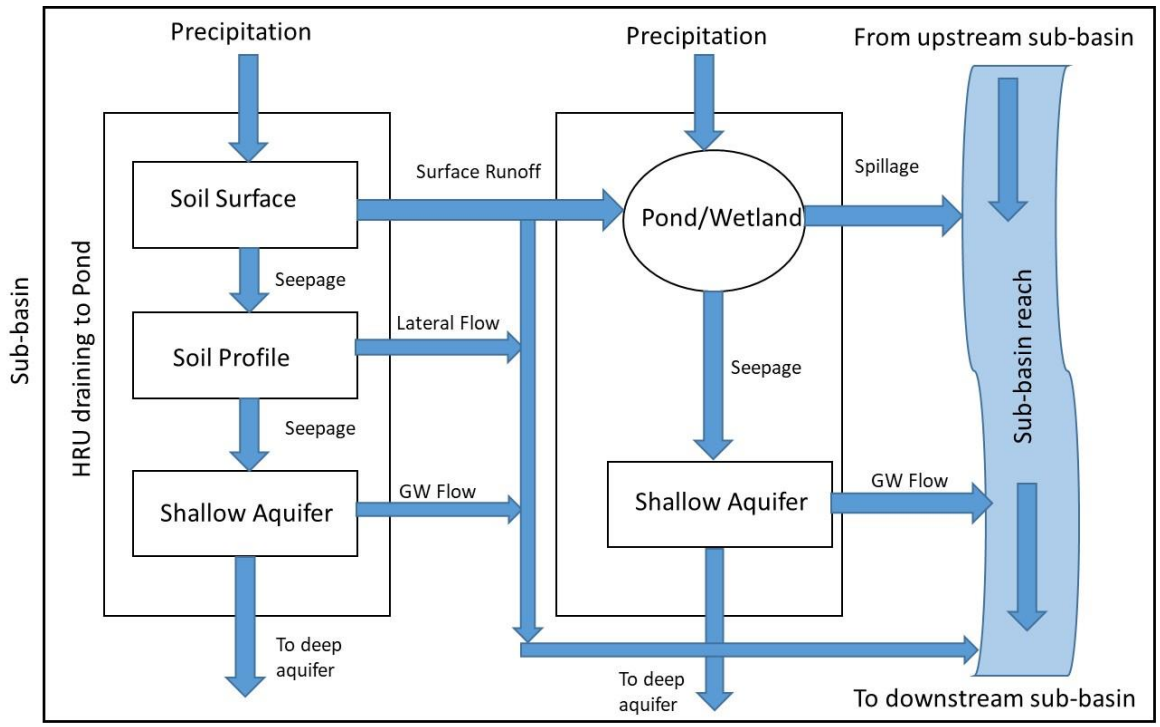


Figure 4.1: SWAT pond module processes (adapted from Evenson *et al*. 2015 and Jalowska and Yuan 2019).

### 4.3 Study Areas

In this study, streamflow and water quality were simulated for three watersheds in Southern Saskatchewan: Swift Current Creek below Rock Creek; Pipestone Creek above Moosomin Lake; and Lightning Creek near Carnduff (Figure 4.2).

Pipestone Creek above Moosomin and Lightning Creek near Carnduff watersheds are located in the southeastern part of the province. The tributary of Pipestone Creek is Montgomery Creek and tributary of Lightning Creek is Gainsborough Creek. The Swift Current Creek watershed (to below Rock Creek) is located in the southwestern part of the province. The tributaries of Swift Current Creek are Bone Creek, Jones Creek, Rock Creek and Pelletier Creek. Nearly 11% of the Pipestone Creek watershed is covered by wetlands (Perez-Valdivia *et al*. 2017). According to

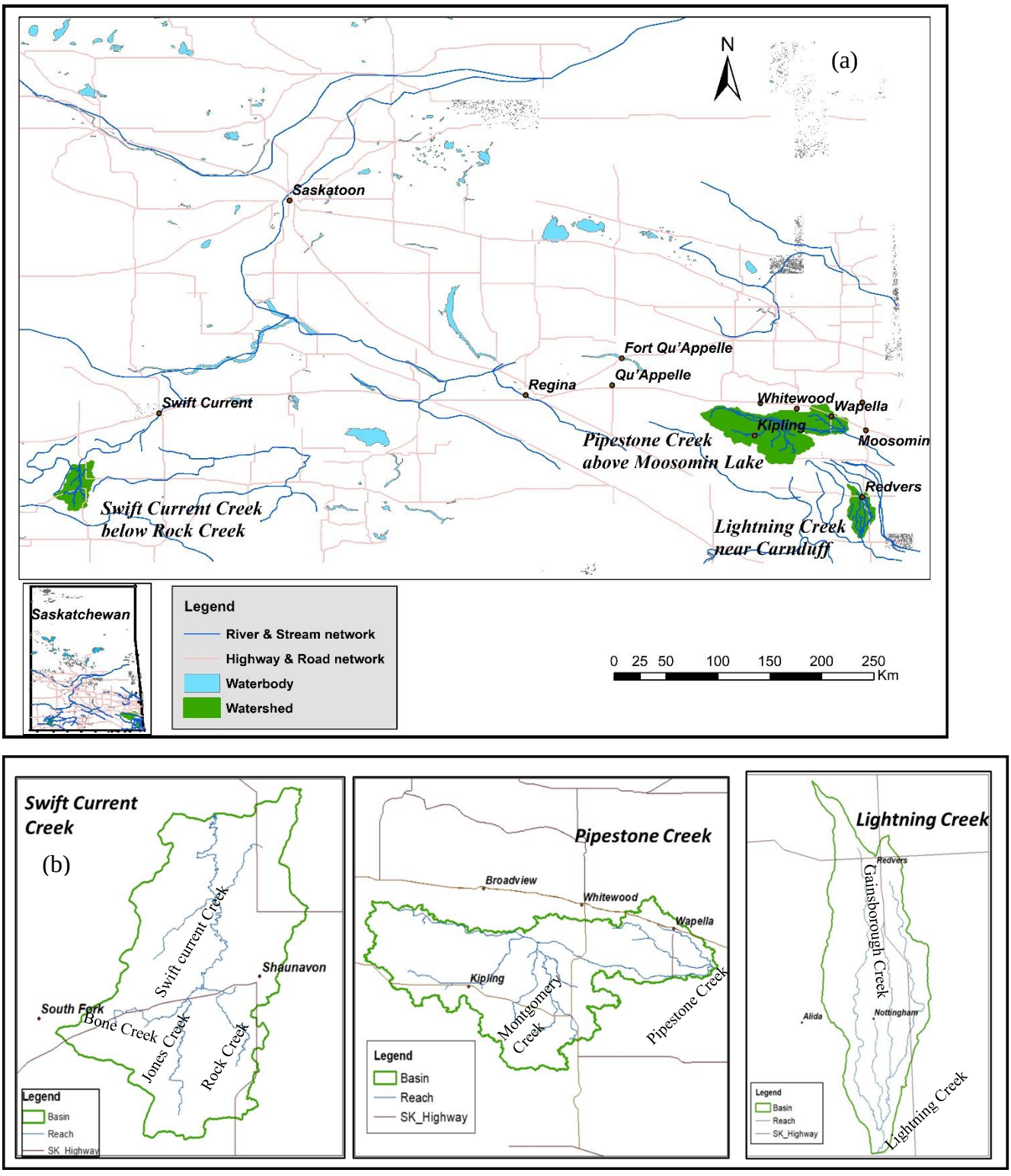


Figure 4.2: Map of watersheds (a) location of catchments in the province (b) individual catchment area (Source: Saskatchewan Open Data, Sask. Interactive Mapping, WSA and mapcruzin.com).

land use maps (Agriculture and Agri-Food Canada) wetland in the Lightning Creek and Swift Current Creek study areas cover around 4% and 2.5% of the watersheds respectively.

The elevation change from headwater to outlet is 804 to 547 m, 1048 to 838 m and 629 to 508 m for Pipestone Creek, Swift Current Creek and Lightning Creek watersheds respectively. The annual average and range in annual average precipitation of Pipestone Creek, Swift Current Creek and Lightning Creek watersheds are 410 mm (300 to 597.5), 352 mm (182 to 597.5) and 460 mm (219 to 619.7) respectively (Canada Weather Stats). It is worth noting that 2010 was a tremendously wet year for all three watersheds. Annual precipitation for 2010 for Pipestone Creek, Swift Current Creek, and Lightning Creek were 597.5 mm, 597.5 mm and 619.7 mm (Canada Weather Stats 2019).

All three watersheds are characterized by a cold climate. Typically, the land is covered by snow and soils are frozen during the winter. The average annual temperature in the Pipestone Creek, Swift Current Creek and Lightning Creek watersheds are 2.6°C, 4.1°C and 3.9 °C respectively. There is a large volume of runoff due to snowmelt in spring but excess evapotranspiration over precipitation in summer (Fang et al. 2007).

## 4.4 Model Input Data

### 4.4.1 Climate Data

Gridded daily total precipitation and maximum and minimum temperature have been collected for several stations within each watershed from 1990 to 2017 from Natural Resources Canada (NRC). The thin plate spline smoothing algorithm (ANUSPLIN) developed by Dr. Michael Hutchinson has been applied to prepare the gridded data (Natural Resources Canada 2019.). The dataset covers the domain from 168.0 to 52.0° W and 25.0 to 85.0° N with a 10 km spatial

resolution for the period of 1900 to 2017. For each sub-basin, SWAT only considers data from a single precipitation gauging station or a single grid point that is nearest to the centroid of the sub-basin (Tuo *et al.* 2016). Note that gridded data was used by Mekonnen *et al.* (2016b), as well as Choi *et al.* (2009) in modelling prairie watersheds, with good model results. In Pipestone Creek watershed climate data was collected for Kipling (50.211° N, -102.733° W), Langbank (50.158° N, -102.395° W), Whitewood (50.35° N, -102.27 W) and Broadview (50.367° N, -102.567° W). In Lightning Creek and Swift Current Creek, the climate data was collected for Carnduff (49.22° N, -101.75° W) and Shaunavon (49.65° N, -108.416° W) respectively.

### 4.4.2 Hydrometric Data

The selected hydrometric stations for Pipestone Creek, Swift Current Creek, and Lightning Creek watersheds are 05NE003 (50°9'7.9"N, 101°50'13.3"W), 05HD036 (49°50'40.0" N, 108°28'46.0" W) and 05NF006 (49°13'15.8" N, 101°43'8.3" W) respectively. Environment Canada maintains a database of daily flow records (HYDAT) at hydrometric stations within the study watersheds. Daily average flow data is available from 1960 to 2018 for Pipestone Creek, 1935-2017 for Lightning Creek, and 1955-2018 for Swift Current Creek watersheds. Recorded maximum average daily streamflow during March- October for Pipestone Creek, Swift Current Creek and Lightning Creek watershed was 87.4, 45.9 and 180 $m^3/s$, whereas maximum mean monthly streamflow was recorded as 4.2, 1.82 and 4.23 $m^3/s$.

Table 4.1 summarizes the watershed area and percentage of agricultural land for each watershed. The gross drainage area is defined as the expected area that is considered for contributing the runoff to the main stream during the extreme wet conditions of the watershed (Pomeroy *et al.* 2005). The effective drainage area is considered based on the contribution of the runoff to the main stream during a flood event of two years return period (Pomeroy *et al.* 2005).

The percentage of agricultural land in each watershed is calculated based on detailed land use data classifications from a land use map (Agriculture and Agri-Food Canada 2015).

### 4.4.3 DEM

A Digital Elevation Model (DEM) with 15 m grid resolution was collected from the Saskatchewan Geospatial Imagery Collaborative (SGIC) for the delineation of sub-basins within each watershed. The DEM has been used to create a continuous flow network and determine landscape geometry within each watershed through the SWAT automatic delineation tool.

Table 4.1: Summary of watershed areas and main land uses.

| **Name of Watershed** | **Average Annual Precipitation (mm)** | **Gross Drainage Area ($km^2$)** | **Effective Drainage Area ($km^2$)** | **Agricultural land ($km^2$)** |
|---|---|---|---|---|
| Swift Current Creek below Rock Creek | 410 | 1430 | 1090 | 85% |
| Pipestone Creek above Moosomin Lake | 460 | 2730 | 655 | 83% |
| Lightning Creek near Cranduff | 352 | 748 | 393 | 87% |

### 4.4.4 Soil Data

Detailed soil information was obtained from the Canadian Soil Information Service (CANSIS) for each watershed ("Canadian Soil Information Service" 2018). According to Soil Landscapes of Canada Version 3.2, two different types of soils are found in the Pipestone Creek watershed. The Orthic Black Chernozem or Oxbow loamy (SKOXA) soil was the dominant type for the Pipestone Creek Watershed. In the Lightning Creek Watershed, two different types of soils are also found but Orthic Brown Chernozem (SKADA) covers most of the watershed. Orthic Dark Brown

Chernozem (SKAMA) is the dominant soil type in the Swift Current Creek watershed among 8 different types present. The dominant soil type in each watershed is well-drained, which means the soil passes water readily but not rapidly (CANSIS).

The important physical soil characteristics required for streamflow and water quality modeling are the number of soil layers to be represented and the bulk density, available water content, saturated hydraulic conductivity, texture class, albedo and percentage of clay, silt and sand of each layer. A customized soil database of the above-mentioned data for each soil type and layer was developed and installed in the model for each watershed.

### 4.4.5 Land Cover and Land Use

Agriculture and Agri-Food Canada (AAFC) recently updated its annual crop inventory digital maps (of 30 m resolution) to 2015 based on satellite imagery for all of Canada (CANSIS). Land cover and land use digital data were collected for each of the study watersheds.

The Pipestone Creek watershed is comprised of 23 different land-use types. Most of the major land-use types represent specific crop types (*e.g.*, canola, spring wheat, winter wheat, barley, lentils, peas, oats, rye, canary seed, and flaxseed). The other significant land-use types are pasture, broadleaf forests, coniferous forest, grassland, shrubland, and wetland.

The major landuse types of the Lightning Creek watershed (21 types) are like those in the Pipestone Creek watershed but with the additional category of canary seed cultivation. Only 18 different land use types were found in Swift Current Creek watershed. Again, most are for specific crop types on agricultural land (*e.g.*, mustard, spring wheat, winter wheat, barley, lentils, peas, rye, and flax seed). Other types of land use in the Swift Current watershed are barren land (exposed or non-vegetated), shrubland, coniferous forest and wetland.

Land use variation is a crucial factor that influences the evapotranspiration rate from the watershed, which plays a major role in the water balance of the watershed (Dwarakish and Ganasri 2015).

### 4.4.6 Nutrient Data

In-stream nutrient and suspended solids data for the three study watersheds was obtained from the Saskatchewan Water Security Agency (WSA). Total suspended solids (TSS), total nitrogen (TN) and total phosphorus (TP) concentration data were collected by WSA once or twice in a month during seasonal flow monitoring period and was available from 2007-2017. The station number of the water quality measuring stations are SK05NE0091, SK05HD0120, and SK05NF0124 for the Pipestone Creek, Swift Current Creek and Lightning Creek watersheds respectively. All three water quality monitoring stations are located at the same locations as the hydrometric stations in the watersheds. The measured suspended solids and nutrient data is used for calibration and validation of the water quality model. The concentration of TSS and nutrients were converted to loading by multiplying by the corresponding streamflow.

### 4.4.7 Tillage Operation and Fertilizer Application

Tillage operation plays a significant role in soil loss in agricultural watersheds. The conventional tillage practice was dominant in the province of Saskatchewan historically, however in the last several decades, conservation tillage and no-tillage practices have increased in use in Saskatchewan (Awada *et al*. 2014). According to Statistics Canada (2007), since 2006, no-tillage operations have been applied on approximately 60% of agricultural land; therefore, in this study, the no-tillage operation was used in the modelling. The general crop plantation period starts at the end of May and the harvesting period starts at the beginning of September (The Old Farmer's

Almanac 2019). In Saskatchewan, cereal crops are cultivated primarily and the remaining crops are different types of oil seeds and pulses (Annual Crop Inventory, Agriculture and Agri-Food Canada 2018).

According to the Saskatchewan Watershed Authority (2010), a large number of agricultural activities and livestock operations are responsible for impacting the water quality of the considered watersheds. In general, soil erosion due to precipitation and runoff, as well as industrial waste disposal will also affect water quality (Vandas *et al.* 2014).

Typical fertilizer (nitrate, orthophosphate and anhydrous ammonia) and manure areal application rates in Saskatchewan agricultural watersheds were collected from the State of the Watershed Report by Saskatchewan Watershed Authority (2010). According to that report, the rate of nitrogen and phosphorus fertilizer application in Saskatchewan ranges from 31.3 to 45.5 kg/ha and 6.0 to 8.5 kg/ha respectively. Most of the fertilizer application (nitrogen and phosphorus) occurs during the seeding period, however, sometimes a limited amount of mid-season phosphorus application is required (Government of Saskatchewan 2020a,b). The amount of manure application ranges between 1098 to 1628 kg/ha, where the portion of nitrogen and phosphorus in the manure application are 7 to 10 kg/ha and 2 to 3 kg/ha respectively (Saskatchewan Watershed Authority 2010). The majority of manure application comes from beef cows (55%) and the other sources are calves (17%), heifers (9%), steers (5%), pigs (4%), bulls (3%), dairy cows (2%) and poultry (1%) and miscellaneous (4%) (Saskatchewan Watershed Authority 2010).

In this study, point source pollution was not considered due to unavailable data. Moreover, in past studies in the prairie region (Mekonnen *et al.* 2016c), point source pollution was considered as insignificant during the spring period due to a high volume of agricultural non-point pollution through surface runoff.

### 4.4.8 Characterization of Landscape Depressions

To incorporate the landscape depressions into the SWAT model in order to observe how storage in depressions impacts the streamflow, it is first required to identify depression geometry (*i.e.,* storage volume, surface area). Depression geometry (pond surface area and pond volume) was computed using the Arc Hydro tools under ArcGIS version 10.5 for each watershed. From the ratio of the pond volume to the pond surface area, the average depth ($c$) was calculated for each pond and an overall mean pond depth ($\overline{c}$) was calculated for each sub-basin within each watershed. For the input in the model the cumulative pond surface area and volume have been used for each sub basin. A high-resolution Ortho-photo image of each watershed was used to visually verify the location and number of depressions identified by the Arc Hydro tools. Visual inspection confirmed the pond locations and sizes.

## 4.5 Model Setup

### 4.5.1 Background

The automatic delineation tool of ArcSWAT (in SWAT 2012) was used to generate initial sub-basins and stream channel locations using DEM information to define basin boundaries and the streamflow network. Next, HRUs were defined after importing the land use and soil data. The automatic delineation was processed after selecting the watershed boundary, which was previously defined by the AAFC Watershed Project (2013)**.**

The SWAT-PDLD model was applied in this research project to improve the streamflow and water quality simulations in comparison to the standard SWAT2012 model. SWAT-PDLD was coded into SWAT by Mekonnen *et al.* (2016a) as an alternative to the existing pond algorithm. The details of the SWAT-PDLD model are described in Mekonnen *et al.* (2016a,b). The PDLD

algorithm introduces a probability distribution into the Pond Module in SWAT, which is used to describe the distribution of pond storage capacity in each sub-basin, and to determine when and to what extent landscape depressions spill and contribute to streamflow for each snowmelt and rainfall event.

In modelling of sediment export from the watershed, the soil erodibility factor (K) is a key parameter for simulating soil erosion that triggers sediment transport in the watershed. SWAT uses an average value of K in the MUSLE equation. However, in cold climate regions like the Canadian prairies, sediment erodibility varies seasonally (McConkey *et al*. 1997, Mekonnen *et al*. 2016b). To consider seasonal variability of sediment transport a seasonally variable soil erodibility factor was introduced by Mekonnen *et al*. (2016b) for four defined seasons in SWAT-PDLD. The four seasons were classified as November 1 to March 15$^{th}$, March 16 to March 31$^{st}$, April 1 to April 30$^{th}$, and May 1 to October 31$^{st}$. The relative weighting of the soil erodibility factor considered for these periods by Mekonnen *et al*. (2016b) was 0.41, 1.18, 1.9 and 1.0 respectively. This modification and weightings has been used in this study.

For the calculation of evapotranspiration, the Hargreaves method has been used in this study for which only temperature data is required.

### 4.5.2 Sensitivity Analysis

Sensitivity analysis is the process of identifying crucial parameters that are the most sensitive to be used in model calibration. The analysis can be done manually or automatically. In this study, it was decided to use SWAT-CUP and the Sequential Uncertainty Fitting Version 2 (SUFI-2) algorithm for sensitivity analysis and calibration. Both local and global sensitivity analysis are available under SUFI-2 and they both have some pros and cons. Local sensitivity analysis or One

Factor at a Time (OAT) is the process of assessing the effect of one parameter on the model result while all other parameters remain constant. It has been used in the field of hydrology on a large scale; however, there are some limitations regarding missing interactions among factors, not obvious to get the most sensitive input factors and the quality of associated uncertainty analysis (Saltelli and Annoni 2010). Moreover, local sensitivity analysis is still using in the field of hydrology (Mekonnen et al. 2016a-b) and it is useful for regional modelling studies specially for semi-distributed hydrological models significantly (Devak and Dhanya 2017). In this study, this method provides better understanding to select parameters than the global sensitivity approach.

In SUFI-2, uncertainty in parameters is expressed as a range that includes all sorts of uncertainties (*i.e.* conceptual model, input variables, parameters and input data). The consequences of the input uncertainties cause the uncertainties of model output variables. SUFI-2 expressed that uncertainty as 95% prediction uncertainty (95PPU) which is calculated at the 2.5% and 97.5% levels of the cumulative distribution of an output variable generated by the propagation of the parameter uncertainties based on Latin hypercube sampling process (Abbaspour *et al.* 2007). So, the goal of the SUFI-2 calibration method is to cover most of the observations within the 95% probability distributions of output variable.

A sensitivity analysis was completed to confirm, expand or reduce the number of sensitive model parameters that were then used to calibrate the model. The sensitive parameters identified with their permissible range and final calibrated value are presented in Table 4.2.

Table 4.2: Sensitive parameters and their calibrated values for the SWAT-PDLD model.

| Type | Parameter | Description | Permissible Range | | Calibrated value | |
|---|---|---|---|---|---|---|
| | | | Lower Limit | Upper Limit | PipeStone Creek | Lightning Creek |
| Streamflow | r_CN2 | SCS runoff curve number | -0.3 | +0.3 | -0.22 | -0.20 |
| | v_TIMP | Snowpack temperature lag factor | 0 | 1 | 0.23 | 0.21 |
| | v_SFTMP | Snowfall temperature (°C) | -5 | 5 | -1.86 | -2.70 |
| | v_SMTMP | Snowmelt base temperature (°C) | -5 | 5 | 0.05 | -0.38 |
| | v_SMFMX | Maximum melt factor (mm /°C/d) | 0 | 9 | 5.79 | 5.50 |
| | v_SMFMN | Minimum melt factor (mm /°C/d) | 0 | 7 | 2.93 | 1.10 |
| | v_SNOCOVMX | Areal snow coverage threshold at 100% (mm $H_2O$) | 0 | 500 | 101.92 | 117.99 |
| | v_SNO50COV | Fraction of areal snow coverage threshold at 50% | 0 | 1 | 0.32 | 0.26 |
| | v_ALPHA_BNK | Baseflow factor for bank storage (day) | 0 | 1 | 0.43 | 0.26 |
| | v_GWQMN | Threshold depth of water in the shallow aquifer required for return flow to occur (mm $H_2O$) | 0 | 5000 | 2770.50 | 2773.70 |
| | r_SOL_Z | Depth from soil surface to bottom of layer (mm) | -0.25 | +0.25 | 0.14 | 0.25 |
| | r_SOL_BD | Moist bulk density ($Mg/m^3$) | -0.2 | +0.2 | 0.02 | 0.10 |
| | v_CH_N2 | Manning's n for the main channel | 0.01 | 0.3 | 0.09 | 0.13 |
| | v_CH_K2 | Effective hydraulic conductivity for the main channel (mm/hr) | 5 | 100 | 35.20 | 50.70 |
| | r_PND_PVOL | Maximum Storage capacity | -0.25 | +0.25 | -0.13 | 0.17 |
| Sediment | v_PRF | Peak rate adjustment factor for sediment | 0 | 2 | 0.01 | 0.09 |
| | v_SPCON | Linear parameter for maximum sediment reentrained | 0 | 0.01 | 0.00 | 0.00 |
| | v_SPEXP | Exponent parameter for sediment reentrained | 0 | 1.5 | 0.50 | N/A |
| | v_USLE_P | USLE support practice | 0 | 1 | 0.61 | 0.73 |
| | v_CH_COV1 | Channel erodibility factor | 0 | 1 | 0.47 | 0.86 |
| | v_CH_COV2 | Channel cover factor | 0 | 1 | 0.79 | 0.43 |
| Phosphorus | v_PSP | P availability index | 0.01 | 0.7 | 0.62 | 0.52 |
| | v_ERORGP | Phosphorus enrichment ratio | 0 | 5 | 0.12 | 0.19 |
| | v_PHOSKD | P soil partitioning coefficient | 100 | 200 | 156.80 | 117.63 |
| | v_P_UPDIS | P uptake distribution parameter | 0 | 100 | 40.01 | 79.60 |
| Nitrogen | v_RCN | N in rainfall (mg N/L) | 0 | 15 | 0.10 | 0.11 |
| | v_NPERCO | Nitrogen percolation coefficient | 0 | 1 | 0.86 | 0.22 |
| | v_ERORGN | Organic N enrichment ratio | 0 | 5 | 0.31 | 0.53 |
| | v_CDN | Denitrification exponential coefficient | 0 | 3 | 1.55 | N/A |
| | v_SDNCO | Denitrification threshold water content | 0 | 2 | 1.10 | N/A |
| | v_N_UPDIS | N uptake distribution parameter | 0 | 100 | 11.24 | 12.30 |

Note: A parameter designated as v_ means the calibrated value replaces with the default parameter value and r_ means initial parameter value is multiplied by (1+calibrated value) that means the parameters will change as percentage (*i.e.* -0.20 means default parameter will decrease 20%).

### 4.5.3 Calibration and Validation

In this research work, the SWAT-PDLD model was used to simulate streamflow, sediment loading and nutrient transport (N and P) in the watersheds. Initially, parameters related to the hydrological process and reported by previous studies in the prairie region were assessed in a sensitivity analysis. After selecting sensitive parameters, calibration was conducted using the SUFI-2 algorithm. Streamflow was calibrated first as it influences other output variables and it is more frequently sampled than water quality data. Many researchers have followed this process, *e.g.*, White and Chaubey (2005), Abbaspour *et al.* (2007), and Mekonnen et al. 2016c).

Streamflow simulations were performed on a daily time-step basis at gauging stations 05NE003 (Pipestone Creek), 05HD036 (Swift Current Creek) and 05NF006 (Lightning Creek). Calibration and validation was conducted following an initial two-year warm-up period for the model to help mitigate the uncertainty of the initial input conditions. The calibration and validation period for streamflow for the Pipestone Creek watershed was 2006-2009 and 2012-2015. For Lightning Creek watershed, the calibration and validation period for streamflow was 1995-1997 and 2015-2017 respectively. The calibration period of Swift Current Creek was initially selected as 2006-2009; however, the model could not be calibrated to provide to the desired model performance. Therefore, no further calibration and validation of Swift Current Creek watershed was continued for streamflow or water quality. Further explanation regarding the Swift Current Creek model calibration will be given in Chapter 6. The calibration periods were chosen to avoid years with extreme flooding (*i.e.* 2010-2011 for Pipestone Creek) or drought that may cause the model unstable. The calibrated parameters are considered in a stable climate condition (not extreme flood or draught). However the model was later validated for different years rather than

calibration period. Calibration and validation periods for streamflow and water quality analysis are summarized in Table 4.3.

Table 4.3: Calibration and validation period used for the modelling

| Simulation Type | Pipestone Creek Watershed | | Lightning Creek Watershed | |
|---|---|---|---|---|
| | Calibration period | Validation period | Calibration period | Validation period |
| **Streamflow** | 2006-2009 | 2012-2015 | 1995-1997 | 2015-2017 |
| **Sediment export** | 2007-2009 | 2012-2015 | 2015-2017 | 2008-2010 |
| **Total Phosphorus export** | 2007-2009 | 2012-2015 | 2015-2017 | 2008-2010 |
| **Total Nitrogen export** | 2007-2009 | 2012-2015 | 2015-2017 | 2008-2010 |

The calibration periods for sediment loading (total suspended solids), total nitrogen and total phosphorus export were 2007-2009 for the Pipestone Creek watershed and 2015-2017 for the Lightning Creek watershed. The validation period for water quality data was 2012-2015 for Pipestone Creek and 2008-2010 for the Lightning Creek watershed. The calibration and validation periods of water quality were selected based on data availability and whether there was similar annual precipitation to the years used for calibration. For the Lightning Creek watershed, water quality data was not available for the streamflow calibration period.

After successful streamflow calibration, the sediment calibration parameters were optimized for a daily time step keeping the flow parameters fixed. A similar process was followed for total phosphorus and total nitrogen loading; the model was calibrated for nutrient processes by keeping the streamflow and sediment export parameters fixed. It is challenging to calibrate the model for nutrient export due to a short annual period of data availability (April-September) and limited number of years for which data is available. As noted above, nutrient and sediment data were collected once or twice in a month from April to September and rarely in October. In the Pipestone Creek watershed, during the calibration period, a total of 80 observations were available and during the validation period a total of 28 observations were available for sediment yield and Total P and

Total N export modelling. However, in the Lightning Creek Watershed, only 19 sediment and nutrient observations were available for the calibration period and 17 observations available for the validation period.

### 4.5.4 Model Evaluation

For evaluation of model performance for streamflow, sediment and nutrients, the Nash and Sutcliffe efficiency index (Nash and Sutcliffe 1970) was used for daily time-step simulations. In this study, NSE has been used for calibration process which tried to optimize the simulated peak values (*i.e.* peak streamflow) with observed data. The Nash and Sutcliffe efficiency index (NSE) used to determine the goodness of fit between observed and simulated streamflow data is given by:

$$\mathrm{NSE} = 1 - \frac{\sum_{i=1}^{n}(Q_i - Q_{sim})^2}{\sum_{i=1}^{n}(Q_i - \bar{Q})^2} \tag{4.1}$$

where, $Q_i$ = observed flow, $Q_{sim}$ = simulated flow, $\bar{Q}$= average observed flow and n= number of observed data.

A standardized version of root mean square error called RSR is also used which is the ratio of root mean square error and standard deviation of the observed dataset (Singh et al. 2007). Root mean square error is the standard deviation of the residuals of simulated values and is given by:

$$\mathrm{RSR} = \frac{\sqrt{\sum_{i=1}^{n}(Q_i - Q_{sim})}}{\sqrt{\sum_{i=1}^{n}(Q_i - \bar{Q})}} \tag{4.2}$$

where, $Q_i$ = observed flow, $Q_{sim}$ = simulated flow, $\bar{Q}$= average observed flow and n= number of observed data.

Percent Bias (PBIAS) was used as an objective function of model performance to check whether average tendency of the simulated dataset underestimates or overestimates the observed data (Gupta *et al.* 1999). The equation for PBIAS is:

$$\text{PBIAS} = \frac{\sum_{i=1}^{n}(Q_i - Q_{sim})*100}{\sum_{i=1}^{n} Q_i} \tag{4.3}$$

where, $Q_i$ = observed flow, $Q_{sim}$= simulated flow and n= number of observed data.

The equations stated above (4.1-4.3) for evaluation of the streamflow model were also used for the evaluation of the model performance of sediment and nutrient loading. However, the notation of discharge Q is replaced with the sediment and nutrient data (*i.e.* daily sediment load, daily total N or total P load).

# CHAPTER 5: RESULTS AND DISCUSSION

## 5.1 Introduction

This chapter describes the modelling work including a discussion of the selection of the sensitive parameters for the SWAT model, model results, and the model performance evaluation based on statistical metrics and visual assessment of model performance using time series plots of streamflow and water quality. Model prediction of when the landscape depressions were spilling and not spilling were used to assess whether spilling from depressions impacts streamflow water quality in the studied watersheds.

## 5.2 Streamflow Modelling

### 5.2.1 Calibration of Parameters for Streamflow

The model calibration parameters were identified based on the results of a sensitivity analysis. The most sensitive and important parameters for calibration of the model are presented in Table 4.2, along with their permissible ranges and final calibrated values. The model calibration simulations were started with initial parameter values selected within a theoretical permissible range (upper and lower limit) based upon a literature review (Mekonnen *et al.* 2016c, Perez-Valdivia *et al.* 2017). The calibration simulation ended when a satisfactory value for the NSE objective function was achieved. The calibration results provided a final calibrated value for each parameter within a refined range. A total of 15 parameters were found to be sensitive for streamflow calibration for the Pipestone Creek, Lightning Creek, and Swift Current Creek watersheds. A separate sensitivity test and calibration was performed for each watershed in SWAT-CUP, and the parameter ranges and calibration results varied for each watershed.

### 5.2.2 Model Performance

To evaluate the performance of the SWAT model in simulating streamflow in the study watersheds, a plot of the time series of the observed and simulated streamflow data, as well as statistical analysis have been considered. The statistical metrics used were the Nash and Sutcliffe efficiency (NSE), the standardized version of root mean square error (RSR), and the percent bias (PBIAS). Statistical metrics were defined in Chapter 4 in Equations 4.1 to 4.3. All simulations were carried out on a daily time-step; statistical metrics were also calculated using daily simulation and observed values.

For the Pipestone Creek watershed, Figure 5.1a) and b) shows the daily streamflow simulation results for the calibration and validation periods using both SWAT-PDLD and the SWAT-lumped models. During the calibration period (2006-2009), both models capture the magnitude and timing of peak flows (spring and summer period) well. However, the SWAT-lumped model underestimated one peak flow during the spring of 2007 (which occurred on June 17, 2007). In the validation period, both models missed some peaks (summer 2014 and spring 2015), but an overall good representation of the timing and magnitude of peak flows was observed. The model was not used for the period from 2010-2011 due to the extreme runoff conditions. Estimation of low flow conditions by both models was satisfactory during the calibration period, but average streamflow was underestimated compared to observed flow during both the calibration and validation periods according to the PBIAS objective function (Table 5.1). The amount of underestimation was noticeably higher in the validation period, probably because of higher annual peak flow conditions in the validation period compared to the calibration period. SWAT-PDLD performed better than SWAT-lumped at simulating peak streamflow in both the calibration and validation periods.

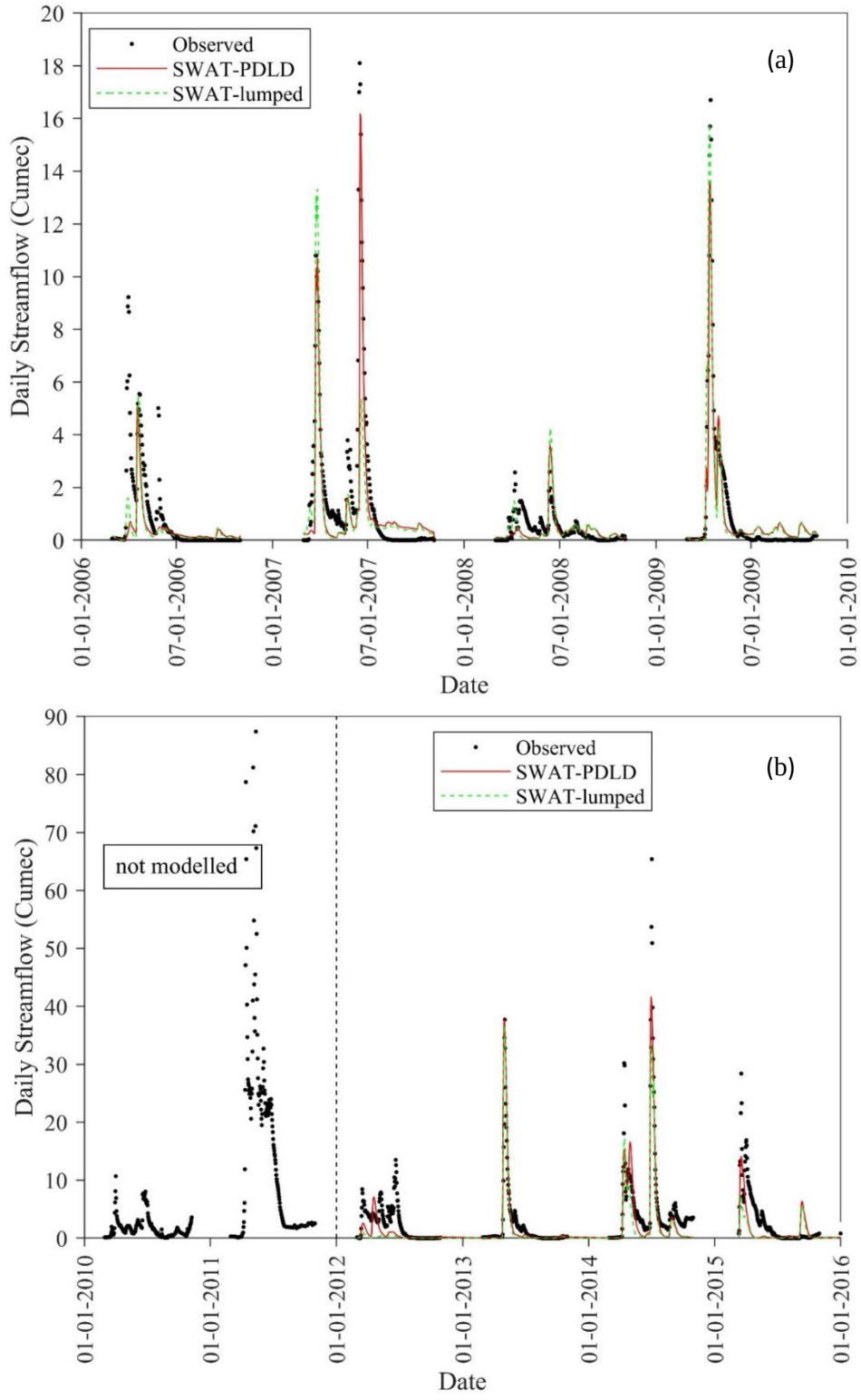


Figure 5.1: Pipestone Creek above Moosomin Lake watershed (Hydrometric Station: 05NE003) for SWAT-PDLD and the SWAT-lumped models (a) calibrated and observed daily streamflow (b) validated and observed daily streamflow.

Furthermore, the total observed flow volumes during the calibration and validation periods were underestimated by the SWAT-PDLD model by 23% and 29%, respectively. The SWAT-lumped model underestimated the observed flow volume for the calibration and validation period by 27% and 48% respectively. The loss of water mainly occurred through evapotranspiration as well as little amount of recharge for aquifers.

Figure 5.2 a) and b) presents the streamflow calibration and validation simulation results for the Lightning Creek watershed. The SWAT-PDLD model underestimated peak flows in spring (April 18, 1995; April 16, 1996; and April 4, 1997) during the calibration period, as well as in validation (again in the spring – April 1, 2015; May 20, 2015; and April 1, 2017). On the other hand, the SWAT-lumped model overestimated peak flows in the spring for the calibration period and overestimated the overall flow in the validation period. The overall performance of SWAT-PDLD is better than the SWAT-lumped model for estimating low flows and peak flows.

Table 5.1 gives a summary of the statistics used in evaluating model performance along with an interpretation of that performance based on the criteria of Moriasi *et al.* (2007). Model results are described as “very good”, “good”, “satisfactory” and “unsatisfactory” as a hierarchical order of performance based on three different objective functions: the NSE, RSR, and PBIAS. Table 5.2 provides a summary of the Moriasi *et al.* (2007) classifications for model results. Based on the three objective function values, the SWAT-PDLD and SWAT-lumped models both performed as “good” for daily streamflow calibration for the Pipestone Creek watershed. However, both models were rated as only “satisfactory” for the validation period. For the Lightning Creek Watershed, the SWAT-PDLD model also performed as “good” for the calibration period and “satisfactory” for the validation period. The SWAT-lumped model was rated as only “satisfactory” for both the calibration and validation periods.

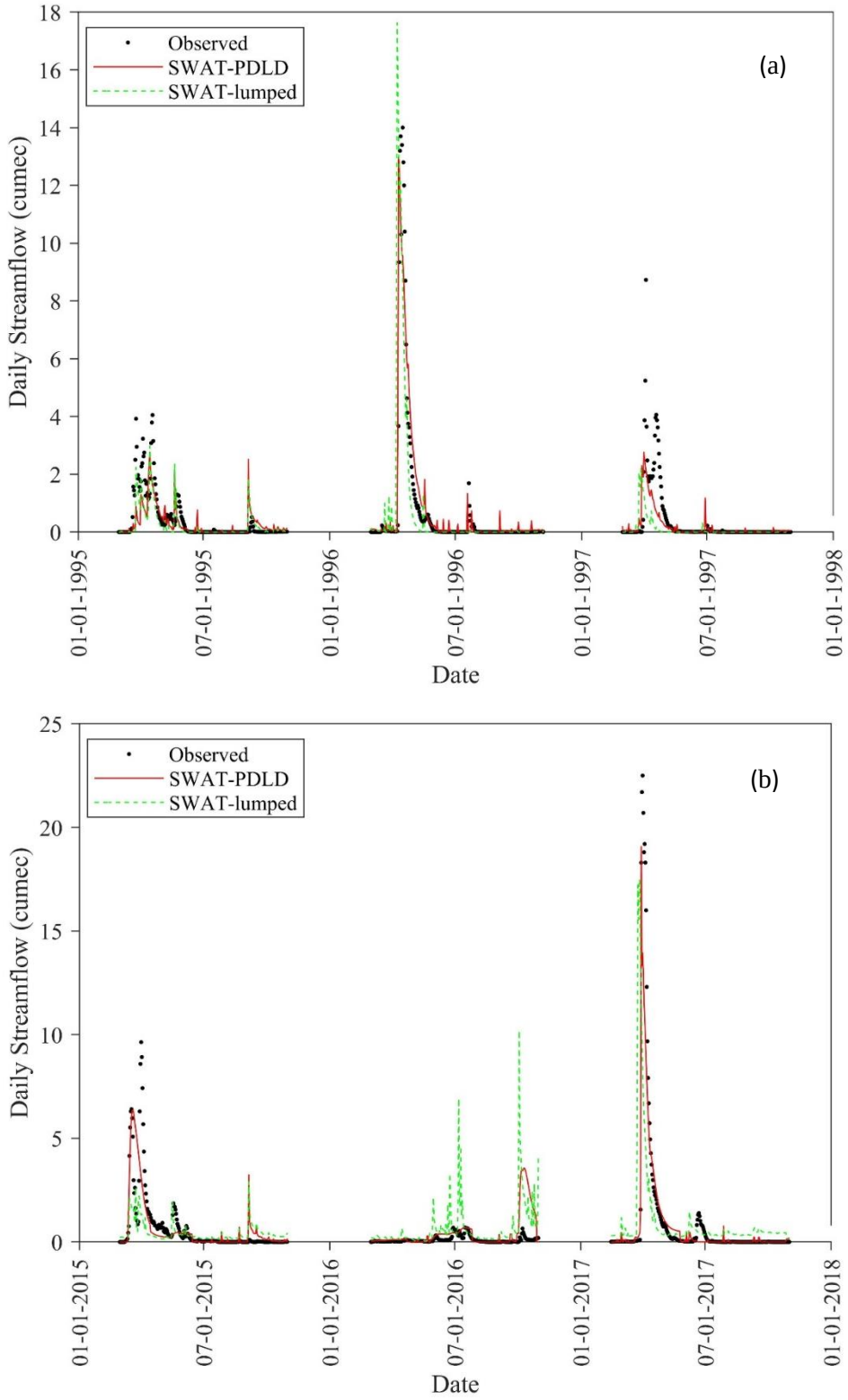


Figure 5.2: Lightning Creek near Carnduff watershed (Hydrometric Station: 05NF006) for the SWAT-PDLD and the SWAT-lumped model (a) calibrated and observed daily streamflow (b) validated and observed daily streamflow.

Table 5.1: Model performance for daily streamflow during calibration and validation periods for the Pipestone Creek and Lightning Creek watersheds.

| Model | Watershed | Simulation type | Period | NSE | RSR | PBIAS (%) | Performance rating (based on Moriasi *et al*. (2007)) |
|---|---|---|---|---|---|---|---|
| SWAT-PDLD | Pipestone Creek | Calibration | 2006-2009 | 0.72 | 0.6 | 8.0 | Good |
| | | Validation | 2012-2015 | 0.6 | 0.63 | 8.6 | Satisfactory |
| | Lightning Creek | Calibration | 1995-1997 | 0.74 | 0.42 | 9.8 | Good |
| | | Validation | 2015-2017 | 0.65 | 0.49 | 10.2 | Satisfactory |
| SWAT-lumped | Pipestone Creek | Calibration | 2006-2009 | 0.65 | 0.59 | 11.5 | Good |
| | | Validation | 2012-2015 | 0.57 | 0.6 | 19.6 | Satisfactory |
| | Lightning Creek | Calibration | 1995-1997 | 0.68 | 0.58 | 18.2 | Satisfactory |
| | | Validation | 2015-2017 | 0.55 | 0.59 | -17.3 | Satisfactory |

Table 5.2: Performance ratings for model output statistics (Moriasi *et al.* 2007).

| Performance Rating | NSE | RSR | PBIAS | | |
|---|---|---|---|---|---|
| | | | Streamflow | Sediment | N,P |
| Very Good | 0.75-1.00 | 0.00-0.50 | <±10 | <±15 | <±25 |
| Good | 0.65-0.75 | 0.50-0.60 | ±10 to ±15 | ±15 to ±30 | ±25 to ±40 |
| Satisfactory | 0.5-0.65 | 0.60-0.70 | ±15 to ±25 | ±30 to ±55 | ±40 to ±70 |
| Unsatisfactory | ≤ 0.50 | > 0.70 | > ±25 | > ±55 | > ±70 |

Unfortunately, no satisfactory calibration results were found for the Swift Current Creek watershed. A plot of the streamflow simulation results for this watershed is given in Figure 5.3. The peak flows estimated by both the SWAT-PDLD and the SWAT-lumped model were close to the observed peak flows for some cases, but both models predicted zero flows during spring seasons, which is unexpected. It is common to get higher streamflow during the spring season in the prairie region due to snowmelt (Pomeroy *et al.* 1998, Fang and Pomeroy 2007). Moreover, the model performance metrics for SWAT-PDLD (NSE=0.39, RSR=0.7, PBIAS=71%) and SWAT-

lumped (NSE=0.21, RSR=0.89, PBIAS=82.5%) both showed that the model performance was "unsatisfactory".

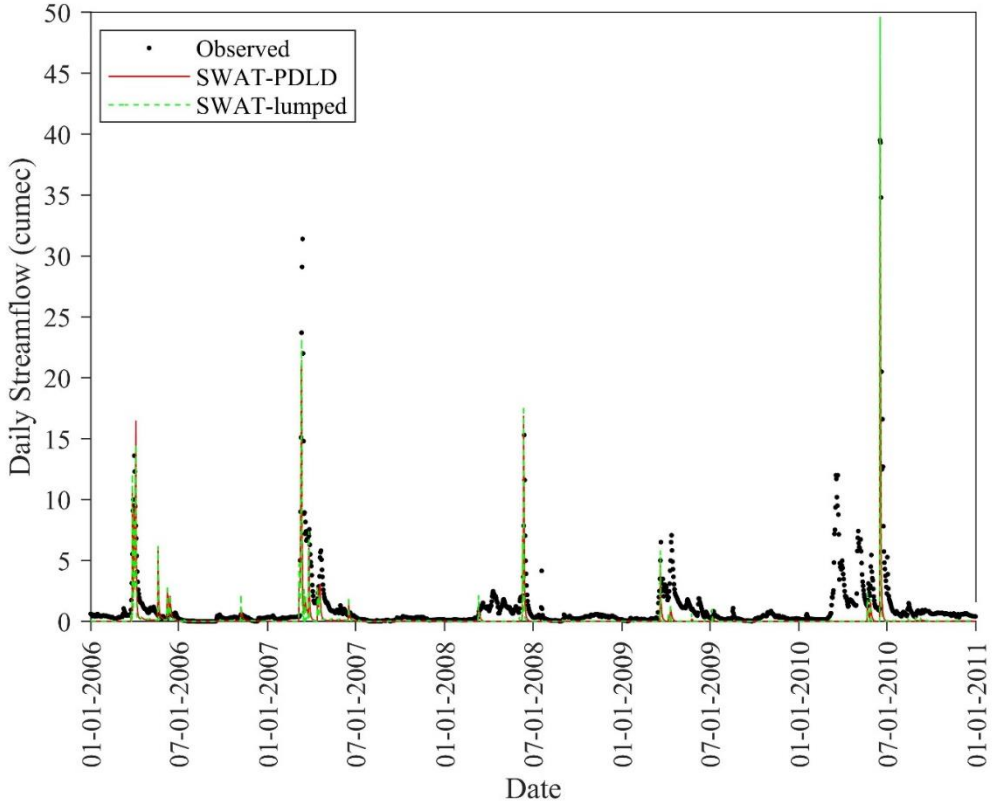


Figure 5.3: Daily streamflow simulation (calibration) of the SWAT-PDLD and SWAT-lumped models for the Swift Current Creek below Rock Creek watershed (Hydrometric Station: 05HD036).

The streamflow of the Swift Current Creek watershed originates from spring runoff and groundwater springs (Rowan *et al*. 2011). The model failed to predict the base flows during spring and summer periods and estimated near zero base flows. The groundwater parameters of the model somehow failed to estimate the recharge and discharge rate of the groundwater aquifers that affected the base flows. Parameters related to the threshold depth of the shallow aquifer for return flow, movement of water between the shallow aquifer and the overlying zone and groundwater flow response to changes in recharge might be the primary responsible factors behind the erroneous base flow.

The Swift Current Creek watershed is warmer than other two prairie watersheds of this study. The annual average temperature is 4.1°C, which is higher than the annual average temperature for the other two watersheds (Pipestone Creek and Lightning Creek watershed) in this study. The watershed is characterized by low precipitation and high evaporation (Peters and Steinley 2018). Compare to other two watersheds, less annual average precipitation has been observed here, which was 352 mm (2006-2017).

In addition, the input gridded data for total precipitation during 2006 and 2008 underestimated the recorded observed precipitation of the Swift Current Creek region. The recorded average annual precipitation from 2006 to 2010 for this watershed was 369.7 mm (Canada Weather Stats 2019); however, the observed (gridded) average annual precipitation that was used in the model was 322 mm. This is likely another important factor behind the low simulated runoff during spring. It is also interesting to note that modelling the watershed with observed precipitation data was tried, but that generated poorer simulation results than those found from gridded data. Recently, Peters and Steinley (2018) indicated annual average evaporation of the Swift Current Creek watershed was 270 mm for the year of 2017. However, the SWAT-lumped and SWAT-PDLD models both overestimated the annual average actual evaporation (around 380 mm), which is a large source of water loss.

In a sum, the zero base flows during spring period might be a reason of inappropriate input precipitation data and overestimated evapotranspiration by the model.

### 5.3 Water Quality Modelling

Like streamflow modeling, the model calibration parameters for water quality modeling were identified based on the results of a sensitivity analysis (Table 4.2). Similarly, the calibration of

water quality model were started with initial parameter values selected within a theoretical permissible range (upper and lower limit) based upon a literature review (Mekonnen *et al.* 2016c).

### 5.3.1 Sediment Export

Daily calibrated and validated sediment export simulations for the Pipestone Creek watershed are plotted in Figure 5.4 a) and b). Both models underestimated the peak sediment export in the spring of 2009 but were reasonably able to predict the sediment export during lower flow conditions. The SWAT-PDLD model achieved a performance rating of "good" for both the calibration and validation periods (see Table 5.3). However, the SWAT-lumped model provided only "satisfactory" performance during both the calibration and validation periods. The SWAT-PDLD model performed better than the SWAT-lumped model likely because of its seasonal soil erodibility factor, which would better represent the seasonal erosion in the watershed.

SWAT-PDLD also achieved a performance rating of "good" for the Lightning Creek watershed in simulating daily sediment export during both the calibration and validation periods (Figure 5.5 a) and b)) based on model performance parameters (Table 5.3). However, the SWAT-lumped model was only able to achieve a "satisfactory" rating for the calibration period, but a "good" rating for the validation period.

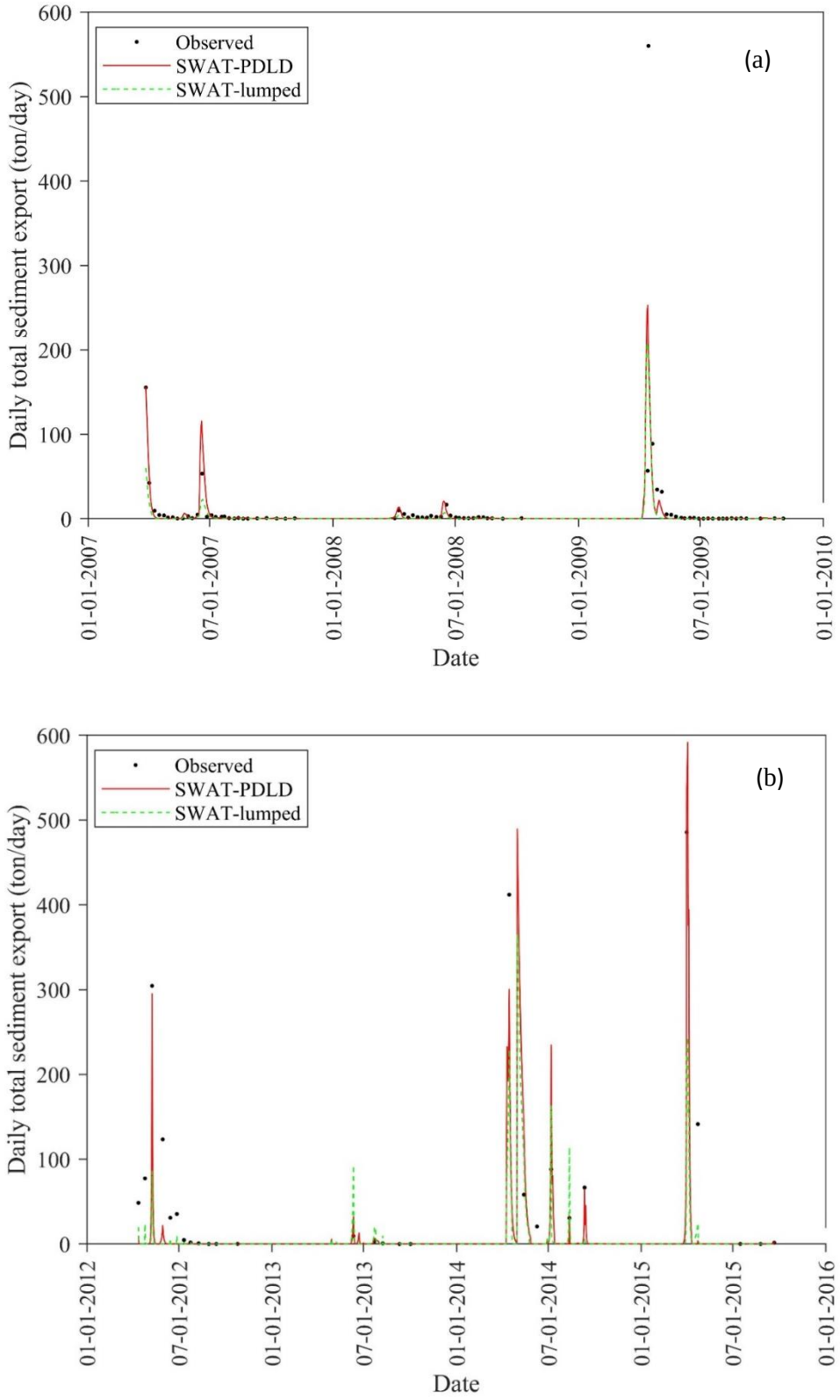


Figure 5.4: Pipestone Creek above Moosomin Lake watershed (WQ Station: SK05NE0091) for SWAT-PDLD and the SWAT-lumped model (a) calibrated and observed daily sediment export (b) validated and observed daily sediment export.

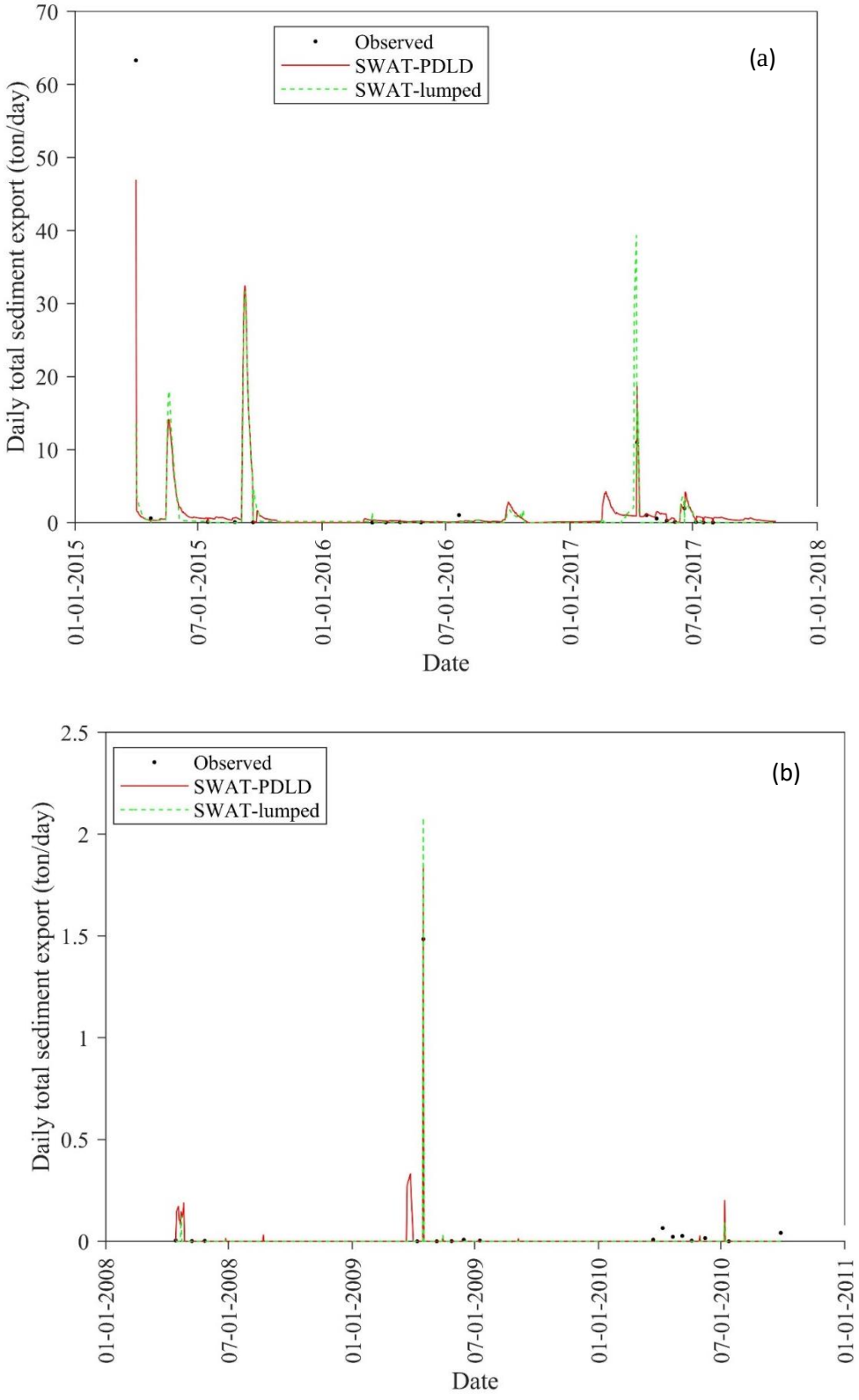


Figure 5.5: Lightning Creek near Carnduff watershed (WQ Station: SK05NF0124) and the SWAT-PDLD and SWAT-lumped models (a) calibrated and observed daily sediment export and (b) validated and observed daily sediment export.

Table 5.3: Model performance for daily total sediment export for calibration and validation periods.

| Model | Watershed | Simulation type | Period | NSE | RSR | PBIAS (%) | Performance rating (based on Moriasi *et al.* (2007)) |
|---|---|---|---|---|---|---|---|
| SWAT-PDLD | Pipestone Creek | Calibration | 2007-2009 | 0.68 | 0.59 | 28.32 | Good |
| | | Validation | 2012-2015 | 0.75 | 0.44 | 14.9 | Good |
| | Lightning Creek | Calibration | 2015-2017 | 0.67 | 0.58 | -18.9 | Good |
| | | Validation | 2008-2010 | 0.8 | 0.26 | -16.5 | Good |
| SWAT-lumped | Pipestone Creek | Calibration | 2007-2009 | 0.6 | 0.63 | 54.1 | Satisfactory |
| | | Validation | 2012-2015 | 0.55 | 0.65 | 36.6 | Satisfactory |
| | Lightning Creek | Calibration | 2015-2017 | 0.65 | 0.56 | 53.2 | Satisfactory |
| | | Validation | 2008-2010 | 0.7 | 0.42 | -23.6 | Good |

In both watersheds, as would be expected, the observed sediment export was related to streamflow and peak sediment export was observed during peak flow. In the Pipestone Creek watershed, both models underestimated the sediment export during the calibration and validation period according to the statistical metrics. However, in the Lightning Creek watershed, SWAT-PDLD overestimated the sediment export for the calibration and validation periods during which streamflow was also overestimated.

### 5.3.2 Total Phosphorus Export

Figures 5.6 a) and b) and 5.7 a) and b) present the simulation results for daily total phosphorus export in comparison to observed values for the Pipestone Creek and Lightning Creek watersheds respectively. From these figures and the model performance statistical metrics (Table 5.4) it can

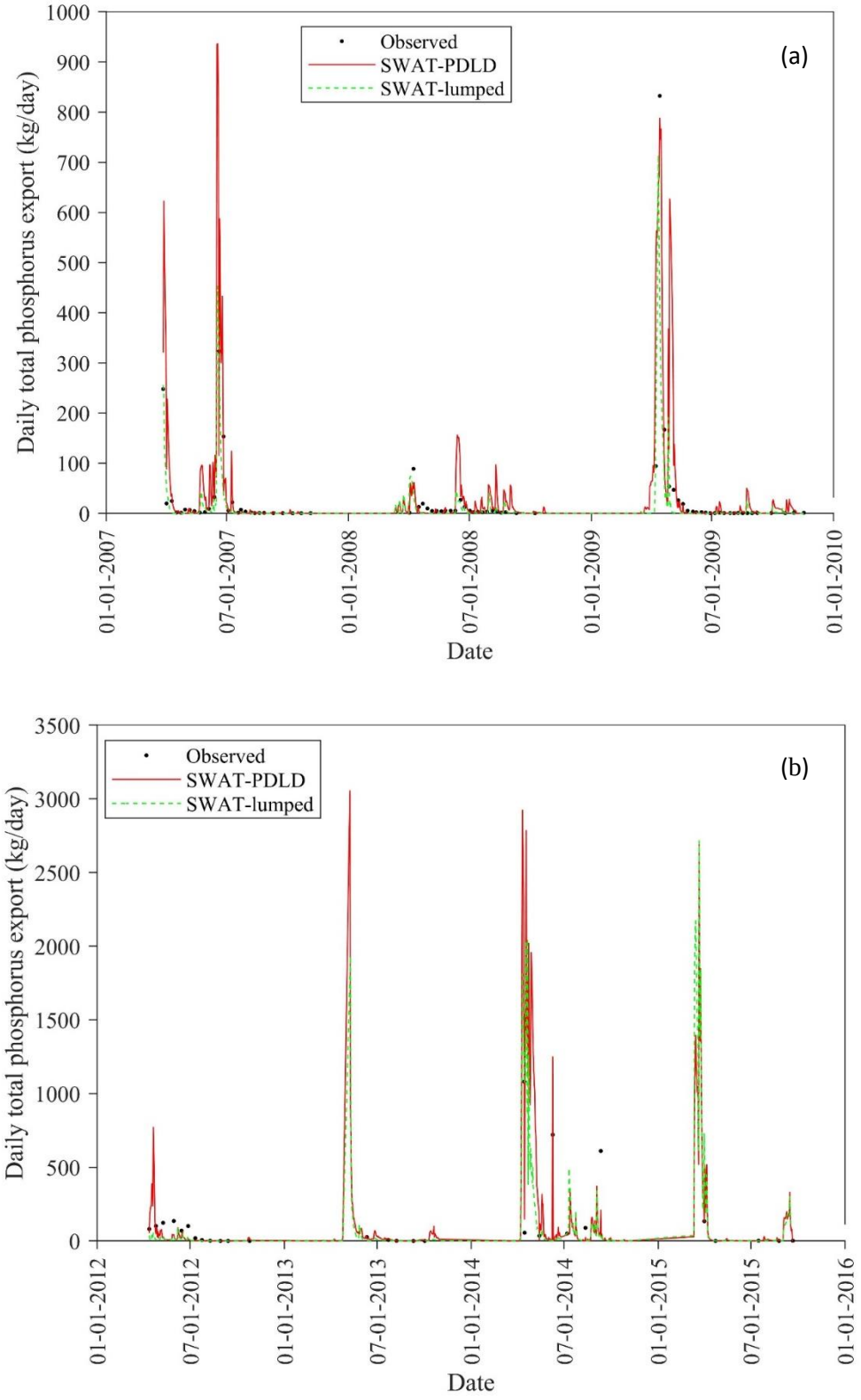


Figure 5.6: Pipestone Creek above Moosomin Lake watershed (WQ Station: SK05NE0091) and the SWAT-PDLD and SWAT-Lumped models (a) calibrated and observed daily total phosphorus export (b) validated and observed daily total phosphorus export.

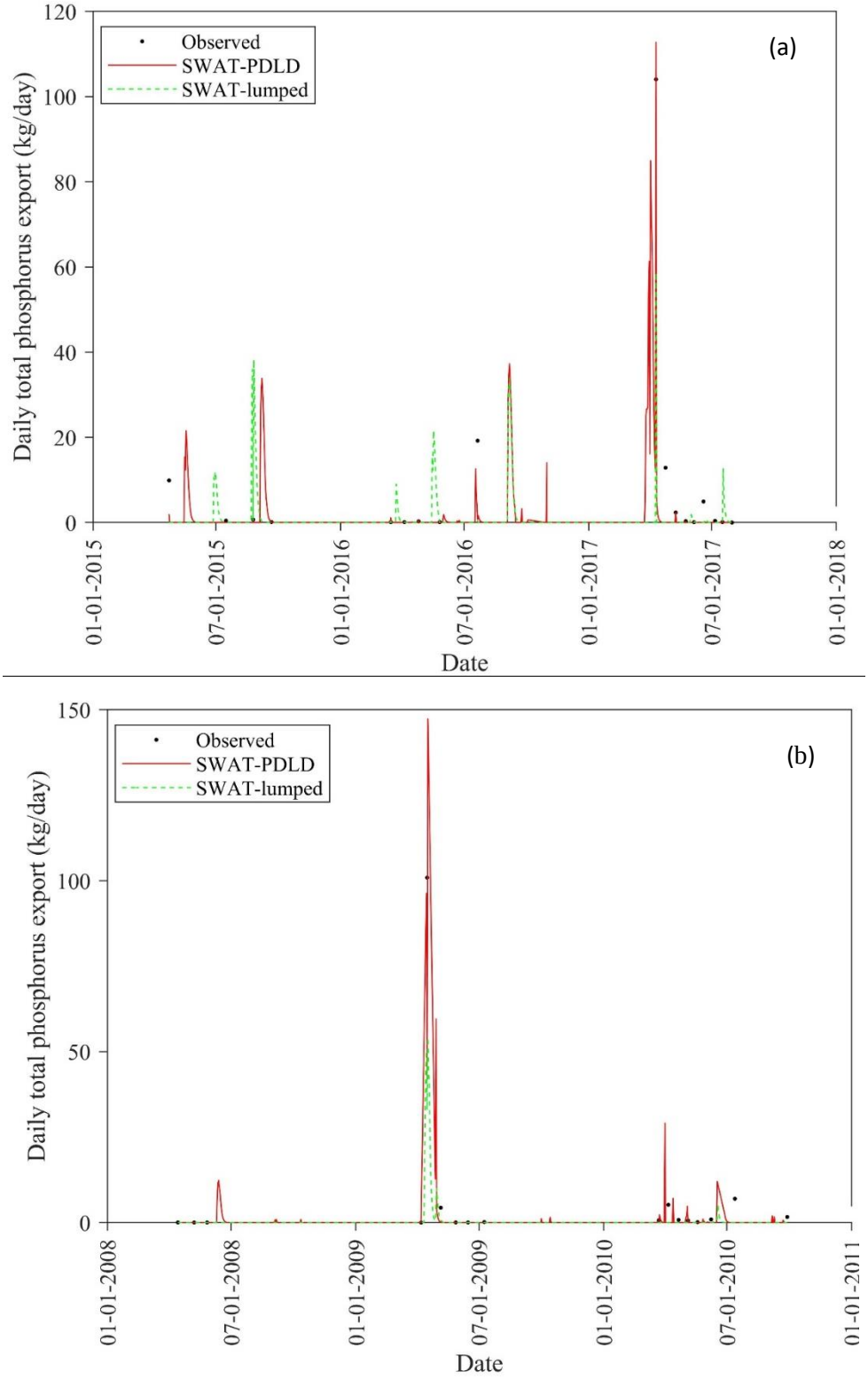


Figure 5.7: Lightning Creek near Carnduff watershed (WQ Station: SK05NF0124) and the SWAT-PDLD and SWAT-lumped models (a) calibrated and observed daily total phosphorus export (b) validated and observed daily total phosphorus export.

be concluded that the SWAT-PDLD model better predicted total phosphorus export than the SWAT-lumped model. This is expected based upon the sediment export model simulation performance because total phosphorus export is highly connected to sediment movement (Mekonnen et al. 2016c). The SWAT-PDLD model achieved a performance rating of "good" for both the calibration and validation periods (Table 5.4) for both watersheds. The SWAT-lumped model only achieved "satisfactory" rating according to the statistical metrics for both watersheds (Table 5.4).

Table 5.4: Model performance for daily total phosphorus export for the calibration and validation periods.

| Model | Watershed | Simulation type | Period | NSE | RSR | PBIAS (%) | Performance rating (based on Moriasi *et al.* (2007)) |
|---|---|---|---|---|---|---|---|
| SWAT-PDLD | Pipestone Creek | Calibration | 2007-2009 | 0.73 | 0.41 | 15.4 | Good |
| | | Validation | 2012-2015 | 0.65 | 0.43 | 5.1 | Good |
| | Lightning Creek | Calibration | 2015-2017 | 0.77 | 0.48 | 25.1 | Good |
| | | Validation | 2008-2010 | 0.62 | 0.22 | 31.9 | Good |
| SWAT-lumped | Pipestone Creek | Calibration | 2007-2009 | 0.7 | 0.44 | 47.5 | Satisfactory |
| | | Validation | 2012-2015 | 0.65 | 0.59 | 58.3 | Satisfactory |
| | Lightning Creek | Calibration | 2015-2017 | 0.73 | 0.52 | 61.4 | Satisfactory |
| | | Validation | 2008-2010 | 0.55 | 0.61 | 65.4 | Satisfactory |

It was challenging to visually compare the SWAT-PDLD and SWAT-lumped models to observed data for the Lightning Creek watershed due to the limited number of observations. Based

on the model statistical performance parameters (Table 5.4), the SWAT-PDLD model achieved a rating of "good" for both the calibration and validation periods. As for Pipestone Creek, in simulating the Lightning Creek watershed, the SWAT-lumped model was only able to achieve a performance rating of "satisfactory" for both the calibration and validation periods.

### 5.3.3 Total Nitrogen Export

Simulation results for daily total nitrogen export have been plotted in Figures 5.8 (a and b) and 5.9 (a and b) for the Pipestone Creek and Lightning Creek watersheds respectively. Here, the SWAT-PDLD model better represented total nitrogen export during the calibration period of both Pipestone Creek and Lightning Creek watersheds as compared to the SWAT-lumped model. Performance was rated as "good" (Table 5.5). Due to the sparse observed data, model performance is not obvious from the visual presentation of the model results during the validation period of both watersheds. During the validation period, SWAT-PDLD is rated as "good" for both watersheds. The SWAT-lumped model underestimated the observed data and rated as "good" for the calibration period of the Pipestone Creek watershed and "satisfactory" for the validation period. The SWAT-lumped model rated as "satisfactory" for both calibration and validation period of Lightning Creek watershed.

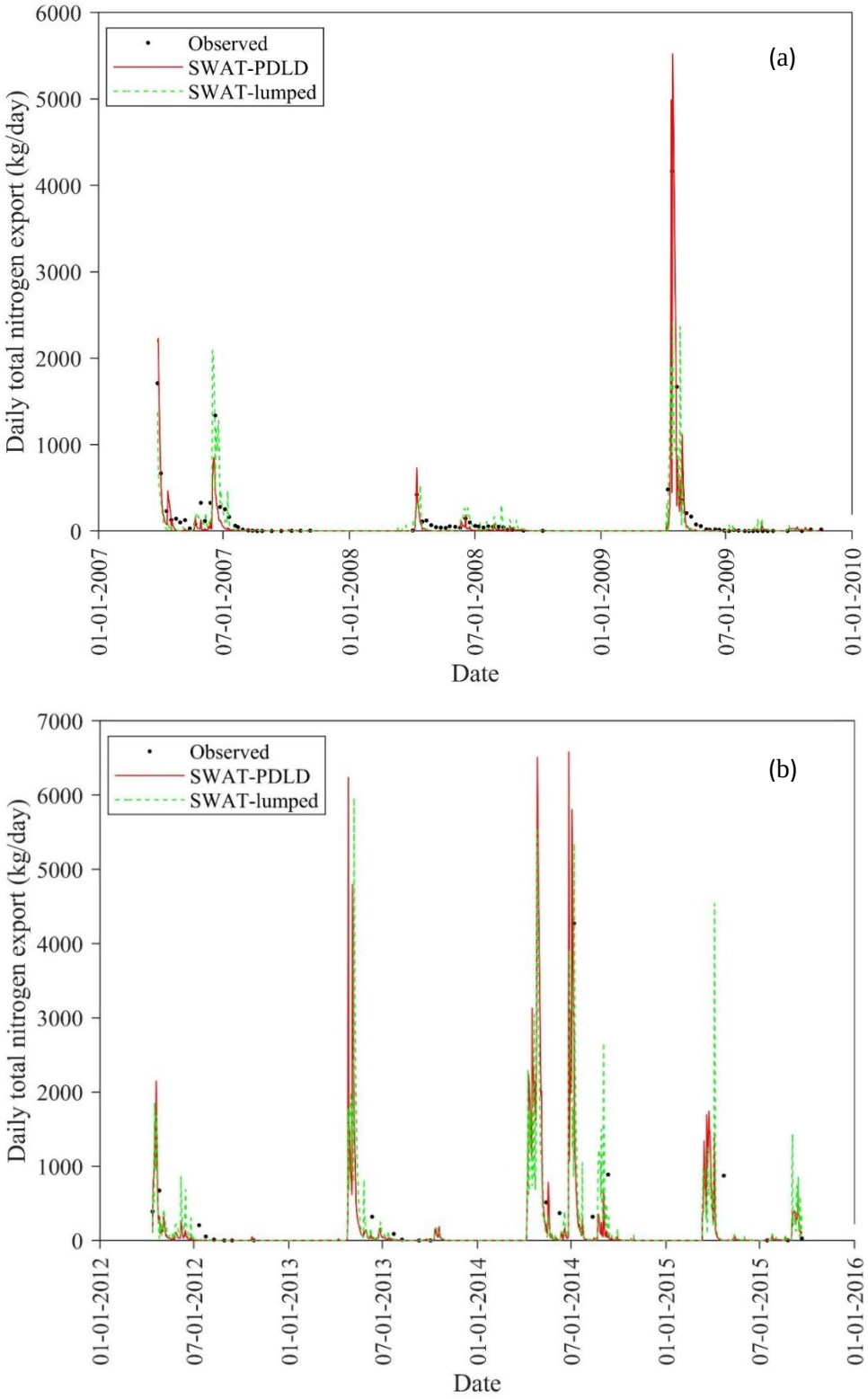


Figure 5.8: Pipestone Creek above Moosomin Lake watershed (WQ Station: SK05NE0091) and the SWAT-PDLD and SWAT-lumped models (a) calibrated and observed daily total nitrogen export (b) validated and observed daily total nitrogen export.

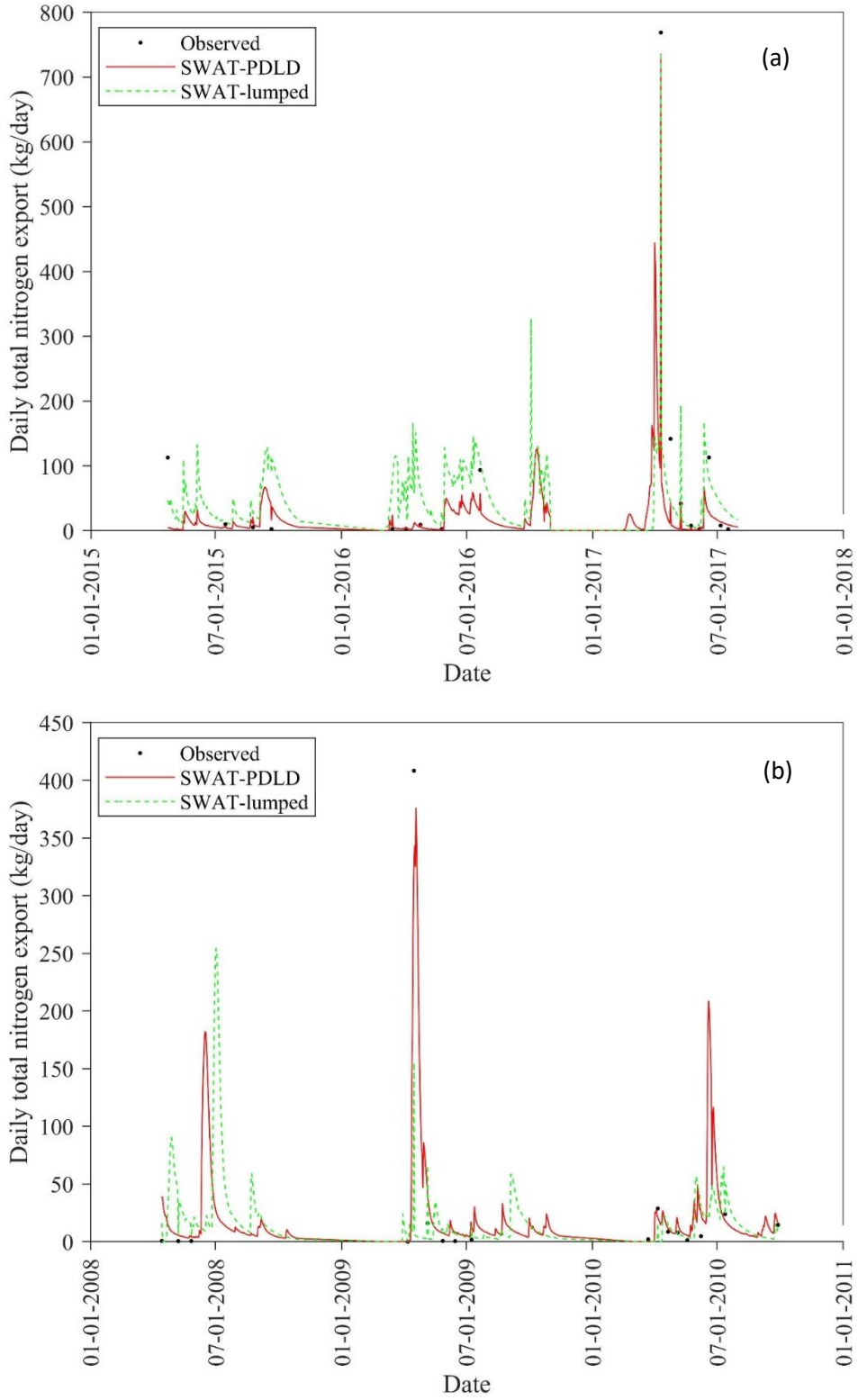


Figure 5.9: Lightning Creek near Carnduff watershed (WQ Station: SK05NF0124) and the SWAT-PDLD and SWAT-lumped models (a) calibrated and observed daily total nitrogen export (b) validated and observed daily total nitrogen export.

Table 5.5: Model performance for daily total nitrogen export.

| Model | Watershed | Simulation type | Period | NSE | RSR | PBIAS (%) | Performance rating (based on Moriasi *et al.* (2007)) |
|---|---|---|---|---|---|---|---|
| SWAT-PDLD | Pipestone Creek | Calibration | 2007-2009 | 0.73 | 0.37 | 22.6 | Good |
| | | Validation | 2012-2015 | 0.62 | 0.5 | 31.2 | Good |
| | Lightning Creek | Calibration | 2015-2017 | 0.68 | 0.53 | 13.6 | Good |
| | | Validation | 2008-2010 | 0.72 | 0.25 | 9.2 | Good |
| SWAT-lumped | Pipestone Creek | Calibration | 2007-2009 | 0.65 | 0.56 | 38.4 | Good |
| | | Validation | 2012-2015 | 0.61 | 0.6 | 51.3 | Satisfactory |
| | Lightning Creek | Calibration | 2015-2017 | 0.65 | 0.53 | -60.5 | Satisfactory |
| | | Validation | 2008-2010 | 0.56 | 0.68 | 27.7 | Satisfactory |

## 5.4 Water Quality during Spilling and Non-Spilling Periods

The second objective of this study was to determine when depressions were spilling and non-spilling using the SWAT-PDLD model and then to examine whether there are any differences in the relationship between streamflow and water quality between spilling and non-spilling periods. Spilling periods can be found from the water balance of depressions given in the SWAT-PDLD model output; the model outputs the daily amount of flow from the ponds.

Initially, a spilling period was deemed to occur when the pond outflow is more than zero. A non-spilling period was considered for the alternate cases (zero outflow). However, to better define a spilling period, the ratio of the cumulative pond outflow to streamflow in a day was instead

considered. Here, the pond outflow is that generated by the model and the streamflow is the measured streamflow at the site. Several different percentage contributions of the pond outflow to the streamflow were tried as the criterion to decide when the ponds would be considered "spilling" in order to test the impact on results: 1%, 2%, 5%, 10% and 20%. The choice of percent contribution as a criterion greatly affected the number of days that were considered spilling and the number of available water quality measurements taken in spilling periods.

Table 5.6 shows the number of days that ponds were spilling according to a range of % contribution criteria, and the number of water quality measurements for Pipestone Creek and Lightning Creek watersheds on spilling days. For example, for the Pipestone Creek watershed and when criteria of 5% contribution was used, there were a total of 252 days with pond spilling during 2007-2018. However, there were only 16 spilling days with available water quality data out of the 256 spilling days.

For the Lightning Creek watershed, water quality observations were limited in number compared to the Pipestone Creek watershed. A total of only 49 water quality observations were available from 2008-2017 (no streamflow was available beyond 2017). However, water quality observations were only available for 6 spilling days among the 159 spilling days that occurred for the 5% contribution criteria. Further, the spilling days with water quality measurements were poorly distributed over the percent contribution categories. The number of water quality observations available for spilling days defined by the 1%, 2%, and 5% contribution to streamflow were the same; similarly, the number of water quality observations for the 10% and 20% contribution to streamflow were the same.

Table 5.6: Summary of spilling days and available water quality observations

| Category | Pipestone Creek Watershed (2007-2018) | | | | | Lightning Creek Watershed (2008-2017) | | | | |
|---|---|---|---|---|---|---|---|---|---|---|
| Pond contribution (%) | 1% | 2% | 5% | 10% | 20% | 1% | 2% | 5% | 10% | 20% |
| Spilling days | 346 | 299 | 252 | 216 | 176 | 258 | 209 | 159 | 124 | 93 |
| Available water quality measurements (for spilling days) | 29 | 29 | 16 | 10 | 8 | 6 | 6 | 6 | 3 | 3 |
| Total available water quality measurements (days) | 157 | | | | | 49 | | | | |

### 5.4.1 Streamflow versus Water Quality in the Lightning Creek Watershed

Daily streamflow versus sediment export, total phosphorus, and total nitrogen plots are presented separately in Figures 5.10 to 5.12 for the Lightning Creek watershed. It has been noticed that water quality observations under spilling condition were found mainly during low flow periods. There were some cases in 2013-2014 where spilling periods were found during high flow conditions, however observed water quality data was not available at that time. For sediment export in this watershed, there is no observable difference in the sediment load between periods of spilling and non-spilling. This is perhaps reasonable because ponds would tend to act as a sediment sink. Similarly, there was no observable difference between spilling and non-spilling periods in total phosphorus loads. This is shown in Figure 5.11.

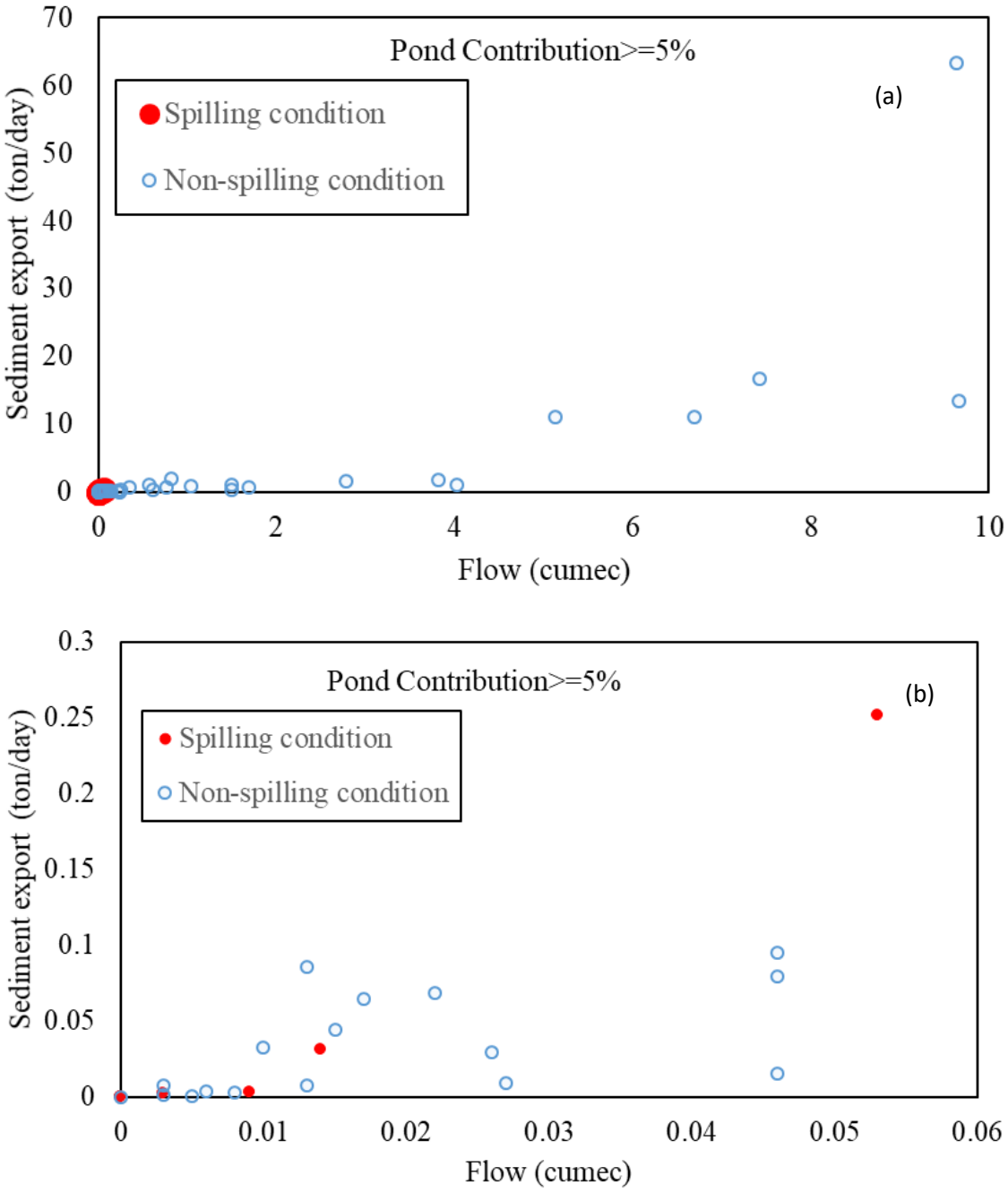


Figure 5.10: Relation between daily streamflow and sediment export during spilling and non-spilling conditions for Lightning Creek near Carnduff watershed (a) full flow range observed (5% pond contribution) (b) low flow conditions (5% pond contribution) (c) full flow range(20% pond contribution) (d) low flow condition (20% pond contribution)

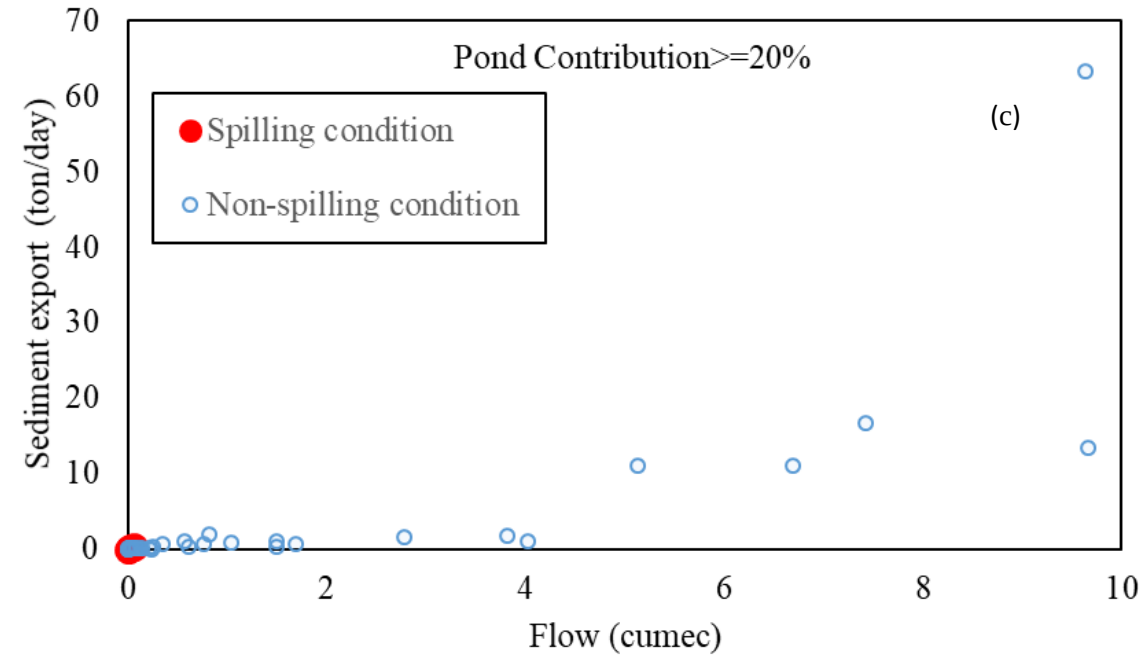


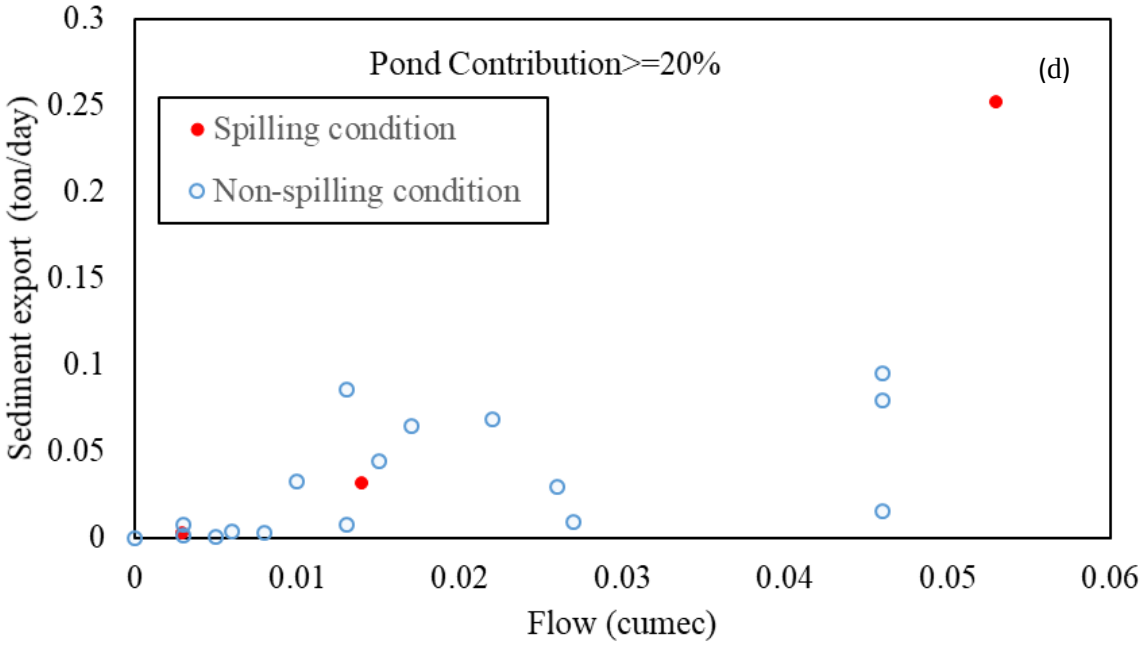


Figure 5.10 continued

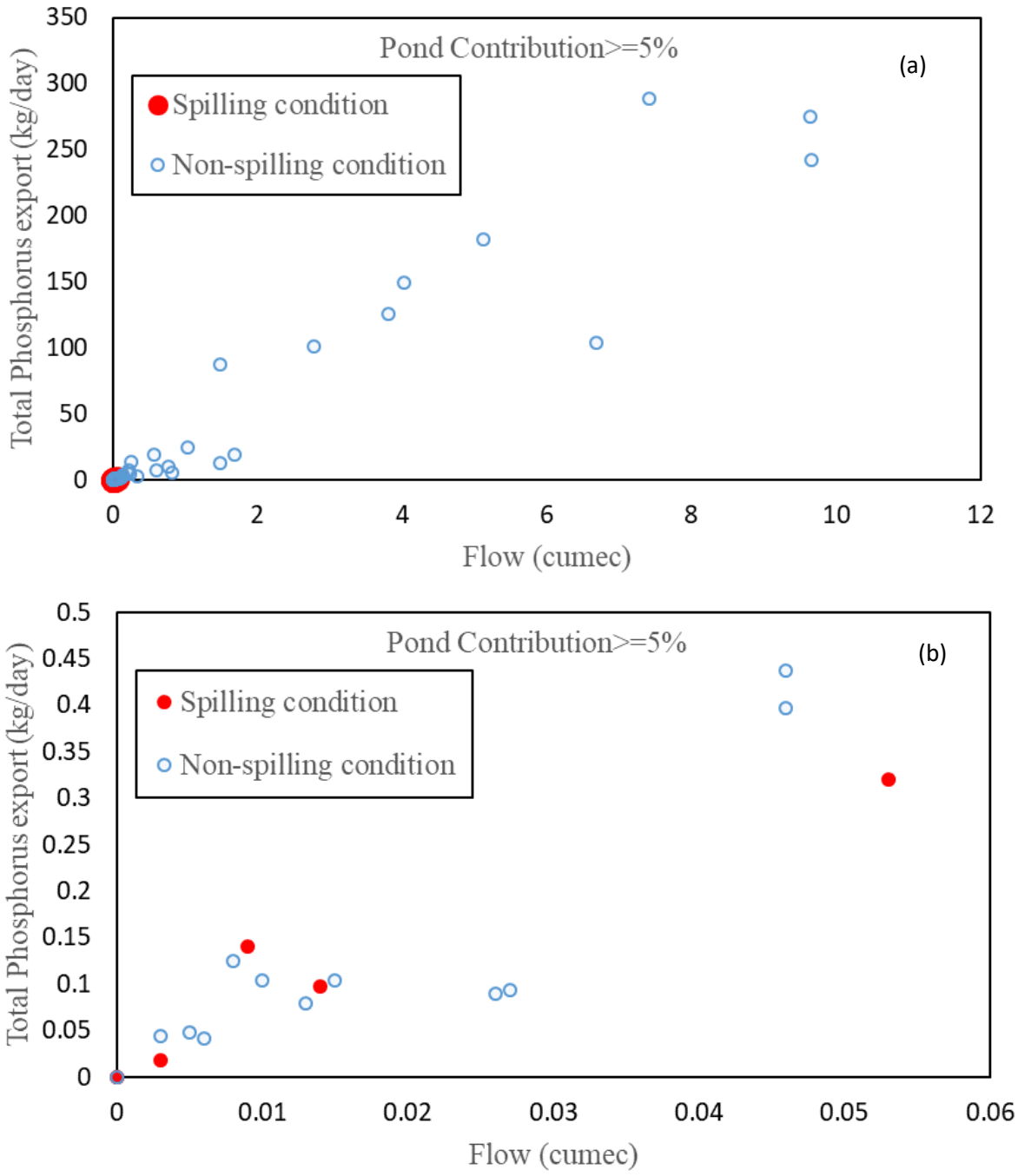


Figure 5.11: Relation between daily streamflow and total phosphorus export during spilling and non-spilling conditions for Lightning Creek near Carnduff watershed (a) considering all flow condition (5% pond contribution) (b) low flow condition (5% pond contribution) (c) considering all flow condition (20% pond contribution) (d) low flow condition (20% pond contribution)

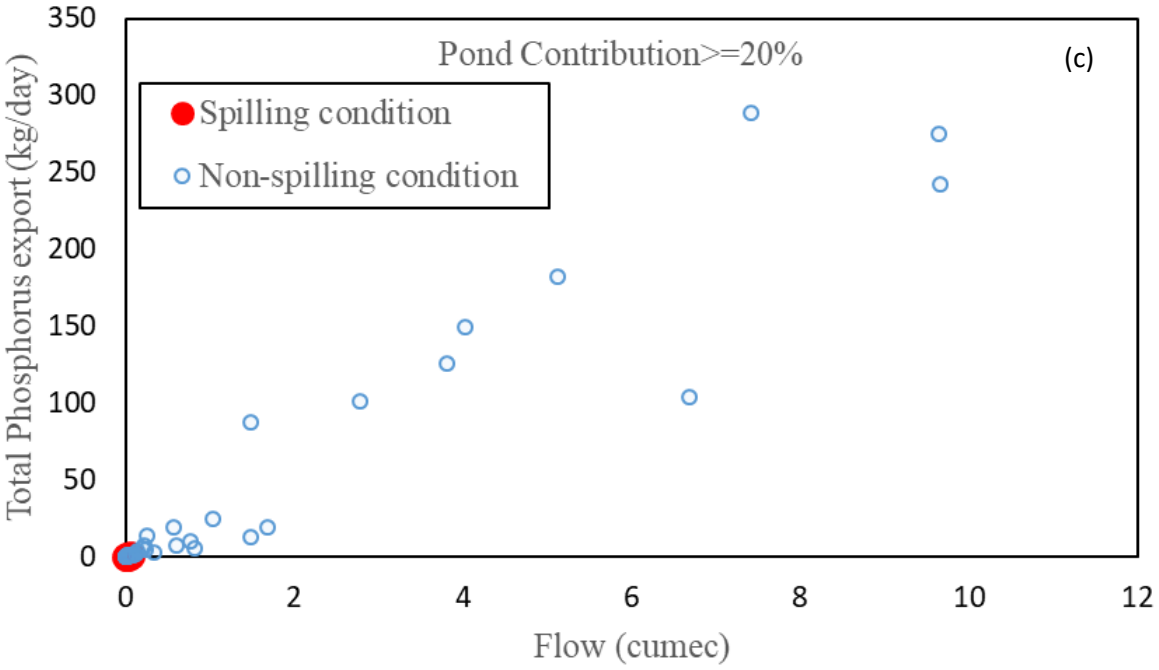


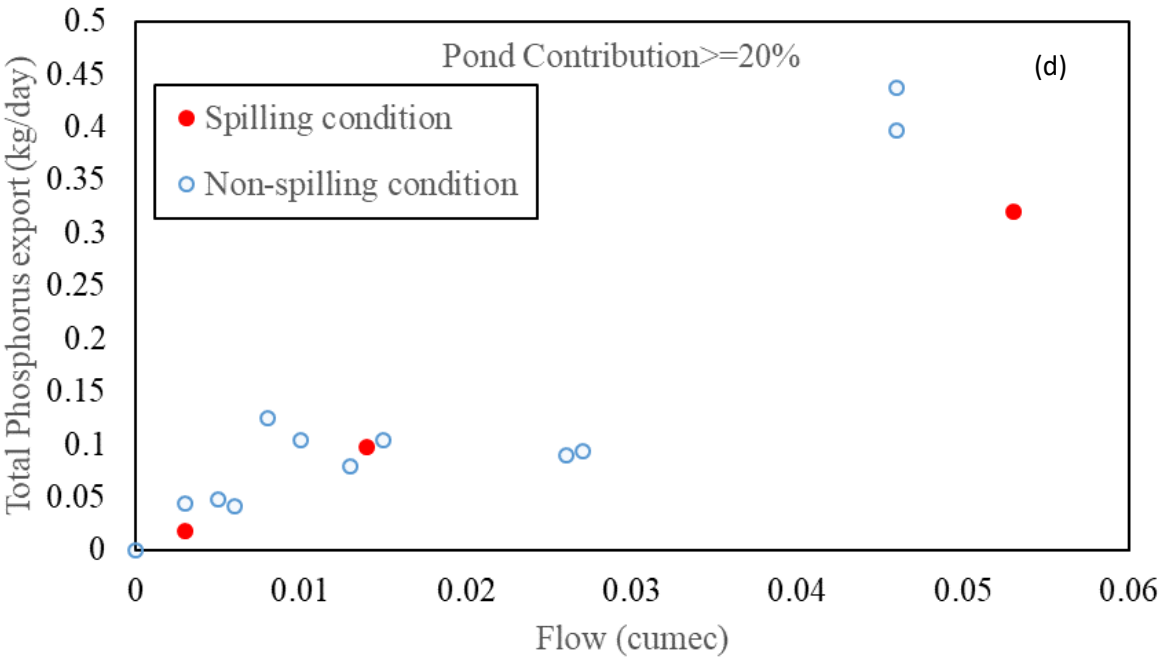


Figure 5.11 continued

However, a different observation was made for total nitrogen export (Figure 5.12). Even for the different pond percentage contributions to streamflow, the volume of total nitrogen export was

clearly higher for spilling than non-spilling conditions. It should be noted again that the observations of water quality where taken during spilling periods during times of low flow.

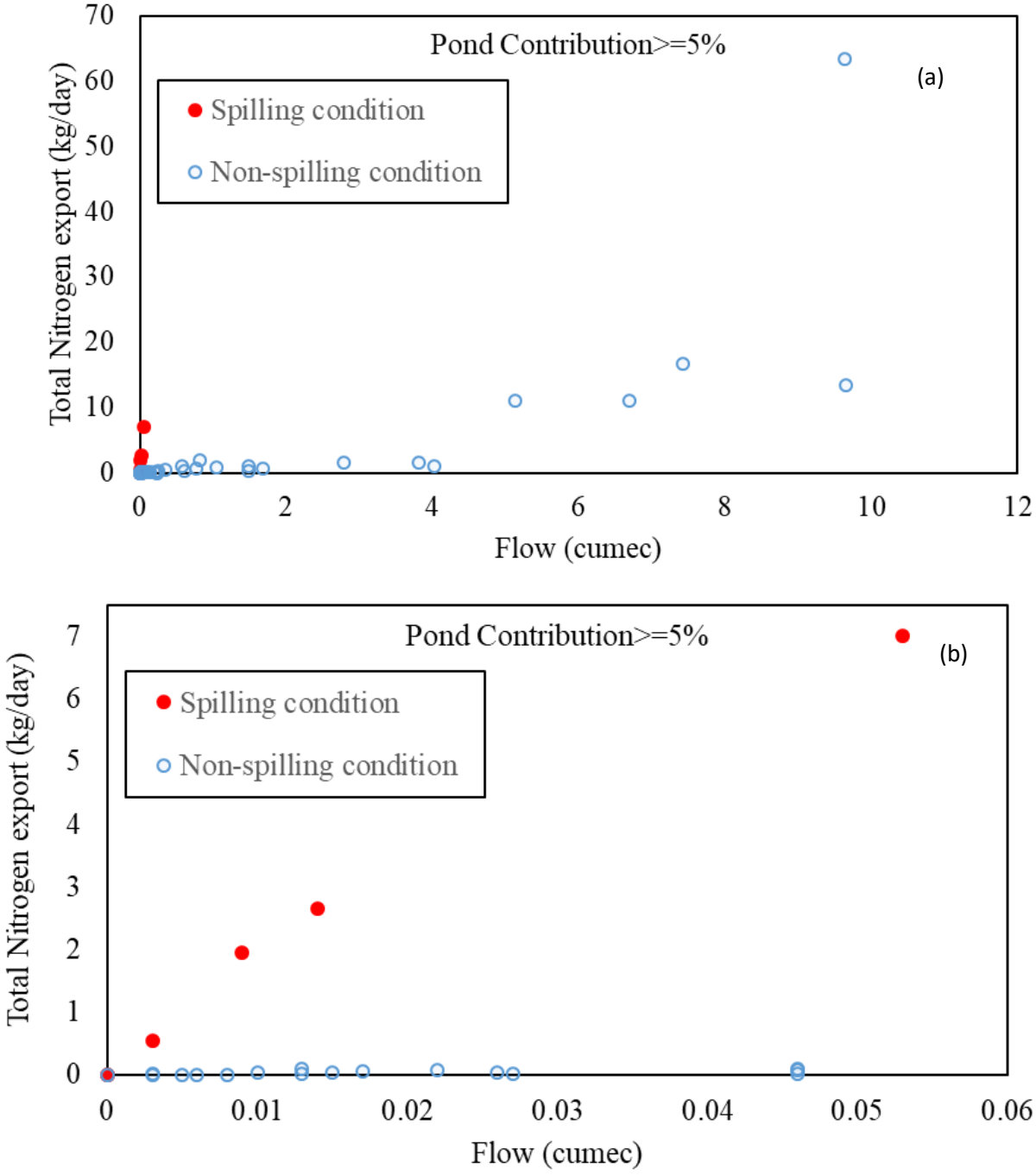


Figure 5.12: Relation between daily streamflow and total nitrogen export during spilling and non-spilling conditions for Lightning Creek near Carnduff watershed (a) full flow range (5% pond contribution) (b) low flow conditions (5% pond contribution) (c) full flow range (20% pond contribution) (d) low flow conditions (20% pond contribution)

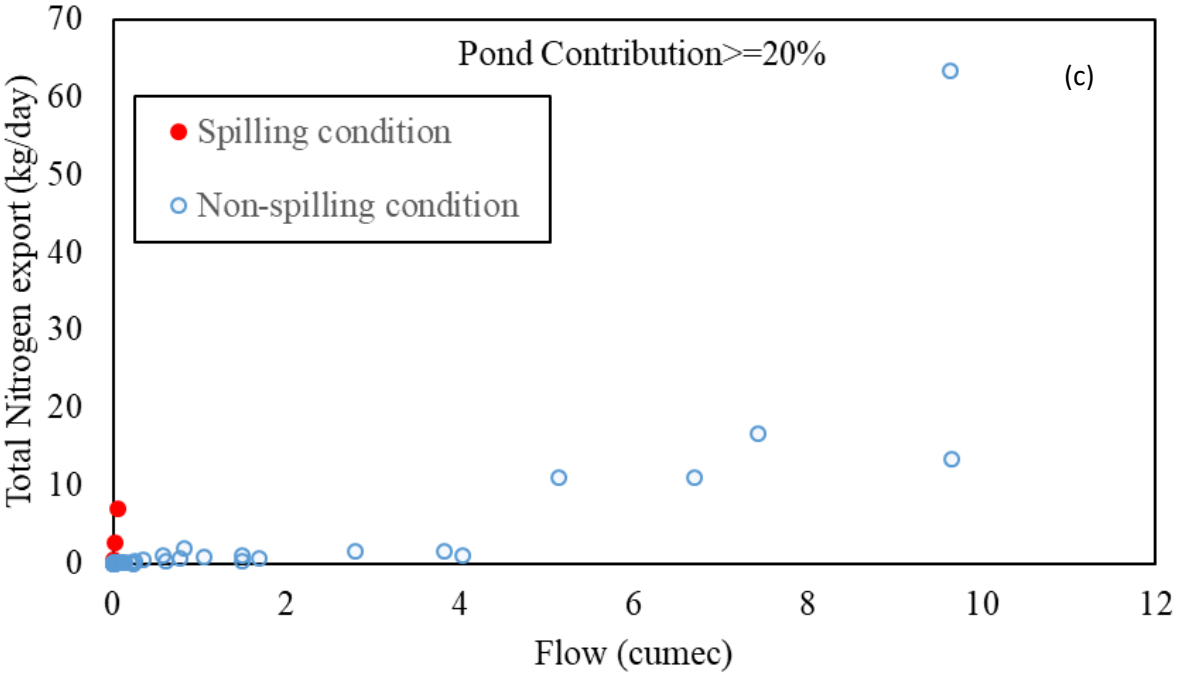


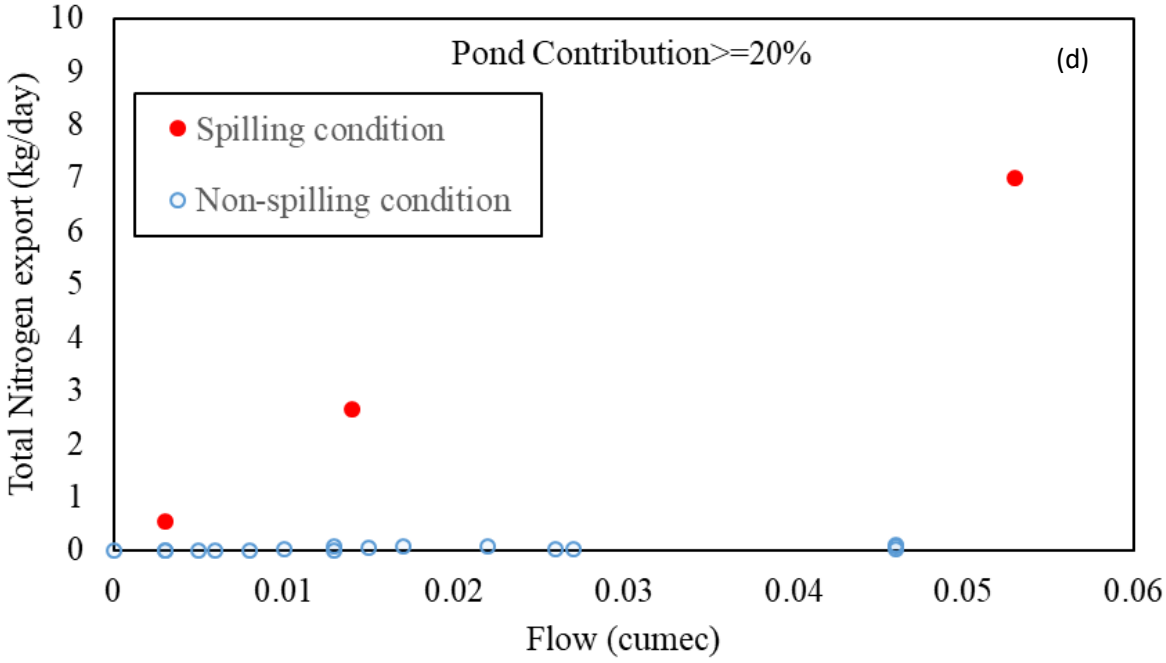


Figure 5.12 continued

### 5.4.2 Streamflow versus Water Quality in the Pipestone Creek Watershed

Observed sediment export versus streamflow during spilling and non-spilling periods are shown for the Pipestone Creek watershed in Figure 5.13. Unlike the Lightning Creek watershed, water quality observations (sediment, total phosphorus and total nitrogen export) during spilling periods were available for both high and low flow periods for Pipestone Creek for pond contributions to streamflow up to 5%. It is interesting to note that many of the spilling periods for low flows occurred during the later period of the year (July-October). Also, the sediment measurements that were taken during higher pond contributions to streamflow (greater than 20%) were for the low flow conditions. There also appears to be a range of flows for which no spilling was observed. In Figure 5.13, this appears to be from about 2 to 8 $m^3/s$. This was checked for all results where the model showed contribution to streamflow. Overall, there was no indication that sediment export was increased or decreased during spilling periods.

Figures 5.14 and 5.15 shows the observed streamflow versus total phosphorus export and nitrogen export for the Pipestone Creek watershed respectively. Like the Lightning Creek watershed, spilling from ponds does not appear to impact the total phosphorus export in the stream. However, unlike the Lightning Creek watershed, this also appears to be case for nitrogen export; spilling does not appear to impact nitrogen export in the watershed.

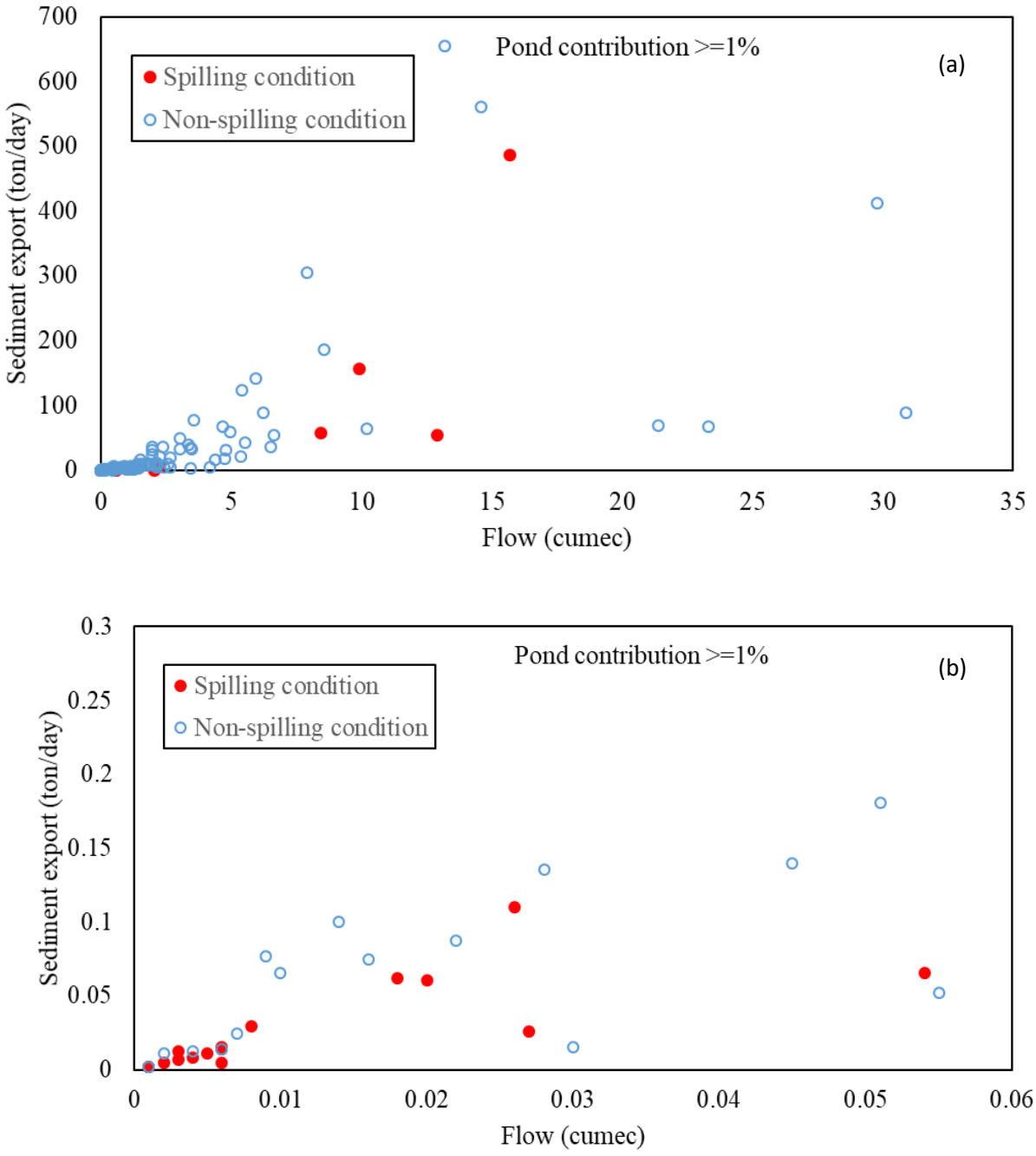


Figure 5.13: Relation between daily streamflow and sediment export during spilling and non-spilling conditions for Pipestone Creek above Moosomin Lake watershed (a) full flow range (1% pond contribution) (b) low flow conditions (1% pond contribution) (c) full flow range (5% pond contribution) (d) low flow conditions (5% pond contribution) (e) full flow range (20% pond contribution) (f) low flow conditions (20% pond contribution).

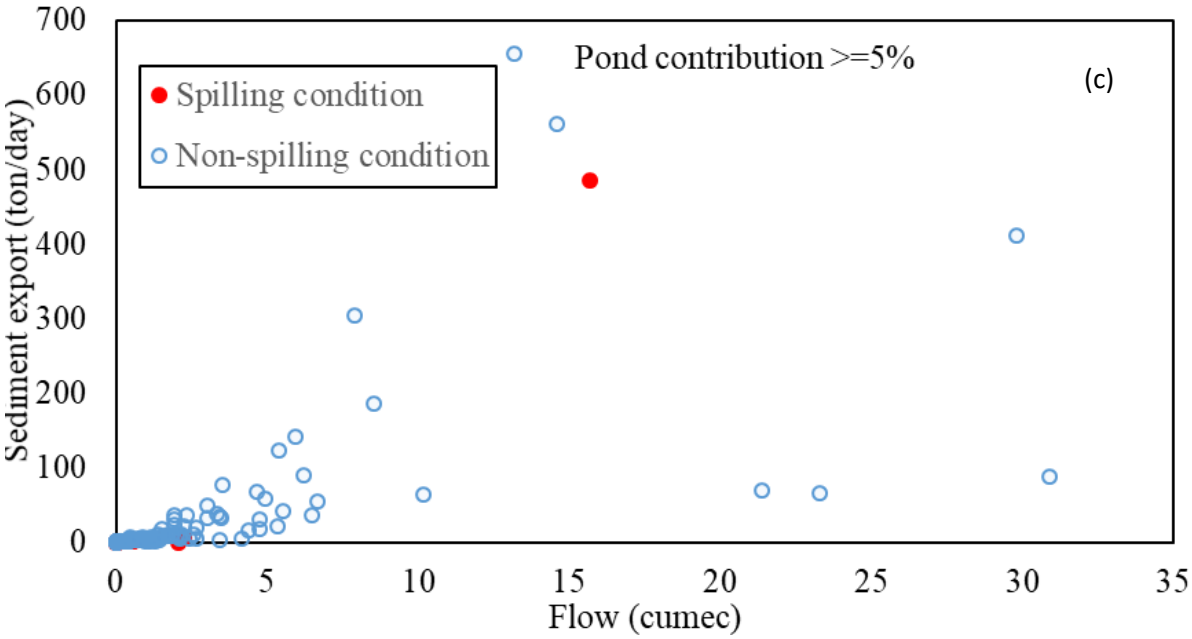


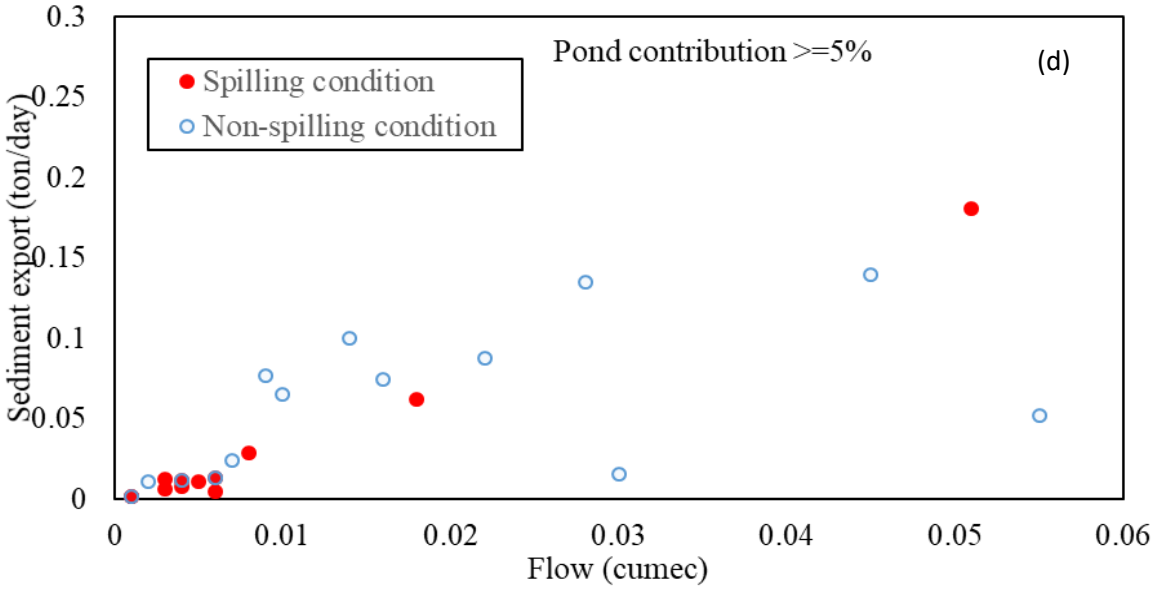


Figure 5.13 continued

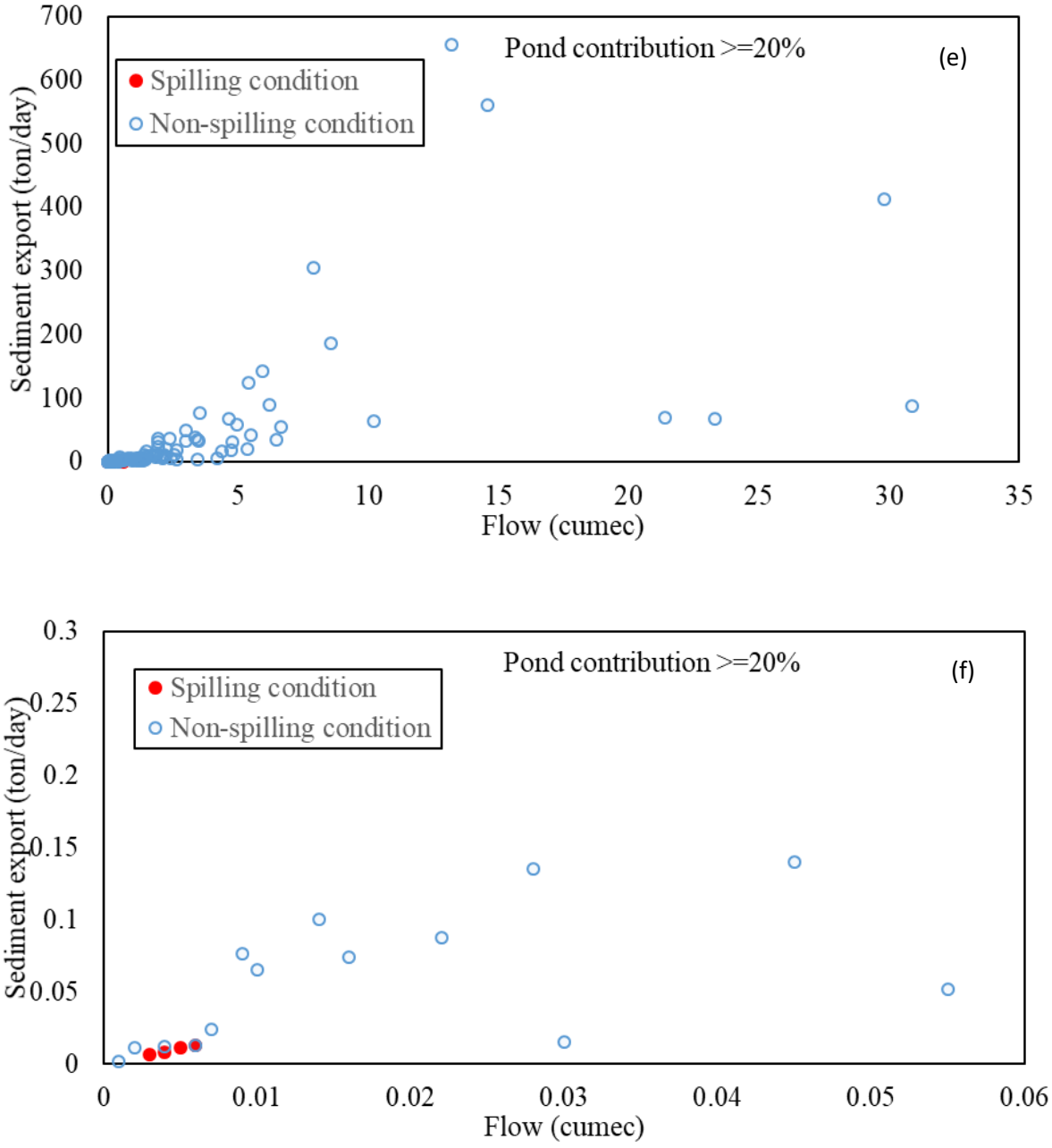


Figure 5.13 continued

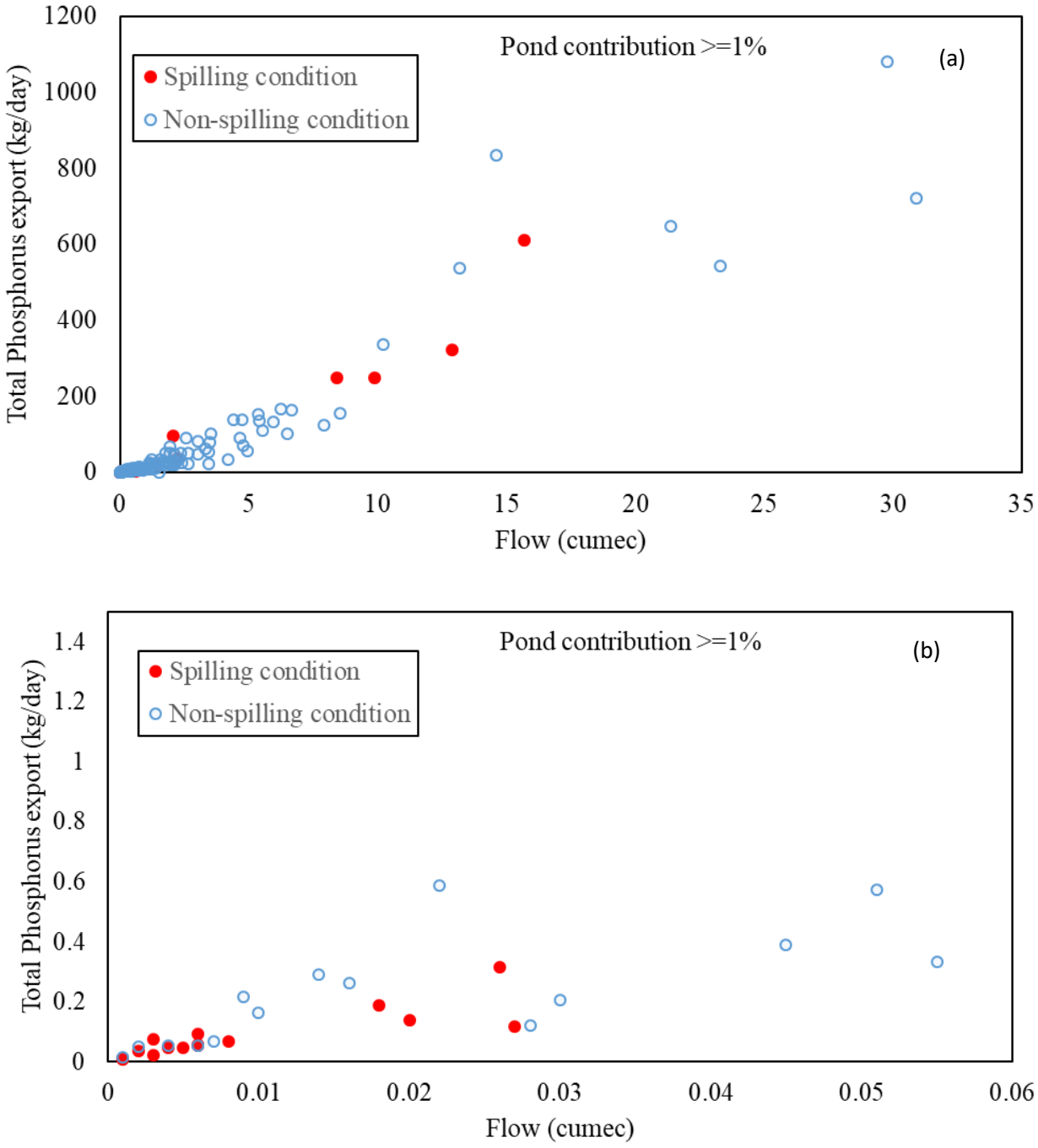


Figure 5.14: Relation between daily streamflow and total phosphorus export during spilling and non-spilling conditions for the Pipestone Creek above Moosomin Lake watershed (a) full range of flows (1% pond contribution) (b) low flow conditions (1% pond contribution) (c) full range of flows (5% pond contribution) (d) low flow conditions (5% pond contribution) (e) full range of flows (20% pond contribution) (f) low flow conditions (20% pond contribution).

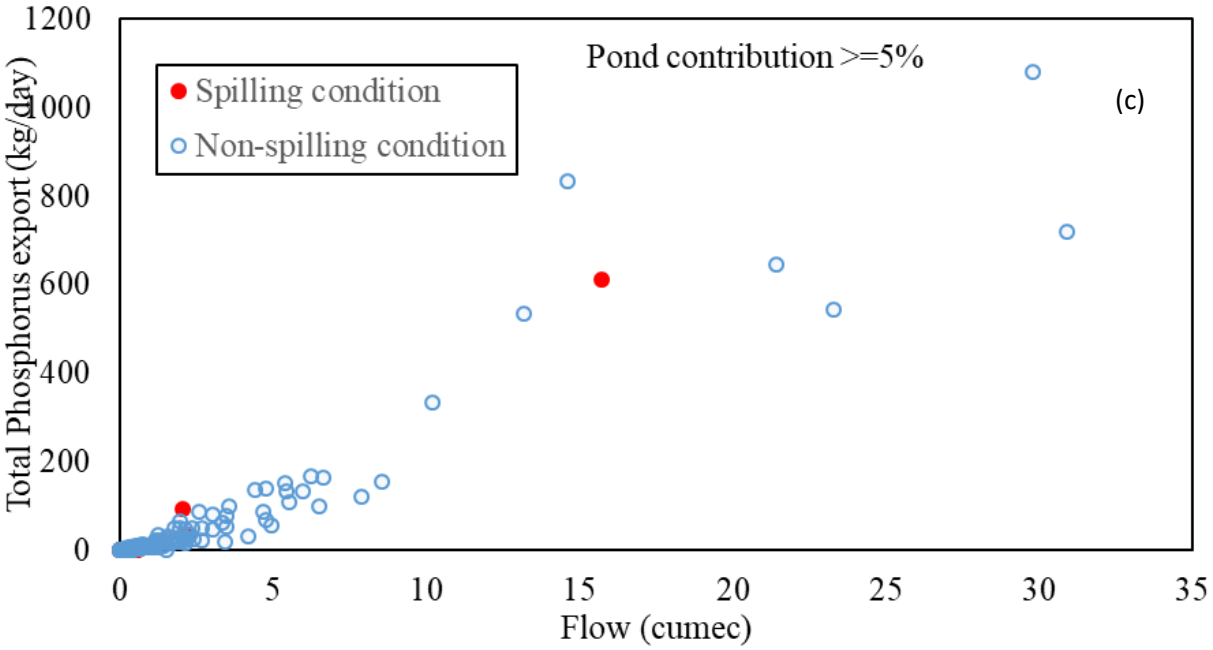


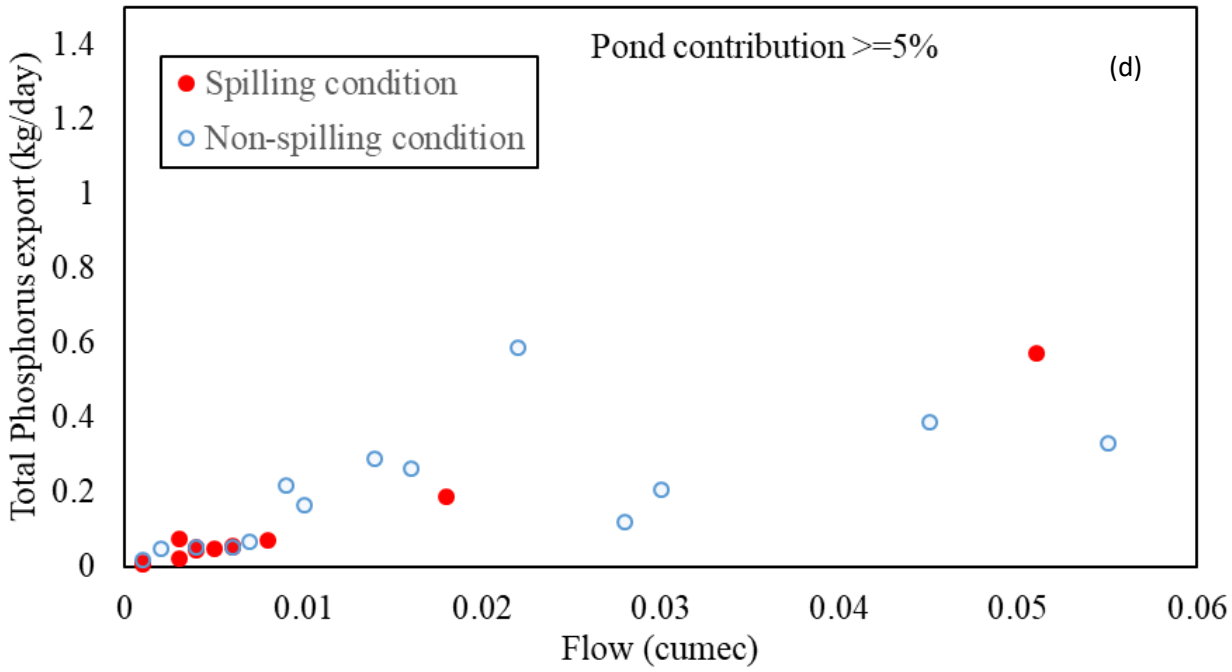


Figure 5.14 continued

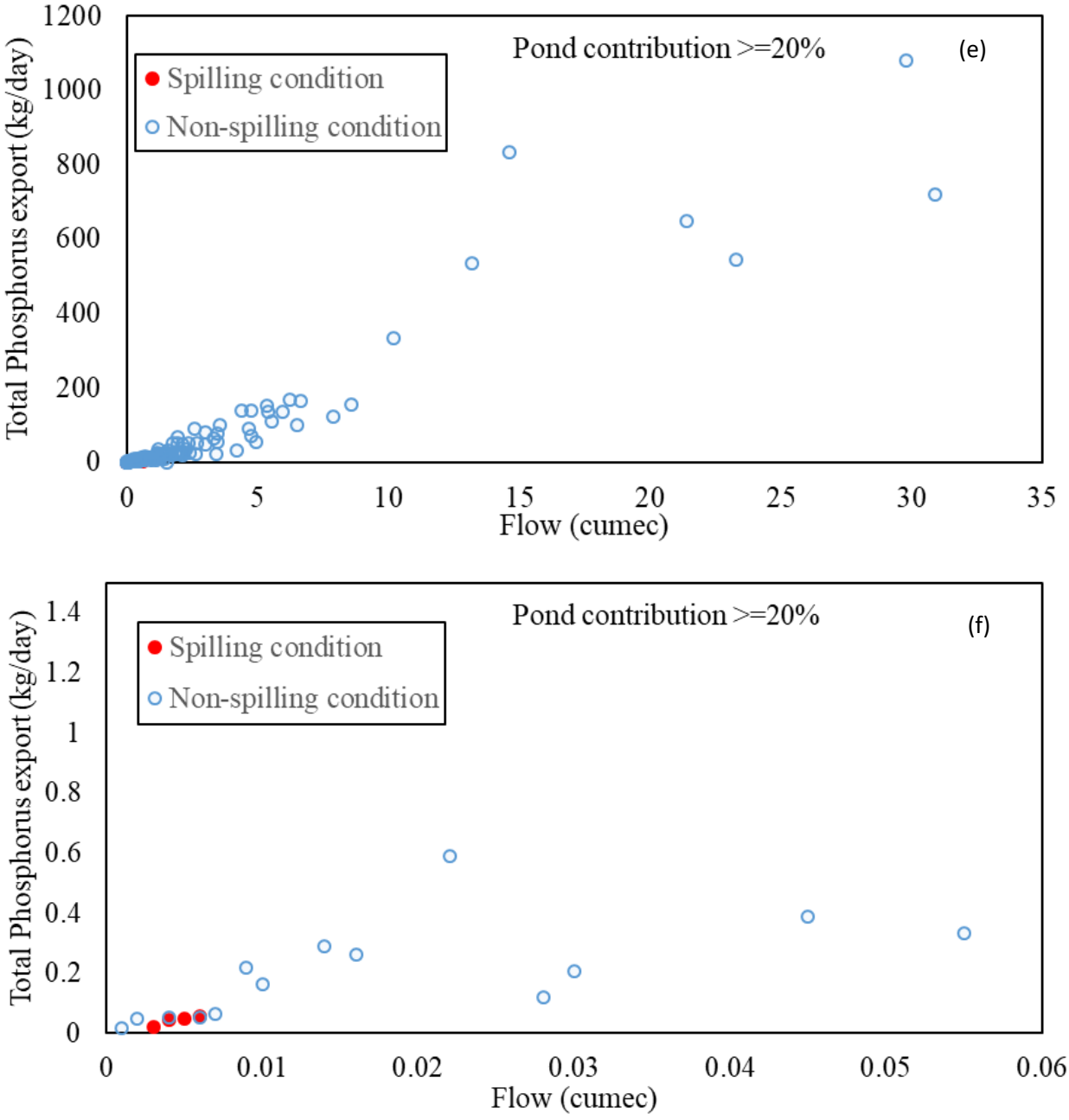


Figure 5.14 continued

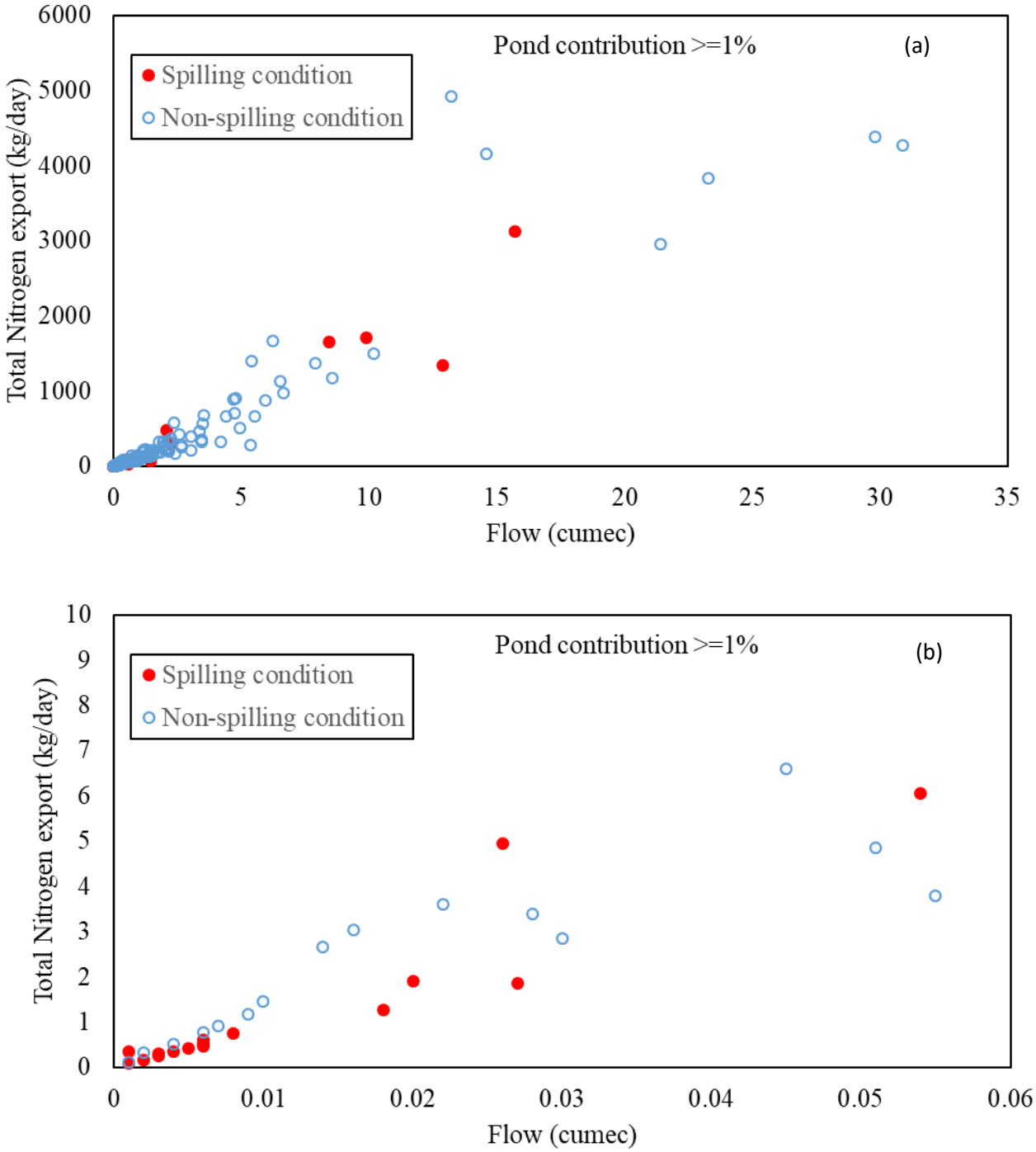


Figure 5.15: Relation between daily streamflow and total nitrogen export during spilling and non- spilling conditions for the Pipestone Creek above Moosomin Lake watershed (a) full range of flows (1% pond contribution) (b) low flow conditions (1% pond contribution) (c) full range of flows(5% pond contribution) (d) low flow conditions (5% pond contribution) (e) full range of flows (20% pond contribution) and (f) low flow conditions (20% pond contribution).

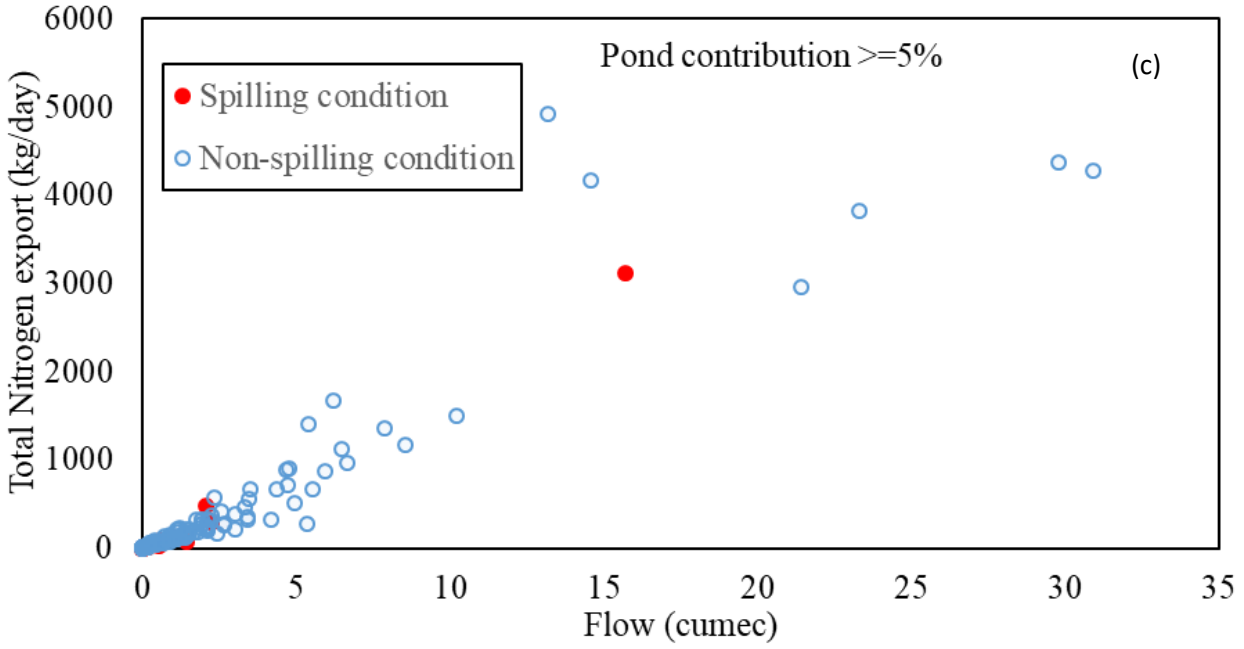


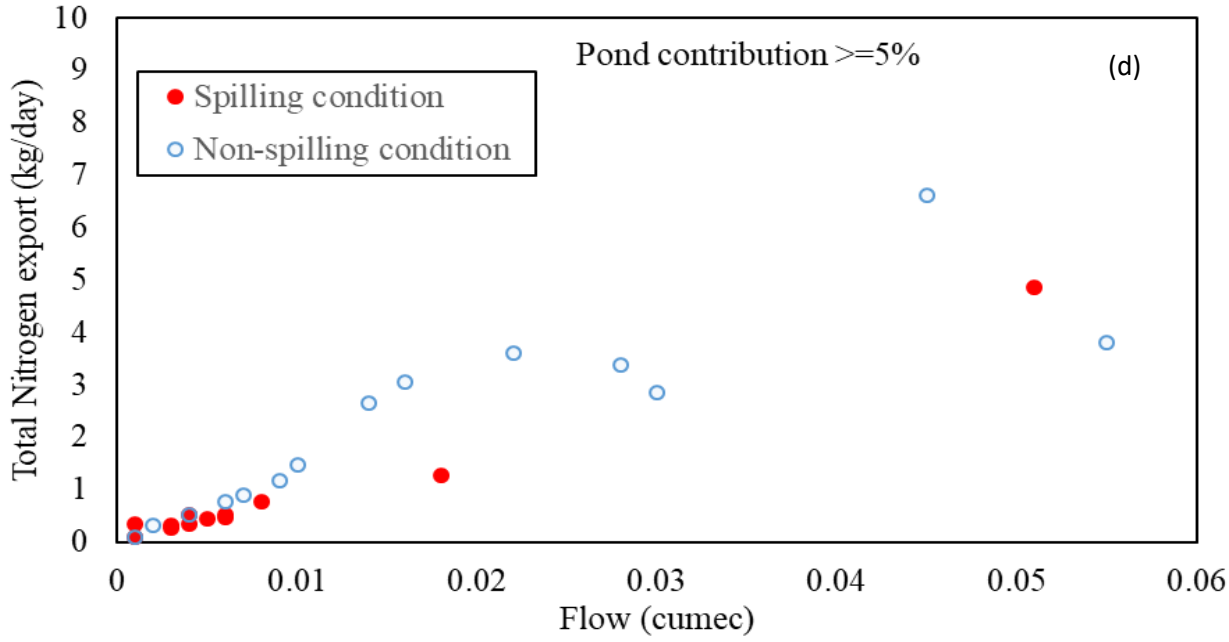


Figure 5.15 continued

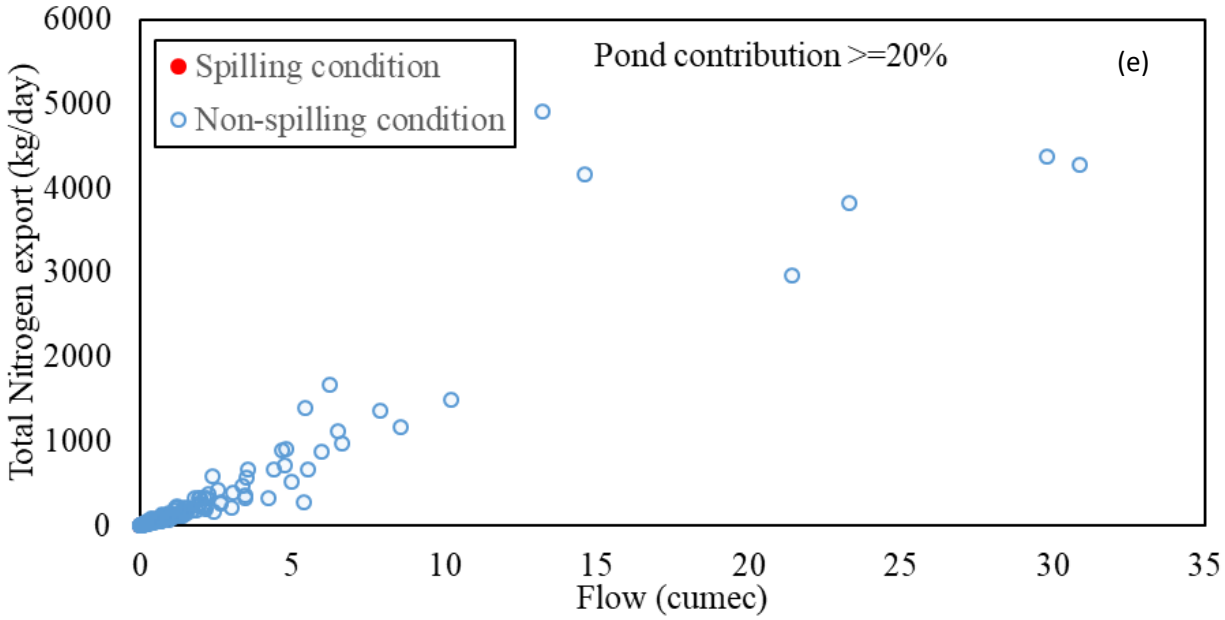


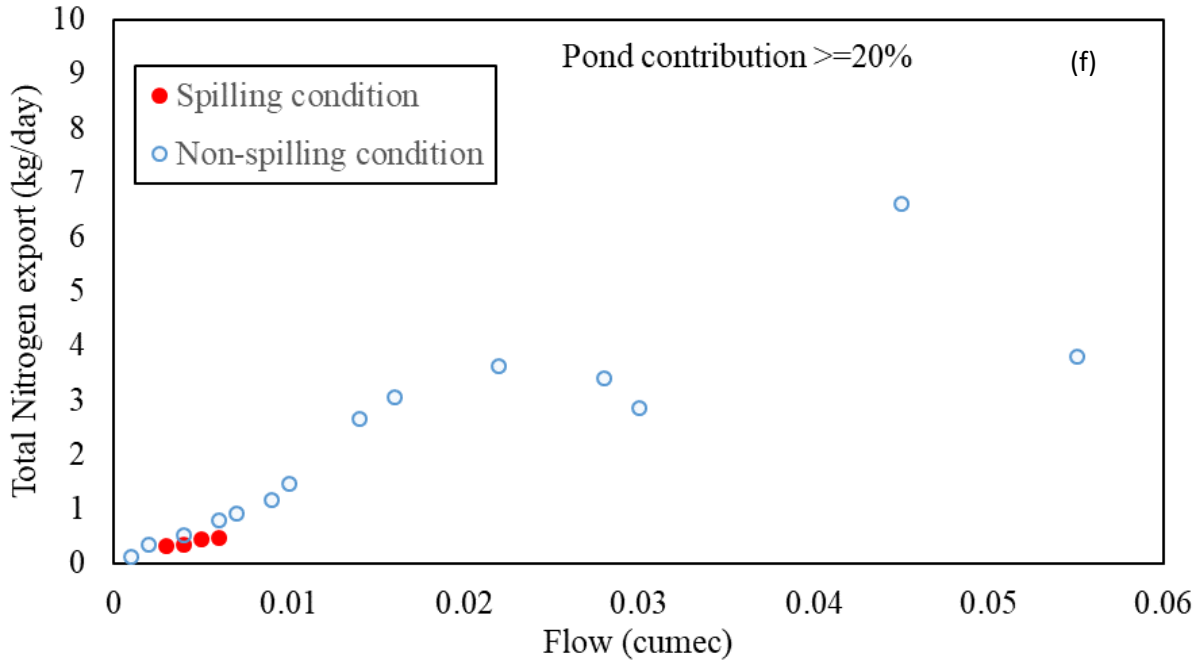


Figure 5.15 continued

## 5.5 Summary

Streamflow simulations using SWAT-PDLD and SWAT-lumped for three southern Saskatchewan watersheds have been presented above. SWAT-PDLD provides better simulation than SWAT-lumped during calibration and validation periods and specially better estimating peak flows for Pipestone Creek watershed. However, both models missed one peak during the validation period. It is worth noting that the validation period of Pipestone Creek watershed is comparatively wetter than the calibration period and a much larger than average annual rainfall recorded for the year 2014 than the surrounding years. Both models underestimated the total annual flow in the calibration and validation periods and the objective function PBIAS also indicates this observation.

In Lightning Creek watershed, the SWAT-lumped model overestimated the streamflow in many cases for both calibration and validation periods. SWAT-PDLD performed better for simulating streamflow; however, it missed the magnitude and timing of one peak for both calibration and validation period separately. It has been observed that one set of gridded precipitation data maybe not perfectly represent the actual scenario of all the simulated years. But for maintaining consistency of the model, only one source of gridded data has been used. Like the Pipestone Creek watershed, both models underestimated the observed flow in all cases except the validation period of the SWAT-lumped model. It is worth noting that, in the study described in this thesis, it was found that up to a maximum of 65 percent of surface runoff from a prairie watershed area drains into depressions before reaching the stream network.

In this study, unsatisfactory calibration results were found for the Swift Current Creek watershed. The limitations of the model were zero base flow during spring seasons and a lack of ability to predict the duration and magnitude of streamflow during both high and low flows. The

probable reasons behind that are inadequate climate data that caused inappropriate groundwater parameter values as well as overestimates of the evapotranspiration.

Water quality simulation was done for the similar periods of streamflow (except 2006) for the Pipestone Creek watershed using the SWAT-PDLD and SWAT-lumped model. Satisfactory visual representation, as well as statistical matrices, were found for daily sediment export, daily total phosphorus and daily total nitrogen export for both models. SWAT-PDLD achieved better statistical performance ratings than SWAT-lumped for simulating all three water quality models.

Spilling and non-spilling periods were identified based on SWAT-PDLD predicted pond outflow percent contribution to observed streamflow for the Pipestone Creek and Lightning Creek watersheds. In the Lightning Creek watershed percent pond contribution to streamflow during low flow was comparatively higher than the high flow periods when spilling occurred. Sediment and phosphorus export with streamflow did not show any different characteristics for spilling and non-spilling conditions. Interestingly, total nitrogen export loading was higher with streamflow during the spilling condition than the non-spilling condition.

Significant pond contributions to streamflow have been noticed for both low flow and high flow conditions for the Pipestone Creek watershed. Sediment export, total phosphorus and total nitrogen export with observed streamflow for the Pipestone Creek watershed did not show any difference for spilling and non-spilling periods. In sum, in this study, it was found that the calibrated SWAT-PDLD model can identify spilling and non-spilling periods for the prairie pothole region and assess the characteristics of sediment and nutrient export with streamflow.

# CHAPTER 6: CONCLUSIONS AND RECOMMENDATIONS

## 6.1 Summary of the Study

The first objective of this study was to apply the SWAT-PDLD model (considering variable seasonal soil erodibility) to three southern Saskatchewan watersheds to simulate streamflow and water quality. The model successfully simulated streamflow for the Pipestone Creek and Lightning Creek watersheds. The calibration results were rated as "good" and validation results were rated as "satisfactory" for both Pipestone Creek watershed and Lightning Creek watershed according to the Moriasi *et al.* (2007) criteria. The validation period for the Pipestone Creek watershed was wetter (more precipitation input) than the calibration period, which appeared to reflect in the simulation results. Further, both statistical measures and graphical representations (hydrographs) of observed and simulated flow showed that SWAT-PDLD performed better for both calibration (NSE=0.72) and validation (NSE=0.6) periods than the calibration (NSE=0.65) and validation (NSE=0.57) results of the standard SWAT-lumped model.

It was not possible to adequately calibrate the model for the Swift Current Creek watershed. During the spring and summer periods, the model predicted zero flows, which was unexpected. The probable reasons behind this were unreasonable value of groundwater parameters and evapotranspiration due to unrepresentative climate data during the spring period.

Based on the SWAT-PDLD streamflow simulations in the Lightning Creek watershed, spilling occurred from landscape depressions mostly during low flow conditions. In the Pipestone Creek watershed, only 48% of landscape depression spilling events occurred when streamflow was less than 1 $m^3/s$, whereas in the Lightning Creek watershed, 75% of the spilling events occurred for streamflow under 1 $m^3/s$.

With respect to the simulation of water quality, the SWAT-PDLD model with seasonal soil erodibility performed better than the standard SWAT lumped model for simulating sediment export for both Pipestone Creek and Lightning Creek watersheds based on the criteria of Moriasi *et al.* (2007). The performance rating of the SWAT-PDLD model for daily sediment export during the calibration and validation periods for Pipestone Creek and Lightning Creek watershed was "Good", whereas the performance of the standard SWAT lumped model for the same periods was only "Satisfactory" for both watersheds except for the validation period for Lightning Creek watershed which was ("Good").

The second goal of this study was to identify the periods when landscape depressions contribute to streamflow (spilling period) and to try and assess whether there is any noticeable impact of spilling from depressions on water quality. It should be noted that the density of landscape depressions differs significantly in Pipestone Creek and Lightning Creek watershed. Only 24% effective drainage area has been reported for Pipestone Creek watershed by Environment Canada (HYDAT), whereas there is more than twice the amount of effective drainage area (52%) for Lightning Creek.

In the Lightning Creek watershed, total nitrogen export with streamflow during spilling and non-spilling period was identical and total nitrogen export was higher during the spilling period. However, the relationship for sediment export and total phosphorus export with streamflow was missing during spilling and non-spilling periods. Furthermore, for Pipestone Creek watershed, no specific relationship had been found between water quality and streamflow during spilling and non-spilling events.

## 6.2 Recommendations

To improve the SWAT-PDLD model performance for further application to simulation of streamflow and water quality in the prairie region watershed, the following guidelines are recommended.

- Use the best possible climate data available to represent the overall water balance of the watershed during the simulation periods. If required, a combination of observed and gridded climate data can be used to avoid missing data to represent the best possible climate scenario.
- Different tools *i.e.* the Wetland DEM Ponding Model (WDPM) other than Arc-Hydro tools can be used to calculate pond geometry and contributing drainage area of the pond to compare the difference in case of pond water balance effect on streamflow simulation that can ensure better pond water balance. In this study, the contributing drainage area of the pond was calculated indirectly based on the difference between effective and non-effective drainage areas of the watershed, which can be calculated directly using alternate tools.
- Simulate water quality model for organic nutrients separately instead of total nitrogen or phosphorus to analyze and improve model performance for more specific water quality variables.
- Frequent water quality measurements specially during peak streamflows are necessary to assess model performance for nutrient export during that time more effectively. Frequent sampling is required specially during the spring period, where most of the peak flows occurred.

## REFERENCES


Abbaspour, K.C., Yang, J., Maximov, I., Siber, R., Bogner, K., Mieleitner, J., Zobrist, J., and Srinivasan, R. 2007. Modelling hydrology and water quality in the pre-alpine/alpine Thur watershed using SWAT. Journal of Hydrology, **333**(2–4): 413–430. doi:10.1016/j.jhydrol.2006.09.014.

Acton, D.F., and Gregorich, L.J. 1995. Health of our soils: toward sustainable agriculture in canada. center for land and biological resources research, Agriculture and Agri-Food Canada, Ottawa, Canada.

Agriculture and Agri-Food Canada. 2018. Annual crop inventory. Geospatial material. Available from http://www.agr.gc.ca/atlas/aci/. [accessed 3 December 2019].

Almendinger, J.E., Murphy, M.S., and Ulrich, J.S. 2014. Use of the soil and water assessment tool to scale sediment delivery from field to watershed in an agricultural landscape with topographic depressions. Journal of Environmental Quality, **43**(1): 9–17. doi:10.2134/jeq2011.0340.

Arnold, J.G., Engel, B.A., and Srinivasan, R. 1993. Continuous time, grid cell watershed model, application of advanced information technologies. Effective management of natural resources. ASAE Publication, 04–93. American Society of Agricultural Engineers 267–278.

Arnold, J.G., Moriasi, D.N., Gassman, P.W., Abbaspour, K.C., White, M.J., Srinivasan, M.S., Santhi, C., Harmel, R.D., van Griensven, A., van Liew, M.W., Kannan, N., and Jha, M.K. 2012. SWAT: model use, calibration, and validation. Transactions of the ASABE, **55**(4): 1491–1508. doi:10.13031/2013.42256.

Awada, L., Lindwall, C.W., and Sonntag, B. 2014. The development and adoption of conservation tillage systems on the Canadian prairies. International Soil and Water Conservation Research, **2**(1): 47–65. doi:10.1016/S2095-6339(15)30013-7.

Bechmann, M. E., Kleinman, P. J. A., Sharpley, A. N., and Saporito L.S. 2005. Freeze-thaw effects on phosphorus loss in runoff from manured and catch-cropped soils. j. environ. Qual. **34**(6): 2301-2309. doi:10.2134/jeq2004.0415.

Beegle, D.B., and Durst, P.T. 2002. Managing phosphorus for crop production (Pennsylvania nutrient management program). Available from https://extension.psu.edu/programs/nutrient-management/educational/soil-fertility/managing-phosphorus-for-crop-production. [accessed 17 December 2019].

Bengtson, M.L., and Padmanabhan, G. 1999. A hydrologic model for assessing the influence of wetlands on flood hydrographs in the red river basin. Development and application. North Dakota Water Resources Research Institute, North Dakota State University Fargo, North Dakota.

Berg, M., and Meehan, M. 2017. Nitrogen behavior in the environment. NDSU extension Service, North Dakota State University. Available from https://www.ag.ndsu.edu/publications/environment-natural-resources/nitrogen-behavior-in-the-environment. [accessed 16 December 2019].

Berg, M., and Meehan, M. 2018. Phosphorus behavior in the environment. NDSU extension Service, North Dakota State University. Available from https://www.ag.ndsu.edu/publications/environment-natural-resources/phosphorus-behavior-in-the-environment. [accessed 17 December 2019].

Beven, K.J. 2000. Down to basics: runoff processes and the modeling process. Rainfall-runoff modelling: the primer. John Wiley & Sons Inc., West Sussex, UK.

Bioteau, T., Bordenave, P., and Laurent, F. 2002. Assessment of the risks of diffuse pollution by nitrogen of agricultural origin on the scale of watersheds: advantages of a modeling approach with SWAT. Article paru dans Ingénieries – EAT, 32: 3–13.

Brown, L.C., and Barnwell, T.O. 1987. The enhanced stream water quality models QUAL2E and QUAL2E-UNCAS: documentation and user manual. USEPA, Athens, GA.

Buda, A.R., Kleinman, P.J.A., Srinivasan, M.S., Bryant, R.B., and Feyereisen, G.W. 2009. Effects of hydrology and field management on phosphorus transport in surface runoff. Published in J. Environ. Qual. **38**: 2273–2284. doi:10.2134/jeq2008.050.

Burford, M.A., Johnson, S.A., Cook, A.J., Packer, T.V., Taylor, B.M., and Townsley, E.R. 2007. Correlations between watershed and reservoir characteristics, and algal blooms in subtropical reservoirs. Water Research, **41**(18): 4105–4114. doi:10.1016/j.watres.2007.05.053.

Burwell, R.E., Schuman, G.E., Heinemann, H.G., and Spomer, R.G. 1977. Nitrogen and phosphorus movement from agricultural watersheds. Reprinted from the Journal of Soil and Water Conservation, **32**(5): 226-230.

Canadian Soil Information Service (CANSIS). 2018. Available from http://sis.agr.gc.ca/cansis/. [accessed 18 February 2020].

Canada Weather Stats 2019. Available from https://www.weatherstats.ca/.[accessed 18 February 2020].

Chislock, M.F., Doster, E., Zitomer, R.A., and Wilson, A.E. 2013. Eutrophication: causes, consequences, and controls in aquatic ecosystems. Nature Education Knowledge, **4**(4): 10.

Choi, W., Kim, S.J., Rasmussen, P.F., and Moore, A.R. 2009. Use of the North American regional reanalysis for hydrological modelling in Manitoba. Canadian Water Resources Journal, **34**(1): 17–36. doi:10.4296/cwrj3401017.

Christopher, S. F., Mitchell, M.J., McHale, M. R., Boyer, E.W., Burns, D. A., and Kendall, C. 2007. Factors controlling nitrogen release from two forested catchments with contrasting hydrochemical responses. Hydrological Processes, **22**(1): 46–62. doi:10.1002/hyp.6632.

Cohen, M.J., Creed, I.F., Alexander, L., Basu, N.B., Calhoun, A.J.K., Craft, C., D'Amico, E., DeKeyser, E., Fowler, L., Golden, H.E., Jawitz, J.W., Kalla, P., Kirkman, L.K., Lane, C.R., Lang, M., Leibowitz, S.G., Lewis, D.B., Marton, J., McLaughlin, D.L., Mushet, D.M., Raanan-Kiperwas, H., Rains, M.C., Smith, L., and Walls, S.C. 2016. Do geographically isolated wetlands influence landscape functions? Proceedings of the National Academy of Sciences, **113**(8): 1978–1986. doi:10.1073/pnas.1512650113.

Connelly, N.A., O'Neill, C.R., Knuth, B.A., and Brown, T.L. 2007. Economic impacts of zebra mussels on drinking water treatment and electric power generation facilities. environmental management, **40**(1): 105–112. doi:10.1007/s00267-006-0296-5.

Costa, D., Roste, J., Pomeroy, J., Baulch, H., Elliott, J., Wheater, H., and Westbrook, C. 2017. A modelling framework to simulate field-scale nitrate response and transport during snowmelt: The WINTRA model. Hydrological Processes, **31**(24): 4250–4268. doi:10.1002/hyp.11346.

Crumpton, W.G., and Goldsborough, L.G. 1998. Nitrogen transformation and fate in prairie wetlands. Great Plains Research: A Journal of Natural and Social Sciences, 8(1): 57-72.

de Boer, D.H., Hassan, M.A., MacVicar, B., and Stone, M. 2005. Recent (1999–2003) Canadian research on contemporary processes of river erosion and sedimentation, and river mechanics. Hydrological Processes, **19**(1): 265–283. doi:10.1002/hyp.5767.

de Jonge, V.N., and Elliott, M. 2001. Eutrophication. *In* encyclopedia of ocean sciences (Second Edition). *Edited by* J.H. Steele. Academic Press, Oxford, UK. pp. 306–323.

DeLaney, T.A. 1995. Benefits to downstream flood attenuation and water quality as a result of constructed wetlands in agricultural landscapes. Journal of Soil and Water Conservation, **50**(6): 620–626.

Devak, M., and Dhanya, C.T. 2017. Sensitivity analysis of hydrological models: Review and way forward. Journal of Water and Climate Change, **8**(4): 557–575. doi:10.2166/wcc.2017.149.

Dickinson, W.T., Rudra, R.P., and Wall, G.J. 1986. Identification of soil erosion and fluvial sediment problems. Hydrological Processes, **1**(1): 111–124. doi:10.1002/hyp.3360010110.

Dickinson, W.T., Scott, A., and Wall, G. 1975. Fluvial sedimentation in southern ontario. Canadian Journal of Earth Sciences, **12**(11): 1813–1819. doi:10.1139/e75-162.

Donald, D.B., Gurprasad, N.P., Quinnett-Abbott, L., and Cash, K. 2000. Diffuse geographic distribution of herbicides in northern prairie wetlands. Environmental Toxicology and Chemistry, **20**(2): 273–279. doi:10.1002/etc.5620200207.

Du, B., Arnold, J.G., Saleh, A., and Jaynes, D.B. 2005. Development and application of SWAT to landscapes with tiles and potholes. American Society of Agricultural Engineers, **48**(3): 1121-1133.

Dwarakish, G.S., and Ganasri, B.P. 2015. Impact of land use change on hydrological systems: A review of current modeling approaches. Cogent Geoscience, **1**(1): 1115691. doi:10.1080/23312041.2015.1115691.

Eisenlohr, W.S., and Sloan, C.E. 1968. Generalized hydrology of prairie potholes on the Coteau du Missouri, North Dakota. USGS Numbered Series, 558, U.S. Geological Survey, Washington, D.C. doi:10.3133/cir558

Erisman, J.W., and Draaijers, G.P. 1995. Atmospheric deposition-in relation to acidification and eutrophication. *In* 1st edition. Elsevier Science, Amsterdam, Netherlands.

Euliss, N.H., Johnson, D.H., and Mushet, D.M. 2002. Using aquatic invertebrates to delineate seasonal and temporary wetlands in the prairie pothole region of North America. The Society of Wetland Scientists. Wetlands, 22(2): 256–262.

Evenson, G.R., Golden, H.E., Lane, C.R., and D'Amico, E. 2015. Geographically isolated wetlands and watershed hydrology: A modified model analysis. Journal of Hydrology, **529**: 240–256. doi:10.1016/j.jhydrol.2015.07.039.

Evenson, G.R., Golden, H.E., Lane, C.R., and D'Amico, E. 2016. An improved representation of geographically isolated wetlands in a watershed-scale hydrologic model. Hydrological Processes, **30**(22): 4168–4184. doi:10.1002/hyp.10930.

Fang, X., Minke, A., Pomeroy, J., Brown, T., Westbrook, C., Guo, X., and Guangul, S. 2007. A review of Canadian prairie hydrology: principles, modelling and response to land use and drainage change. Centre for Hydrology Report, 2, University of Saskatchewan, Saskatoon, SK.

Fang, X., and Pomeroy, J.W. 2007. Snowmelt runoff sensitivity analysis to drought on the Canadian prairies. Hydrological Processes, **21**(19): 2594–2609. doi:10.1002/hyp.6796.

Fang, X., and Pomeroy, J.W. 2008. Drought impacts on Canadian prairie wetland snow hydrology. Hydrological Processes, **22**(15): 2858–2873. doi:10.1002/hyp.7074.

Faria, D.A., Pomeroy, J.W., and Essery, R.L.H. 2000. Effect of covariance between ablation and snow water equivalent on depletion of snow-covered area in a forest. Hydrological Processes, **14**(15): 2683–2695. doi:10.1002/1099-1085(20001030)14:15<2683::AID-HYP86>3.0.CO;2-N.

Fontaine, T.A., Cruickshank, T.S., Arnold, J.G., and Hotchkiss, R.H. 2002. Development of a snowfall–snowmelt routine for mountainous terrain for the soil water assessment tool (SWAT). Journal of Hydrology, **262**(1–4): 209–223. doi:10.1016/S0022-1694(02)00029-X.

Franzblau, E., and Popp, C.J. 1989. Nitrogen oxides produced from lightning. Journal of Geophysical Research: Atmospheres, **94**(D8): 11089–11104. doi:10.1029/JD094iD08p11089.

Garcia, J.L., and Tiedje, J.M. 1982. Denitrification in rice soils. *In* Microbiology of Tropical Soils and plant productivity. Springer Netherlands, Dordrecht, The Netherlands. pp. 187–208.

Gassman, P.W., Reyes, M.R., Green, C.H., and Arnold, J.G. 2007. The Soil and Water Assessment Tool: historical development, applications, and future research directions. Transactions of the ASABE, **50**(4): 1211–1250. doi:10.13031/2013.23637.

Gorham, E. 1991. Biogeochemistry: its origins and development. Biogeochemistry, **13**(3): 199–239.

Government of Saskatchewan 2020. Publication Saskatchewan, CA. Available from https://publications.saskatchewan.ca/#/products/75197. [accessed 29 January 2020].

Granger, R.J., Gray, D.M., and Dyck, G.E. 1984. Snowmelt infiltration to frozen prairie soils. Canadian Journal of Earth Sciences, **21**(6): 669–677. doi:10.1139/e84-073.

Grath, B. 2016. Simulation of discharge and nitrate-nitrogen loads in the Raab catchment with the hydrological model SWAT. Master Thesis, Department for Water-Atmosphere-Environment, University of Natural Resources and Life Sciences, Vienna, Austria.

Gupta, H.V., Sorooshian, S., and Yapo, P.O. 1999. Status of automatic calibration for hydrologic models: comparison with multilevel expert calibration. Journal of Hydrologic Engineering, **4**(2): 135–143. doi:10.1061/(ASCE)1084-0699(1999)4:2(135).

Hansen, N.C., Daniel, T.C., Sharpley, A.N., and Lemunyon, J.L. 2002. The fate and transport of phosphorus in agricultural systems. Journal of Soil and Water Conservation, **57**(6): 408–417.

Hargrave, A.P., and Shaykewich, C.F. 1997. Rainfall induced nitrogen and phosphorus losses from Manitoba soils. Canadian Journal of Soil Science, **77**(1): 59–65. doi:10.4141/S95-034.

Harmel, D., Potter, S., Casebolt, P., Reckhow, K., Green, C., and Haney, R. 2006. Compilation of measured nutrient load data for agricultural land uses in the united states. Journal of the American Water Resources Association, **42**(5): 1163–1178. doi:10.1111/j.1752-1688.2006.tb05292.x.

Hay, L., Norton, P., Viger, R., Markstrom, S., Regan, R.S., and Vanderhoof, M. 2017. Modelling surface-water depression storage in a Prairie Pothole Region. Hydrological Processes, **32**(4): 462–479. doi:10.1002/hyp.11416.

Hayashi, M., van der Kamp, G., and Rudolph, D.L. 1998. Water and solute transfer between a prairie wetland and adjacent uplands. Water balance. Journal of Hydrology, **207**(1): 42–55. doi:10.1016/S0022-1694(98)00098-5.

Hayashi, M., Quinton, W.L., Pietroniro, A., and Gibson, J.J. 2004. Hydrologic functions of wetlands in a discontinuous permafrost basin indicated by isotopic and chemical signatures. Journal of Hydrology, **296**(1): 81–97. doi:10.1016/j.jhydrol.2004.03.020.

Hofmann, L., Ries, R.E., and Gilley, J.E. 1983. Relationship of runoff and soil loss to ground cover of native and reclaimed grazing land. agronomy Journal, **75(4)**: 599–602.

Hossain, K. 2017. Towards a systems modelling approach for a large-scale Canadian Prairie watershed. M.Sc. thesis, Department of Civil, Geological & Environmental Engineering, University of Saskatchewan, Saskatoon, SK.

Howerter, D. 2014. Wetlands: biodiversity offsets: challenges and considerations. Conservation Science, Ducks Unlimited, Canada.

Huber, W.C., and Dickinson, R.E. 1988. Storm water management model, version 4: user's manual. U.S. Environmental Protection Agency, Athens, GA.

Jalowska, A.M., and Yuan, Y. 2019. Evaluation of SWAT impoundment modeling methods in water and sediment simulations. Journal of the American Water Resources Association, **55**(1): 209–227. doi:10.1111/1752-1688.12715.

Jamieson, A., Madramootoo, C.A., and Enright, P. 2003. Phosphorus losses in surface and subsurface runoff from a snowmelt event on an agricultural field in Quebec. Brace Centre for Water Resources Management, Ste-Anne-de-Bellevue, Quebec, **45**.

Jantunen, L.M., Helm, P.A., Ridal, J.J., and Bidleman, T.F. 2008. Air–water gas exchange of chiral and achiral organochlorine pesticides in the great lakes. Atmospheric Environment, **42**(36): 8533–8542. doi:10.1016/j.atmosenv.2008.05.052.

Kjelland, M.E., Woodley, C.M., Swannack, T.M., and Smith, D.L. 2015. A review of the potential effects of suspended sediment on fishes: potential dredging-related physiological,

behavioral, and transgenerational implications. Environment Systems and Decisions, **35**(3): 334–350. doi:10.1007/s10669-015-9557-2.

Koroluk, S.L., and de Boer, D.H. 2007. Land use change and erosional history in a lake catchment system on the Canadian prairies. CATENA, **70**(2): 155–168. doi:10.1016/j.catena.2006.08.006.

Köchy, M., and Wilson, S.D. 1997. Litter decomposition and nitrogen dynamics in aspen forest and mixed-grass Prairie. Ecology, **78**(3): 732–739. doi:10.1890/0012-9658(1997)078[0732:LDANDI]2.0.CO;2.

LaBaugh, J.W., Winter, T.C., and Rosenberry, D.O. 1998. Hydrologic functions of prairie wetlands. Great Plains Research, **8**(1): 17-37.

Leibowitz, S.G., and Vining, K.C. 2003. Temporal connectivity in a prairie pothole complex. Wetlands, **23**(1): 13–25. doi:10.1672/0277-5212(2003)023[0013:TCIAPP]2.0.CO;2.

Lintern, A., Webb, J.A., Ryu, D., Liu, S., Bende-Michl, U., Waters, D., Leahy, P., Wilson, P., and Western, A.W. 2018. Key factors influencing differences in stream water quality across space. Wiley Interdisciplinary Reviews: Water, **5**(1): e1260. doi:10.1002/wat2.1260.

Liu, K., Elliott, J.A., Lobb, D.A., Flaten, D.N., and Yarotski, J. 2013. Critical factors affecting field-scale losses of nitrogen and phosphorus in spring snowmelt runoff in the Canadian prairies. Journal of Environmental Quality; Madison, **42**(2): 484–96.

Liu, Y., Yang, W., Shao, H., Yu, Z., and Lindsay, J. 2018. Development of an integrated modelling system for evaluating water quantity and quality effects of individual wetlands in an agricultural watershed. Water, **10**(6): 774. doi:10.3390/w10060774.

Ludden, A.P., Frink, D.L., and Johnson, D.H. 1983. Water storage capacity of natural wetland depressions in the Devils lake basin of North Dakota. Journal of Soil and Water Conservation, **38**(1): 45–48.

Malhotra, H., Vandana, Sharma, S., and Pandey, R. 2018. Phosphorus nutrition: plant growth in response to deficiency and excess. *In* Plant Nutrients and Abiotic Stress Tolerance. Springer, Singapore. pp. 171–190.

McConkey, B.G., Nicholaichuk, W., Steppuhn, H., and Reimer, C.D. 1996. Sediment yield and seasonal soil erodibility for semiarid cropland in western Canada. Canadian Journal of Soil Science, **77**(1): 33-40. doi:10.4141/S95-060.

Mekonnen, B.A. 2016. Modeling and management of water quantity and quality in cold-climate prairie watersheds. Phd Thesis, Department of Civil and Geological Engineering, University of Saskatchewan, Saskatoon, SK.

Mekonnen, B.A., Mazurek, K.A., and Putz, G. 2016a. Incorporating landscape depression heterogeneity into the Soil and Water Assessment Tool (SWAT) using a probability distribution. Hydrological Processes, **30**(13): 2373–2389. doi:10.1002/hyp.10800.

Mekonnen, B.A., Mazurek, K.A., and Putz, G. 2016b. Sediment export modeling in cold-climate prairie watersheds. Journal of Hydrologic Engineering, **21**(5): 05016005. doi:10.1061/(ASCE)HE.1943-5584.0001336.

Mekonnen, B.A., Mazurek, K.A., and Putz, G. 2016c. Modeling of nutrient export and effects of management practices in a cold-climate prairie watershed: Assiniboine river watershed, Canada. Agricultural Water Management, **180**: 235–251. doi:10.1016/j.agwat.2016.06.023.

Mekonnen, B.A., Nazemi, A., Mazurek, K.A., Elshorbagy, A., and Putz, G. 2015. Hybrid modelling approach to prairie hydrology: fusing data-driven and process-based hydrological models. Hydrological Sciences Journal, **60**(9): 1473-1489. doi:10.1080/02626667.2014.935778.

Melles, S.J., Benoy, G.B., Booty, B., León, L.F., Vanrobaeys, J., and Wong, I.W.S. 2010. Scenarios to investigate the effect of wetland position in a watershed on nutrient loadings. *In* Proceedings of the 5th international congress on environmental modelling and software, July 2010. International Environmental Modelling and Software Society, Ottawa, Ontario, Canada, pp. 400

Mendas, A., Errih, M., Benhanifia, K., and Rahmani, M.A. 2006. Hydrologic model and GIS to estimate hydrologic balance at watershed scale - application to the watershed of Macta (Western Algerian). Division of Geomatic, National Center of Spatial Techniques, Azew, Algeria.

Messing, P.G., Farenhorst, A., Waite, D.T., McQueen, D.A.R., Sproull, J.F., Humphries, D.A., and Thompson, L.L. 2011. Predicting wetland contamination from atmospheric deposition measurements of pesticides in the Canadian Prairie Pothole Region. Atmospheric Environment, **45**(39): 7227–7234. doi:10.1016/j.atmosenv.2011.08.074.

Mitsch, W.J., and Gosselink, J.G. 1993. Wetlands, 2nd Edition, John Wiley & Sons, Inc, Hoboken, N.J.

Molina-Navarro, E., Hallack-Alegría, M., Martínez-Pérez, S., Ramírez-Hernández, J., Mungaray-Moctezuma, A., and Sastre-Merlín, A. 2016. Hydrological modeling and climate change impacts in an agricultural semiarid region. Case study: Guadalupe River basin, Mexico. Agricultural Water Management, **175**: 29–42. doi:10.1016/j.agwat.2015.10.029.

Moog, D.B., and Whiting, P.J. 2002. Climatic and agricultural factors in nutrient exports from two watersheds in Ohio. Journal of Environmental Quality, **31**(1): 72–83. doi:10.2134/jeq2002.7200.

Morales-Marín, L.A., Wheater, H.S., and Lindenschmidt, K.E. 2017. Assessment of nutrient loadings of a large multipurpose prairie reservoir. Journal of Hydrology, **550**: 166–185. doi:10.1016/j.jhydrol.2017.04.043.

Moriasi, D.N., Arnold, J.G., Van Liew, M.W., Bingner, R.L., Harmel, R.D., and Veith, T.L. 2007. Model evaluation guidelines for systematic quantification of accuracy in watershed simulations. Transactions of the ASABE, **50**(3): 885-900.

Mosbahi, M. 2012. Determination of critical source areas for sediment loss : Sarrath river basin, Tunisia. International Journal of Environmental, Chemical, Ecological, Geological and Geophysical Engineering, **5**(8): 467-471.

Muhammad, A., Evenson, G.R., Stadnyk, T.A., Boluwade, A., Jha, S.K., and Coulibaly, P. 2019. Impact of model structure on the accuracy of hydrological modeling of a Canadian prairie watershed. Journal of Hydrology: Regional Studies, **21**: 40–56. doi:10.1016/j.ejrh.2018.11.005.

Murphy, S. 2007. BASIN: General information on phosphorus. Available from http://bcn.boulder.co.us/basin/data/BACT/info/TP.html. [accessed 17 December 2019].

Mushet, D.M., Calhoun, A.J.K., Alexander, L.C., Cohen, M.J., DeKeyser, E.S., Fowler, L., Lane, C.R., Lang, M.W., Rains, M.C., and Walls, S.C. 2015. Geographically isolated wetlands: rethinking a misnomer. Wetlands, **35**(3): 423–431. doi:10.1007/s13157-015-0631-9.

Nasab, M.T., Singh, V., and Chu, X. 2017. SWAT modeling for depression-dominated areas: how do depressions manipulate hydrologic modeling? Water, **9**(1): 58. doi:10.3390/w9010058.

Nash, J.E., and Sutcliffe, J.V. 1970. River flow forecasting through conceptual models part I - a discussion of principles. Journal of Hydrology, **10**(3): 282–290. doi:10.1016/0022-1694(70)90255-6.

Natural Resources Canada. 2020. Regional, national and international climate modeling. Natural Resources Canada. Available from https://cfs.nrcan.gc.ca/projects/3. [accessed 18 February 2020].

Nazemi, A., and Wheater, H.S. 2015. On inclusion of water resource management in earth system models – Part 1: problem definition and representation of water demand. Hydrol. Earth Syst. Sci., **19**(1): 33–61. doi:10.5194/hess-19-33-2015.

Neely, R.K., and Baker, J.L. 1989. Nitrogen and phosphorous dynamics and fate of agricultural runoff. Northern Prairie Wetlands, Iowa State University Press, Ames, Iowa. pp. 92-131.

Neitsch, S., Arnold, J., Kiniry, J., and Williams, J. 2011. Soil and water assessment tool theoretical documentation version 2009, Texas Water Resources Institute, Texas A&M University System, College Station, Texas, USA.

Nitrogen Fertilization in crop production 2020. Ministry of Agriculture, Government of Saskatchewan. Available from https://publications.saskatchewan.ca/#/products/75197. [accessed 29 January 2020].

Novotny, V. 2003. Water quality: diffuse pollution and watershed management, 2nd Edition. John Wiley & Sons, Inc., Hoboken, NJ, USA.

Perez-Valdivia, C., Cade-Menun, B., and McMartin, D.W. 2017. Hydrological modeling of the pipestone creek watershed using the Soil Water Assessment Tool (SWAT): assessing impacts of wetland drainage on hydrology. Journal of Hydrology: Regional Studies, **14**: 109–129. doi:10.1016/j.ejrh.2017.10.004.

Peters, D., and Steinley, K. 2018. Swift Current Creek water monitoring project 2017. Final Report, Swift Current Creek Watershed Stewards, Swift Current, SK.

Pidwirny, M. 2006. “Evaporation and transpiration”. Fundamentals of physical geography, 2nd Edition. Available from http://www.physicalgeography.net/fundamentals/8i.html. [accessed 21 January 2020]

Pietroniro, A., Fortin, V., Kouwen, N., Neal, C., Turcotte, R., Davison, B., Verseghy, D., Soulis, E.D., Caldwell, R., Evora, N., and Pellerin, P. 2006. Using the MESH modelling system for hydrological ensemble forecasting of the Laurentian great lakes at the regional scale. Hydrology and Earth System Sciences Discussions, **3(4)**: 2473–2521.

Pomeroy, J.W., de Boer, D., and Martz, L.W. 2005. Hydrology and water resources of Saskatchewan. Centre for Hydrology Report 1, University of Saskatchewan, Saskatoon, SK.

Pomeroy, J.W., Gray, D.M., Brown, T., Hedstrom, N.R., Quinton, W.L., Granger, R.J., and Carey, S.K. 2007. The cold regions hydrological model: a platform for basing process representation and model structure on physical evidence. Hydrological Processes, **21**(19): 2650–2667. doi:10.1002/hyp.6787.

Quinton, W.L., Hayashi, M., and Pietroniro, A. 2003. Connectivity and storage functions of channel fens and flat bogs in northern basins. Hydrological Processes, **17**(18): 3665–3684. doi:10.1002/hyp.1369.

Reddy, K.R., Khaleel, R., Overcash, M.R., and Westerman, P.W. 1979. A nonpoint source model for land areas receiving animal wastes. II. Ammonia volatilization. Transactions of the ASAE, 22(6): 1398-1405. doi: 10.13031/2013.35219

Rehman, O. ur, Rashid, M., Kausar, R., Alvi, S., and Hussain, R. 2015. Slope gradient and vegetation cover effects on the runoff and sediment yield in hillslope agriculture. Turkish Journal of Agriculture - Food Science and Technology, **3**(6): 478–483.

Ritchie, J.T. 1972. Model for predicting evaporation from a row crop with incomplete cover. Water Resources Research, **8**(5): 1204–1213. doi:10.1029/WR008i005p01204.

Rowan, K., Pittman, J., Wittrock, V., and Unvoas, A. 2011. Drought and excessive moisture preparedness plan, Swift Current Creek watershed. Saskatchewan Watershed Authority, Swift Current, SK.

Saltelli, A., and Annoni, P. 2010. How to avoid a perfunctory sensitivity analysis. Environmental Modelling & Software, **25**(12): 1508–1517. doi:10.1016/j.envsoft.2010.04.012.

Saskatchewan Watershed Authority. 2010. State of the watershed report. science, information and monitoring stewardship division, Regina, Saskatchewan.

Sharpley, A.N., and Syers, J.K. 1979. Phosphorus inputs into a stream draining an agricultural watershed. Water, Air, and Soil Pollution, **11**(4): 417–428. doi:10.1007/BF00283433.

Shaw, D.A., Vanderkamp, G., Conly, F.M., Pietroniro, A., and Martz, L. 2011. The fill–spill hydrology of Prairie wetland complexes during drought and deluge. Hydrological Processes, **26**(20): 3147–3156. doi:10.1002/hyp.8390.

Smith, V.H., and Schindler, D.W. 2009. Eutrophication science: where do we go from here? Trends in Ecology & Evolution, **24**(4): 201–207. doi:10.1016/j.tree.2008.11.009.

Statistics Canada. 2007. Percentage of total land prepared for seeding, 1991 and 2006, Saskatchewan. Available from https://www150.statcan.gc.ca/t1/tbl1/en/tv.action?pid=3210040801. [accessed 21 January 2020]

Statistics Canada. 2011. Fertilized land area in Canada by ecozone, selected years, 1971 to 2006. Available from https://www150.statcan.gc.ca/n1/pub/16-201-x/2009000/t235-eng.htm. [accessed 21 January 2020]

Shrestha, R.R., Dibike, Y.B., and Prowse, T.D. 2012a. Modelling of climate-induced hydrologic changes in the Lake Winnipeg watershed. Journal of Great Lakes Research, **38**: 83-94. doi:10.1016/j.jglr.2011.02.004.

Shrestha, R.R., Dibike, Y.B., and Prowse, T.D. 2012b. Modeling climate change impacts on hydrology and nutrient loading in the Upper Assiniboine Catchment. Journal of the American Water Resources Association, 48(1): 74–89. doi:10.1111/j.1752-1688.2011.00592.x.

Singh, J., Knapp, H.V., Arnold, J.G., and Demissie, M. 2007. Hydrological modeling of the Iroquois river watershed using HSPF and SWAT. Journal of the American Water Resources Association, 4**1**(2): 343–360. doi:10.1111/j.1752-1688.2005.tb03740.x.

Sloan, P.G., and Moore, I.D. 1984. Modeling subsurface stormflow on steeply sloping forested watersheds. Water Resources Research, **20**(12): 1815–1822. doi:10.1029/WR020i012p01815.

Southwest Booster. 2002. Water in the Swift Current Creek watershed. The Swift Current Creek Watershed Stewards (SCCWS), Saskatchewan.

Stichling, W., and Blackwell, S.R. 1957. Drainage area as a hydrologic factor on the glaciated Canadian prairies. Prairie Farm Rehabilitation Administration, Regina, Canada.

The old farmer's Almanac. 2019. Planting calendar for places in Saskatchewan. Available from https://www.almanac.com/gardening/planting-calendar/SK. [accessed 3 December 2019].

Tiner, R.W. 2003. Estimated extent of geographically isolated wetlands in selected areas of the United States. Wetlands, **23**(3): 636–652. doi:10.1672/0277-5212(2003)023[0636:EEOGIW]2.0.CO;2.

Tisseuil, C., Wade, A.J., Tudesque, L., and Lek, S. 2008. Modeling the stream water nitrate dynamics in a 60,000 $km^2$ european catchment, the Garonne, Southwest France. Journal of Environmental Quality, **37**(6): 2155–2169. doi:10.2134/jeq2007.0507.

Tolson, B.A., and Shoemaker, C.A. 2007. Cannonsville reservoir watershed SWAT2000 model development, calibration and validation. Journal of Hydrology, **337**(1): 68–86. doi:10.1016/j.jhydrol.2007.01.017.

Townsend-Small, A., McClelland, J.W., Holmes, R.M., and Peterson, B.J. 2011. Seasonal and hydrologic drivers of dissolved organic matter and nutrients in the Upper Kuparuk River, Alaskan Arctic. Biogeochemistry, **103**(1-3): 109–124. doi:10.1007/s10533-010-9451-4.

Tuo, Y., Duan, Z., Disse, M., and Chiogna, G. 2016. Evaluation of precipitation input for SWAT modeling in Alpine catchment: a case study in the Adige river basin (Italy). Science of The Total Environment, **573**: 66–82. doi:10.1016/j.scitotenv.2016.08.034.

United States Environmental Protection Agency (USEPA). 1983. Results of the nationwide urban runoff program. Final Report, USEPA, Water Planning Division, Washington, D.C., USA.

Upadhyay, P., Pruski, L.O.S., Kaleita, A.L., and Soupir, M.L. 2018. Evaluation of AnnAGNPS for simulating the inundation of drained and farmed potholes in the Prairie Pothole Region of Iowa. Agricultural Water Management, **204**: 38–46. doi:10.1016/j.agwat.2018.03.037.

Vandas, S.J., Winter, T.C., and Battaglin, W.A. 2014. What affects the quality of surface and groundwater? American Geosciences Institute. Available from

https://www.americangeosciences.org/critical-issues/faq/what-affects-quality-surface-and-groundwater. [accessed 29 January 2020].

van der Kamp, G., and Hayashi, M. 2009. Groundwater-wetland ecosystem interaction in the semiarid glaciated plans of North America. Hydrogeology Journal **17**(1):203-214. doi:10.1007/s10040-008-0367-1.

van Groenigen, J.W., Huygens, D., Boeckx, P., Kuyper, T.W., Lubbers, I.M., Rütting, T., and Groffman, P.M. 2015. The soil N cycle: new insights and key challenges. SOIL, **1**(1): 235–256. doi:10.5194/soil-1-235-2015.

Vining, K.C. 2002. Simulation of streamflow and wetland storage, Starkweather Coulee subbasin, North Dakota, water years 1981-98. USGS Numbered Series 4113, U.S. Geological Survey, Reston, VA, USA.

Waite, D.T., Cessna, A.J., Grover, R., Kerr, L.A., and Snihura, A.D. 2002. Environmental concentrations of agricultural herbicides. Journal of Environmental Quality, **31**(1): 129–144. doi:10.2134/jeq2002.1290.

Waite, D.T., Sommerstad, H., Grover, R., Kerr, L., and Westcott, N.D. 1992. Pesticides in ground water, surface water and spring runoff in a small Saskatchewan watershed. Environmental Toxicology and Chemistry, **11**(6): 741–748. doi:10.1002/etc.5620110603.

Wall, G.J., Dickinson, W.T., Rudra, R.P., and Coote, D.R. 1988a. Seasonal soil erodibility variation in Southwestern Ontario. Canadian Journal of Soil Science, **68**(2): 417–424. doi:10.4141/cjss88-038.

Wall, G.J., Dickinson, W.T., Rudra, R.P., and Coote, D.R. 1988b. Seasonal soil erodibility variation in Southwestern Ontario. Canadian Journal of Soil Science, **68**(2): 417–424. doi:10.4141/cjss88-038.

Wang, X., Yang, W., and Melesse, A.M. 2008. Using hydrologic equivalent wetland concept within SWAT to estimate streamflow in watersheds with numerous wetlands. Transactions of the ASABE, **51**(1): 55–72. doi:10.13031/2013.24227.

Wheater, H., and Gober, P. 2013. Water security in the Canadian prairies: science and management challenges. Philosophical Transactions of the Royal Society A: Mathematical, Physical and Engineering Sciences, 371: 20120409. doi:10.1098/rsta.2012.0409.

White, K.L., and Chaubey, I. 2005. Sensitivity analysis, calibration, and validations for a multisite and multivariable SWAT model. JAWRA Journal of the American Water Resources Association, **41**(5): 1077–1089. doi:10.1111/j.1752-1688.2005.tb03786.x.

Winter, T.C., and LaBaugh, J.W. 2003. Hydrologic considerations in defining isolated wetlands. Wetlands, **23**(3): 532. doi:10.1672/0277-5212(2003)023[0532:HCIDIW]2.0.CO;2.

Wischmeier, W.H., and Smith, D.D. 1978. Predicting rainfall-erosion losses: a guide to conservation planning. USDA, Washington, D.C.

Woo, M.K., and Rowsell, R.D. 1992. Hydrology of a prairie slough. Journal of Hydrology, **146**: 175-207. doi:0022-1694/93.

Xu, Y., Cai, Q., Han, X., Shao, M., and Liu, R. 2010. Factors regulating trophic status in a large subtropical reservoir, China. Environmental Monitoring and Assessment, **169**: 237–248. doi:10.1007/s10661-009-1165-5.

Yang, W., Wang, X., Liu, Y., Gabor, S., Boychuk, L., and Badiou, P. 2010. Simulated environmental effects of wetland restoration scenarios in a typical Canadian prairie watershed. Wetlands Ecology and Management, **18**(3): 269–279. doi:10.1007/s11273-009-9168-0.

Zhao, D., Xie, D., Zhou, H., Jiang, H., and An, S. 2012. Estimation of leaf area index and plant area index of a submerged macrophyte canopy using digital photography. PLoS ONE, **7**(12): e51034. doi:10.1371 /journal.pone.0051034.